

Fall 1-2021

## Viral Factors Influencing Early Infection Events During Ex-Vivo KSHV Infection

Ramina Nabiee  
*Chapman University*

Follow this and additional works at: [https://digitalcommons.chapman.edu/  
pharmaceutical\\_sciences\\_dissertations](https://digitalcommons.chapman.edu/pharmaceutical_sciences_dissertations)

 Part of the [Immunology of Infectious Disease Commons](#), [Investigative Techniques Commons](#), and the [Other Pharmacy and Pharmaceutical Sciences Commons](#)

---

### Recommended Citation

Nabiee, R. *Viral Factors Influencing Early Infection Events During Ex-Vivo KSHV Infection*. [dissertation]. Irvine, CA: Chapman University; 2021. <https://doi.org/10.36837/chapman.000224>

This Dissertation is brought to you for free and open access by the Dissertations and Theses at Chapman University Digital Commons. It has been accepted for inclusion in Pharmaceutical Sciences (PhD) Dissertations by an authorized administrator of Chapman University Digital Commons. For more information, please contact [laughtin@chapman.edu](mailto:laughtin@chapman.edu).

VIRAL FACTORS INFLUENCING EARLY INFECTION  
EVENTS DURING EX-VIVO KSHV INFECTION

A Dissertation by

Ramina Nabiee

Chapman University

Irvine, CA

Chapman University School of Pharmacy (CUSP)

Submitted in partial fulfillment of the requirements for the degree of

Doctor of Philosophy in Pharmaceutical Sciences

January 2021

Committee in charge:

Dr. Jennifer E. Totonchy, Ph.D., Chair

Dr. Innokentiy Maslennikov, Ph.D.

Dr. Ajay Sharma, Ph.D.

Dr. Moom Roosan, Ph.D.

Dr. Khalid Elsaid, Ph.D.



The dissertation of Ramina Nabiee is approved.



---

Jennifer E. Totonchy, Ph.D., Chair



---

Innokentiy Maslennikov, Ph.D.



---

Ajay Sharma, Ph.D.



---

Moom Roosan, Ph.D.



---

[Khaled Elsaid \(Jan 21, 2021 11:46 PST\)](#)

---

Khaled Elsaid, Ph.D.

January 2021

# Viral Factors Influencing Early Infection Events During Ex-Vivo KSHV Infection

Copyright © 2021

by Ramina Nabiee

## ACKNOWLEDGEMENTS

The world is built by those who dare to dream, those who are not afraid of challenging themselves and venturing into the unknown. But it is preserved by those who vow to train and document; those who graciously take in the inexperienced and mentor them, lift them up and internalize the joy of perseverance and knowledge acquirement in them.

This dissertation is dedicated to all of my mentors who took a chance on a wide eyed, eager girl, and showed her the wonders of being a seeker of truth and sciences, those whose constant encouragement and support not only affected my professional life but my personal life as well. Particularly my advisors, Dr. Jennifer E. Totonchy whose eagerness to educate me, and participating in scientific chats provided me with a chance to exercise my love of scientific debates and discovery. Thanks for your encouragement and unconditional support, it has been an honor for me to be a part of your lab.

I like to express the depth of my gratitude to my family and friends for their unconditional love and support, and most importantly for keeping up with me and my stress induced *Romina-ness*. Thanks for keeping me on the path of light and thanks for not giving up on me even when I was about to; a big part of what I am today is shaped by you and because of you and I am and shall be eternally grateful to you.

And finally, I would like to acknowledge the arduous work and sacrifices that all humans in all life endeavors constantly go through as that was what mostly inspired me years ago to pursue a life of sciences and embark on a mission through which I could help alleviate the pain of humans, and help elevate the world towards a lighter path as small as those contributions may be, as a sign of gratitude to all the people I have encountered on my journey so far.

## VITA

Ramina Nabiee is currently a PhD. Student in Pharmaceutical Sciences at Chapman University School of Pharmacy. Prior to her PhD. She was enrolled in Chapman University School of Pharmacy's Master of Sciences in Pharmaceutical Sciences and graduated in June 2017. She graduated with her Bachelor of Applied Sciences degree in Biotechnology Engineering in May 2015 from Jahrom University.

During her studies at Chapman University School of Pharmacy she has achieved the following awards/ scholarships:

Trainee Award at the 22nd International Workshop on Kaposi's Sarcoma Herpesvirus (KSHV) and Related Agents.

2019 Graduate Student Research Showcase 1st place poster award.

Graduate student 3MT® Award 2nd place at Chapman University 2019.

Full PhD Fellowship and scholarship from Chapman University August 2017-Present.

The winner of James L. Doti Outstanding Graduate Student Award 2017 awarded for exhibition of academic excellence and outstanding professional leadership as a graduate student at Chapman University July 2017.

Dean's list of honor scholarships Chapman University School of Pharmacy August 2016 and February 2017.

## LIST OF PUBLICATIONS

During the PhD program the following manuscripts have been published as a result of direct work on the thesis project or collaborative works. The manuscripts have been listed chronologically.

1. Totonchy, J., Osborn, J. M., Chadburn, A., **Nabiee, R.**, Argueta, L., Mikita, G., & Cesarman, E. (2018). KSHV induces immunoglobulin rearrangements in mature B lymphocytes. *PLoS pathogens*, 14(4), e1006967. <https://doi.org/10.1371/journal.ppat.1006967>
2. Mulama, D. H., Mutsvunguma, L. Z., Totonchy, J., Ye, P., Foley, J., Escalante, G. M., Rodriguez, E., **Nabiee, R.**, Muniraju, M., Wussow, F., Barasa, A. K., & Ogembo, J. G. (2019). A multivalent Kaposi sarcoma-associated herpesvirus-like particle vaccine capable of eliciting high titers of neutralizing antibodies in immunized rabbits. *Vaccine*, 37(30), 4184–4194. <https://doi.org/10.1016/j.vaccine.2019.04.071>
3. Muniraju, M., Mutsvunguma, L. Z., Foley, J., Escalante, G. M., Rodriguez, E., **Nabiee, R.**, Totonchy, J., Mulama, D. H., Nyagol, J., Wussow, F., Barasa, A. K., Brehm, M., & Ogembo, J. G. (2019). Kaposi Sarcoma-Associated Herpesvirus Glycoprotein H Is Indispensable for Infection of Epithelial, Endothelial, and Fibroblast Cell Types. *Journal of virology*, 93(16), e00630-19. <https://doi.org/10.1128/JVI.00630-19>
4. Aalam, F., **Nabiee, R.**, Castano, J. R., & Totonchy, J. (2020). Analysis of KSHV B lymphocyte lineage tropism in human tonsil reveals efficient infection of CD138+ plasma cells. *PLoS pathogens*, 16(10), e1008968. <https://doi.org/10.1371/journal.ppat.1008968>
5. **Nabiee, R.**; Syed, B.; Ramirez Castano, J.; Lalani, R.; Totonchy, J.E. An Update of the Virion Proteome of Kaposi Sarcoma-Associated Herpesvirus. *Viruses* 2020, 12, 1382.

## ABSTRACT

Viral Factors Influencing Early Infection Events During Ex-Vivo KSHV Infection

by Ramina Nabiee

The enigma of Kaposi Sarcoma Herpes Virus infection, and its persistence despite a quarter century of research on the virus, has given rise to an immediate need for addressing fundamental questions about basic immunology and virology knowledge regarding this virus. Kaposi Sarcoma Herpes Virus (KSHV), also known as Human Herpesvirus 8 (HHV8), is the etiological agent of Kaposi Sarcoma (KS) and other lymphoproliferative cancers, such as Multicentric Castleman's Disease (MCD), Primary Effusion Lymphoma (PEL), and a newly discovered rare disease called KSHV Inflammatory Cytokines Syndrome (KICS). Epidemic KS, also known as AIDS-KS, is the most common cancer in untreated HIV patients. This epidemic in western countries mostly affects the homosexual population, while in the malaria-belt, both men and women can be affected equally. All forms of diseases caused by KSHV are uniformly fatal highlighting the need for research into KSHV virology for the identification of possible druggable targets to address the public health burden and help further develop vaccines, therapies, or treatments.

The thesis presented herein will focus on the study of early infection events and the persistence of infection within the oral cavity. We have identified and characterized virion-associated factors critical for the earliest stages of KSHV infection; in three specific aims:

1. Examining Host-Specific Differences and Viral Tropism in KSHV Infection of Tonsil-Derived B Lymphocytes
2. Validating the Proteomic Composition of KSHV Virions
3. Establishing the Contribution of KSHV-ORF11 Tegument Protein in *de novo* Infection of B Lymphocytes.

We have demonstrated that gamma-herpesvirus conserved tegument factors play critical but uncharacterized roles in the establishment of infection in B lymphocytes, and that utilizing our study model provides us with the unique chance to observe this infection process at an early stage. Thus, in short, we have attempted to provide an answer to the long-forgotten questions within the field of KSHV virology about the proteins the virion packages and introduces in early stages of infection and what that could mean in the bigger picture for the host -pathogen interactions.

# TABLE OF CONTENTS

	<u>Page</u>
ACKNOWLEDGEMENTS .....	IV
VITA .....	V
LIST OF PUBLICATIONS .....	VI
ABSTRACT .....	VII
LIST OF TABLES.....	XIII
LIST OF FIGURES.....	XIV
LIST OF ABBREVIATIONS.....	XVI
LIST OF SYMBOLS.....	XVIII
<b>1. CHAPTER I: KSHV EARLY INFECTION EVENTS AND HOST-PATHOGEN INTERACTIONS, A ROAD LESS TRAVELED.....</b>	<b>1</b>
<b>1.1 Introduction .....</b>	<b>2</b>
1.1.1 KSHV Discovery .....	3
1.1.2 KSHV's Pathophysiology .....	8
1.1.3 KSHV Host Cell Tropism .....	13
1.1.4 Difficulties in KSHV Research .....	15
<b>1.2 Rationale and Hypothesis .....</b>	<b>15</b>
<b>1.3 Specific Aims .....</b>	<b>19</b>
<b>1.3.1 Examining Host-Specific Differences in KSHV Infection of Tonsil-Derived B Lymphocytes .....</b>	<b>19</b>
1.3.2 Validating the Proteomic Composition of KSHV Virions .....	20
1.3.3 To Establish the Contribution of KSHV-ORF11 Tegument Protein in <i>de novo</i> Infection of B Lymphocytes.....	21
<b>1.4 Justification for and Significance of the Study .....</b>	<b>22</b>
1.4.1 Global Impact of KSHV on Public Health .....	22
1.4.2. The Black Box of Basic KSHV Virology .....	23
1.4.3. Implementation of Tonsil Lymphatic Tissue as a Novel Study System	23
1.4.4. Targeting Tegument Factors as Potential Novel Druggable Targets .....	24
1.4.5. Studying the Mechanism of Action and Effects of Specific Tegument Proteins	25
<b>1.5 Innovations of the Study .....</b>	<b>25</b>
<b>1.6 Scope of this study .....</b>	<b>26</b>

<b>2 CHAPTER II: ANALYSIS OF KSHV B LYMPHOCYTE LINEAGE TROPISM IN HUMAN TONSIL REVEALS EFFICIENT INFECTION OF CD138+ PLASMA CELLS</b> .....	<b>28</b>
<b>Abstract</b> .....	<b>29</b>
<b>Author summary</b> .....	<b>30</b>
<b>2.1 Introduction</b> .....	<b>31</b>
<b>2.2 Materials and Methods</b> .....	<b>33</b>
2.2.1 Ethics Statement. ....	33
2.2.2 Reagents and Cell Lines. ....	34
2.2.3 Isolation of primary lymphocytes from human tonsils.....	34
2.2.4 Infection of primary lymphocytes with KSHV. ....	35
2.2.5 Flow cytometry staining and analysis of KSHV infected tonsil lymphocytes. ....	36
2.2.6 B lymphocyte lineage isolation by cell sorting. ....	37
2.2.7 RT-PCR. ....	38
2.2.8 Single Cell RT-PCR. ....	40
2.2.9 Heparinase treatment of human fibroblasts and lymphocytes.....	41
2.2.10 T cell depletion studies. ....	42
2.2.11 Statistical Analysis. ....	43
<b>2.3 Results</b> .....	<b>43</b>
2.3.1 Variable immunological composition of human tonsil specimens.....	43
2.3.2 Variable susceptibility of tonsil-derived B cells to ex vivo KSHV infection. ....	49
2.3.3 Specific targeting of individual B cell lineages by KSHV infection.....	53
2.3.4 Viral gene expression in KSHV infected B lymphocytes .....	61
2.3.5 KSHV infection of B lymphocytes does not rely on heparin sulfate proteoglycans ....	64
2.3.6 Immune status alters KSHV infection of B lymphocytes .....	69
<b>2.4 Discussions</b> .....	<b>76</b>
<b>3 CHAPTER III: AN UPDATE OF THE VIRION PROTEOME OF KAPOSI SARCOMA-ASSOCIATED HERPESVIRUS</b> .....	<b>84</b>
<b>Abstract</b> .....	<b>85</b>
<b>3.1 Introduction</b> .....	<b>86</b>
<b>3.2 Materials and methods</b> .....	<b>90</b>
3.2.1. Purification of Cell-Free KSHV Virions .....	90
3.2.2. Trypsin and Detergent Treatment of Purified Virions .....	91
3.2.3. Mass Spectrometry Analysis .....	92
3.2.4. Antibodies and Western Blotting .....	95
<b>3.3 Results</b> .....	<b>97</b>
3.3.1. Purification of Cell Free KSHV Virions and Virion Protein Fractions....	97
3.3.2. Mass Spectrometry Quality Control .....	100
3.3.3. KSHV Virion Protein Identification.....	104

3.4 Discussion .....	120
<b>4 CHAPTER IV: KSHV ORF11 TEGUMENT PROTEIN SUPPRESSES PLASMABLAST AND PLASMA CELL PROLIFERATION .....</b>	<b>127</b>
<b>Abstract .....</b>	<b>128</b>
<b>4.1 Introduction .....</b>	<b>129</b>
<b>4.2 Materials and Methods .....</b>	<b>132</b>
4.2.1 Tissue Culture.....	132
4.2.2 X-ray Irradiation.....	132
4.2.3 Tonsil Tissue Dissociation and Isolation of Primary Lymphocytes.....	133
4.2.4 Generation of KSHV- $\Delta$ ORF11 using BAC16.....	133
4.2.5 Preparation of Cell Free Recombinant KSHV Particles.....	134
4.2.6 Viral Titering .....	135
4.2.7 Infection of Primary Lymphocytes with KSHV.....	136
4.2.8 Multicolor Flow cytometry.....	137
4.2.9 RT-PCR for Viral Gene Expression .....	140
4.2.10 Immunofluorescence assays (IFA).....	141
4.2.11 Construction of ORF11-myc-pCDNA .....	142
4.2.12 Cell Proliferation assays .....	143
4.2.13 UV inactivation studies .....	143
<b>4.3 Results.....</b>	<b>144</b>
4.3.1 ORF11 Protein Localizes to Plasma Membrane and has a Transmembrane Domain. ....	144
4.3.2 KSHV ORF11KO, Mutant Development, And Preliminary Studies Confirm That ORF11 Is Not Essential for Viral Production.....	147
4.3.3 Increased Infection with ORF11KO Is Observed in B lymphocytes However, There Is No Significant Viral Particle Production Change. ....	152
4.3.4 Increased Proliferation In $\Delta$ ORF11 Mutant Virus Infected Cells, Is Linked to Increased Proliferation of Plasmablasts and Plasma Cells. ....	154
<b>4.4 Discussion and Future Directions .....</b>	<b>161</b>
<b>5 CHAPTER V: CONCLUSIONS AND FUTURE DIRECTIONS.....</b>	<b>164</b>
<b>5.1 Conclusions .....</b>	<b>164</b>
5.1.1 In Chapter 2: .....	164
5.1.2 In Chapter 3: .....	166
5.1.3 In Chapter 4: .....	166
<b>5.2 In Summary .....</b>	<b>167</b>
<b>5.3 Future Directions.....</b>	<b>169</b>
<b>REFERENCES .....</b>	<b>171</b>
<b>Appendices.....</b>	<b>184</b>

## LIST OF TABLES

	<b><u>Page</u></b>
Table 2.1 Donor demographics for the tonsil specimens used in the study (n = 40).....	45
Table 2.2 Lineage definitions for lymphocyte subsets used in the study.....	48
Table 3.1. Proteins identified in the VT fraction in our study that were previously reported by mass spectrometry. ....	105
Table 3.2. Proteins identified by mass spectrometry in our study that were previously reported by other methods.....	110
Table 3.3. Virion-associated proteins identified that have not previously been reported by any method.....	113
Table 4.1 B cell lineages used in this study.....	139
Table 4.2: Primer and Probe Sequences used for qPCR Assays. ....	141

# LIST OF FIGURES

	<u>Page</u>
Figure 1. 1 Divergence of Gamma Herpesviruses from the other Herpesvirus Families.....	5
Figure 1. 2 Worldwide KSHV seroprevalence (cumulative data from several studies conducted between 1998-2015).....	7
Figure 1. 3 KSHV Structure and its simplified interaction with Host cell during entry. ....	10
Figure 1. 4 Scheme of the infection model used in our studies.....	18
Figure 2. 1 Variability and age-dependence of B lymphocyte lineage distribution in humans...46	
Figure 2. 2 Tonsil-derived B lymphocytes from diverse donors display variable susceptibility to KSHV infection.....	52
Figure 2. 3 B lymphocyte lineage tropism of KSHV.....	56
Figure 2. 4 CD138 and heparin sulfate proteoglycans as attachment factors for KSHV in B lymphocytes.....	67
Figure 2. 5 The donor specific CD4+ T cell microenvironment influences infection of CD138+ plasma cells.....	71
Figure 2. 6 Manipulation of T cell microenvironment alters KSHV tropism for B cell lineages.	74
Figure 3. 1 Quality control of the virion fraction prior to mass spectrometry.....	99
Figure 3. 2 Statistical data presented from PEAKS analysis on the 17 proteins found uniquely in our study, with false discovery rate (FDR) set at 1%.....	103
Figure 3. 3 CID spectrum of the precursor ion at m/z7792 (z = 2) corresponding to the peptide sequence (DRPLTATEK) of an ORF52.....	116
Figure 3. 4 Example of post-translational modifications (PTMs) detected via PEAKS DB analysis for ORF52.....	117
Figure 4. 1 ORF11 expression is localized to plasma membrane and the expression level is significantly improved by codon optimization.....	146
Figure 4. 2 ORF11 protein Has A Transmembrane Domain. (A)The top panel is confocal microscopy analysis of the HEK293T cells expressing ORF11 pCDNA.....	147

Figure 4. 3 KSHV ORF11 Mutant development. As demonstrated two amino acids genetic codons.....149

Figure 4. 4 Higher GFP Expression Within The  $\Delta$ ORF11 Infected Samples Is Observed Within Similar Doses.....151

Figure 4. 5 Increased Infection with ORF11KO Is Observed However There Is No Significant Viral Particle Production Change.....153

Figure 4. 6 Observed changes in total population of B cells, as well as changes in GFP(Infected) only population of B cells. All B cells are shown as frequency of viable, CD19+ B cells.....155

Figure 4. 7 BrdU analysis shows increased proliferation in total B cell population and individual subset proliferation.....157

Figure 4.8 Total B Cell Proliferation, Plasmablasts and, Plasma Cell Proliferation Increases Significantly Post Infection with ORF11KO, statistical analysis has been done using ggplot ggpaired statistical tests.....158

Figure 4. 9 UV inactivated  $\Delta$ ORF11 infection of B cells does not yield any proliferation, indicating that it is not the ORF11 packaged within the virus that has an effect in the suppression of B cell proliferation but the role of newly expressed ORF11 within the infected cells, analysis is done by ggplot.....160

## LIST OF ABBREVIATIONS

<b><u>Abbreviation</u></b>	<b><u>Meaning</u></b>
AIDS	Acquired immunodeficiency syndrome
BAC16	Bacterial artificial Chromosome 16 containing KSHV genome
CCS	Cosmic calf serum
CD	Cluster of differentiation markers
DMEM	Dulbecco's Modified Eagle Medium
DNA	Deoxyribonucleic acid
EBV	Epstein Barr Virus
FBS	Fetal bovine serum
HEK293T	Human embryonic kidney 293 cell variant that expresses a temperature-sensitive allele of the SV40 T antigen.
HHV8	Human Herpes Virus 8
HIV	human immunodeficiency virus
HVS	Herpes Virus Saimiri
iSLK	Inducible SLK cells
KICS	KSHV Induced Cytokine Syndrome
KS	Kaposi Sarcoma
KSHV	Kaposi's Sarcoma Herpes Virus
LB Broth	Luria-Bertani (LB) broth
MCD	Multicentric Castleman's Disease
ORF	Open Reading Frame

PBS	Phosphate-buffered saline
PEL	Primary Effusion Lymphoma
RNA	Ribonucleic acid
RPMI	Roswell Park Memorial Institute Medium
RTA	Replication and Transcription Activator
TLR	Toll like receptors
UV	Ultraviolet
vIL	Viral interleukin
vIRF	viral interferon regulatory factor

## LIST OF SYMBOLS

Symbol	Meaning
-10lgP	Low scoring peptide identifications are filtered out by setting a desired peptide-spectrum match -10lgP threshold or a desired FDR (false-discovery rate)
ALC%	average local confidence) scores for Peptide <i>de novo</i> sequencing
KO	Knockout
mL	Milliliter
PTM	confidence score of identifying a Modification in a peptide at a specific
Ascore	position
$\alpha$	Alpha- herpesvirus family
$\beta$	Beta-herpesvirus family
$\gamma$	gamma( $\gamma$ )-2 herpesvirus family
$\Delta 11$	Knockout Mutant lacking ORF11
$\mu\text{L}$	Microliter

1. CHAPTER I: KSHV Early Infection Events and Host-Pathogen Interactions, A  
Road Less Traveled

## 1.1 Introduction

Kaposi Sarcoma (KS) is now the 4<sup>th</sup> most common cancer caused by an infectious agent. KS has a high prevalence among AIDS patients, but the enigma of Kaposi's Sarcoma Herpes Virus (KSHV) infection, and its persistence despite quarter century of research on the virus, has given rise to immediate need for addressing fundamental questions about basic immunology and virology knowledge regarding this virus (Martin JN, 2007). Kaposi's Sarcoma was first discovered by Dr. Moritz Kaposi in 1872, when he observed a peculiar multifocal pigmented sarcoma in elderly European males who died within a few years of symptom emergence (Classic KS) (Kaposi, 1872). Years later, several reports described a lymphadenopathic form of KS in African children (Endemic KS) (D'Oliveira, 1972). However, it was the onset of the AIDS epidemic that KS became a major public health burden and a research priority (Epidemic KS) (Gottlieb, 1981), (Ariyoshi, 1998). It is worth noting that there have been two other forms of KS detected: Iatrogenic KS, occurring in people with iatrogenic immunodeficiencies, or people undergoing tissue transplant surgeries (Grulich, 2015); and a newer increasing form of KS in men who have sex with men (MSM) without HIV infection (Denis, 2018).

It was not until 1994 that a directed study suggested that this cancer had an infectious origin independent of HIV (Chang, et al., 1994).

KSHV also known as Human Herpesvirus 8 (HHV8) is known today as the etiological causative of Kaposi Sarcoma (KS) and other lymphoproliferative cancers (Mesri EA, 2010 ) such as Multicentric Castleman's Disease (MCD), and Primary Effusion Lymphoma (PEL), and a newly discovered rare disease called KSHV Inflammatory Cytokines Syndrome (KICS) (Karass M. e., 2017).

Epidemic KS also known as AIDS-KS is the most common cancer in untreated HIV patients, and this epidemic in western countries mostly affects the homosexual population, while in the malaria belt both men and women can be affected equally (Wabinga HR, 1993 ).

All forms of diseases caused by KSHV are uniformly fatal (Mesri EA, 2010 ), highlighting the major need for study and development of possible druggable targets within the virus to address the public health burden and help further develop vaccines, therapies, and treatments.

### 1.1.1 KSHV Discovery

KSHV was first discovered twenty-five years ago through the use of representational difference analysis by Chang et.al (Chang, et al., 1994) and about a year later Moore et al. looked into similarities of this virus with other known gamma-herpesviruses and were able to identify it as most similar to HVS (Herpesvirus Saimiri). However, through gene alignment and amino acid sequencing alignments on ORFs suitable for phylogenetic analysis, they noted that

the divergence between them is ancient. Furthermore, they classified the virus as the first human gamma( $\gamma$ )-2 herpesvirus (Moore, et al., 1996).

KSHV is the only viral agent of the rhadinoviral subfamily capable of infecting humans (Chang, et al., 1994). The gamma-herpesvirus subfamily was first classified and distinguished from the other herpesviruses (alpha and beta subfamilies) because of their cellular tropism for lymphocytes (Longnecker R, 2007. ) The Gammaherpesvirinae subfamily is further divided into two superfamilies: Lymphocryptoviridae including EBV, and Rhinoviruses which includes KSHV (**Fig.1.1**).

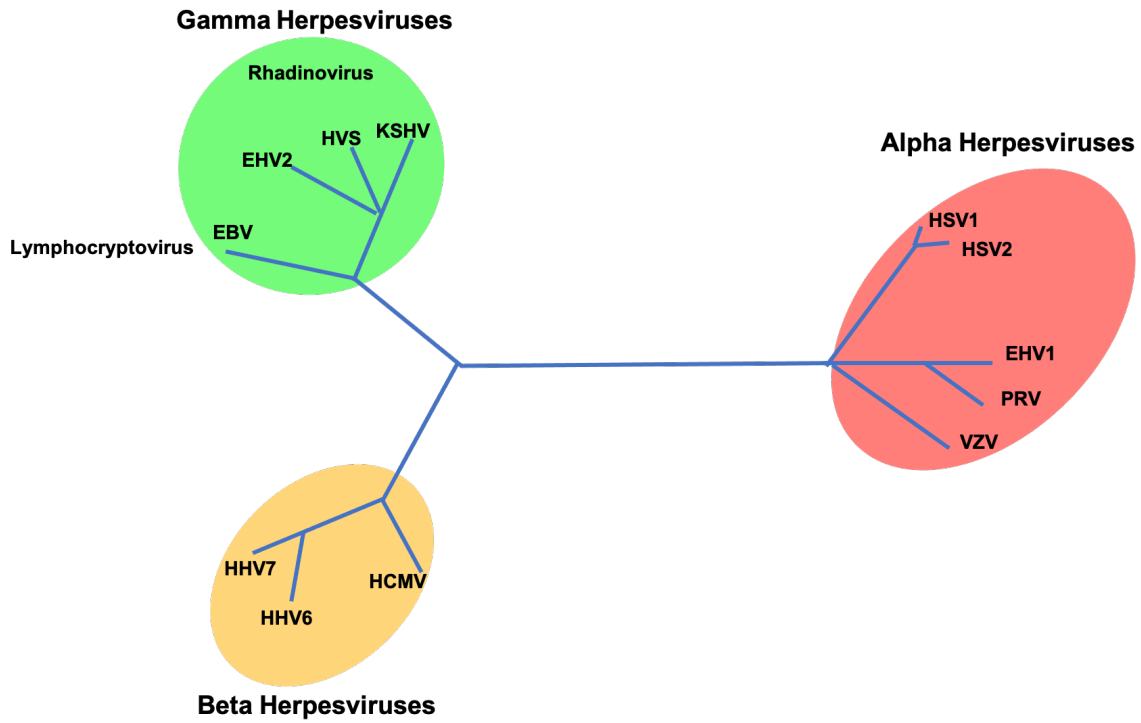


**Figure 1. 1 Divergence of Gamma Herpesviruses from the other Herpesvirus Families.** In 1996 Moore et al. looked into similarities of KSHV virus with other known gamma-herpesviruses of the day and identified it as most similar with HVS (Herpesvirus Saimiri) through gene alignment and amino acid sequencing alignments on ORFs suitable for phylogenetic analysis. He furthermore, classified the virus as the first human gamma( $\gamma$ )-2 herpesvirus.

KSHV's seroprevalence has been connected with KS prevalence (Mesri EA, 2010 ). It is highest in sub-Saharan Africa (up to 90% seroprevalence in some adult populations). In contrast, its prevalence in Europe, Asia, USA where it is prevalent in less than 10% of population (**Fig1.2**) (Cesarman, 2019).

Aside from the infection of endothelial cells that leads to different forms of KS, KSHV is also capable of infecting human B cells, where it can lead to different B cell tumors (Hassman LM, 2011 ), all of which are not only fatal but the current therapy available for them can only prolong patients' lifespan up to two years at most (Carbone A G. A., 2008), (Waterston A, 2004 ).

## KSHV Seroprevalence around the world



**Figure 1. 2 Worldwide KSHV seroprevalence (cumulative data from several studies conducted between 1998-2015).** Figure modified from Cesarman et al. (Cesarman, 2019) and Mesri et al. (Mesri EA, 2010).

### 1.1.2 KSHV's Pathophysiology

KSHV can infect and interact with a range of host cells including B lymphocytes, dendritic cells, endothelial cells, epithelial cells, fibroblasts, and monocytes (Bechtel J. T., 2003). KSHV uses different surface receptors to interact with different host cells, for example it has been recognized that KSHV uses integrins such as heparin sulfate and tyrosine protein kinase receptor EPHA2 for endothelial cell entry (Kumar, 2016), while it has been suggested that KSHV relies on DC-SIGN for B cell entry (Rappocciolo G, 2008 ).

KSHV virions average 120-150 nm in size. The central nucleocapsid has a T = 16 icosahedral structure with vertices formed out of 12 pentons interconnected with 320 triplexes and 150 hexons, that form the faces and edges that together constitute a capsid structure similar to other herpesviruses (Trus BL, 2001). KSHV has a linear double stranded DNA (Damania, 2013) of 165–170 kb, that is encapsulated within the capsid surrounded by a layer of non-structural proteins, and RNA. This amorphous proteinaceous layer is called the tegument layer and proteins in this layer critically affect the cellular and viral biology immediately following viral entry (Minhas, 2014). The tegument layer also separates the capsid from the glycoprotein containing envelope (Roizman, et al., 1981 ). The glycoproteins residing within the envelope interact with cell type specific receptors and facilitate entry (Kumar, 2016), which leads to direct delivery of the viral capsid into host

cytoplasm. Once within the cytoplasm, capsids are transported to the nuclear membrane where KSHV genomes are released and penetrate the nucleus. During latency, the viral genome resides in the form of an extrachromosomal episome and can switch to sporadic onsets of lytic activation (**Fig1.3**) (Bechtel J. T., 2003).

In the very early stages of viral entry, the virion releases tegument proteins within the host cell, which immediately begin modulating host and viral processes including cell cycle modulation (De Oliveira, Ballon, & Cesarman, 2010 ), transcriptional activation of viral genes (Sathish N, 2012 ) inhibition of host gene expression activation (Zhu, Sathish, & Yuan, 2010), translocation of the virion capsid to the nucleus and modulation of innate immune responses (Bergson, et al., 2014 ) in the infected cells.

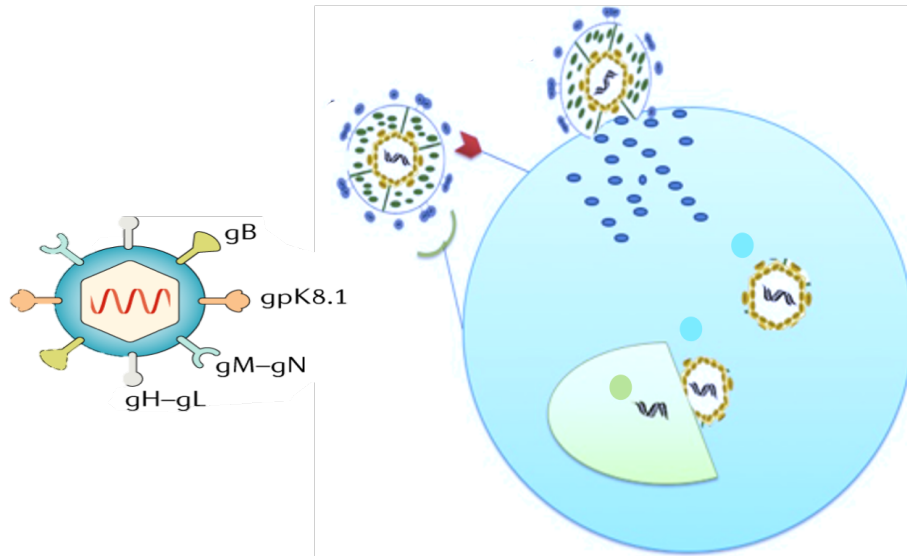


**Figure 1. 3 KSHV Structure and its simplified interaction with Host cell during entry.** The glycoproteins residing within the envelope interact with cell type specific receptors and facilitate entry leading to direct delivery of viral capsid into host cytoplasm. Once within the cytoplasm KSHV genome will be unshathed, however the virion packaged proteins will be released in the early preliminary stages, manipulating the cellular environment

As with other herpesviruses, infection with KSHV is lifelong, and the virus primarily establishes latency and only expresses a few selective loci, such as ORF71 (also called ORFK13; encoding viral FLICE inhibitory protein (vFLIP), ORF72 (encoding vCyclin), ORF73 (encoding latency-associated nuclear protein (LANA), ORFK12, and low levels of expression for some other ORFS such as ORFK15, ORFK1 and viral IL-6 (vIL6), as well as several microRNAs (miRNAs) (Cai, 2005), (Chandriani, 2010). The latent genes are expressed in most KSHV-infected tumor cells and are thought to promote tumorigenesis. Also, the viral miRNAs that are expressed during KSHV latency are believed to help keep the infected cell alive, by inhibiting apoptosis, and maintaining virus latency (Dittmer, 2016); these viral miRNAs are also expressed in KS, PEL and MCD (O'Hara, 2009). Similarly, in B cell studies using animals it has been observed that the expression of some latent genes as well as miRNAs leads to lymphoma (Sin, 2013) as well as vascular proliferation and an inflammatory phenotype when expressed in endothelial cells (Ballon, 2015).

Some studies have attempted therapeutic targeting of these latent genes. However, due to a lack of proper cell models, or clinical infeasibility, there have not been significant therapeutic successes (Briggs, 2017) . Another approach has also focused on targeting the host cellular genes that are activated / regulated by KSHV.

This approach seems to have a higher degree of success, especially in the case of mTOR pathway targeting due to its overexpression in latently infected tumor cells of PEL as well as KS (Krown, 2012) and the fact that it acts as a general sensing pathway within all cells.

KSHV is also capable of a lytic life cycle, however, it is not yet clear what physiological stimuli allows spontaneous reactivation (Cesarman, 2019). In the lytic life cycle, KSHV genes have different time-based clusters of expression. Immediate-Early (IE) genes are expressed first. The protein products of most IE genes control transcription and ORF45/RTA, a key protein also known as the reactivation switch, which ensures the expression of viral genes required for replication. The next cluster of lytic genes are Delayed-Early (DE) genes followed finally by late genes (Damania, 2013). The DE genes, in general, control and facilitate viral DNA replication via rolling circle mechanism resulting in linear genomes ready for packaging within the capsids. In the late phase, all viral structural genes are expressed. In contrast to latent genes that are expressed in all tumor cells, lytic genes and the encoded viral proteins are produced by a low proportion of tumor cells (Damania, 2013). Lytic phase genes have also been studied as therapeutic targets. However, the results are inconsistent within distinct patient groups', highlighting the immediate need for development of more effective therapeutics (Uldrick, 2011), (Krown S. E., 2011).

### 1.1.3 KSHV Host Cell Tropism

Although KSHV's route of transmission is still unknown, KSHV has consistently been detected in circulating peripheral blood mononuclear cells (PBMC; mostly of B cell lineage), saliva, prostate, bone, and nerve tissues of AIDS patients with or without KS (Ambroziak JA, 1995). Pauk et al. (Pauk, et al., 2000) showed that, in comparison to other bodily fluids, the percentage of KSHV detection in saliva is the highest. Thus, they concluded that oral exposure to infectious saliva is a potential risk factor for the acquisition of KSHV. In addition, KSHV has been detected in hyperplastic lymph nodes of immune-competent persons, strengthening the hypothesis that HHV-8 may establish persistent infection without inducing clinically evident disease (He, et al., 1998).

The origin of the cell types resulting in KSHV-related diseases is still not fully determined, and how a certain cell types become infected with KSHV needs more research (Ensoli, et al., 2001). In early KS development, it has been observed that the KS nodes are rich in immune cells, suggesting a potential role for immune cells during macule formation. However, the increase in immune cells could be driven by infected cells and not be the source of the virus (Cesarman, Mesri, & Gershengorn, 2000). It has been hypothesized that infected B cells residing in the proximity of endothelial cells may play a role in KS formation. Clinical research has shown that B cells are of critical importance to KSHV by: (1) providing a

reservoir for KSHV latent life cycle in the host (2) being the cell type of origin for PEL and MCD and (3) as a possible source of KSHV in the saliva (Myoung J, 2011). However, B cells are largely refractory to KSHV infection in cell culture models (Akula SM, 2001 ), (Dyson, Traylen, & Akula, 2010). One plausible reason for this observation could be the utilization of PBMC cells instead of secondary lymphoid tissue residing cells (Hassman LM, 2011 ).

In B cell cancers it has long been believed that the transformed B cells will still mirror the phenotype of their cell type of origin (Salmon & Seligmann, 1974 ) However, it has been a topic of discussion in the infectious lymphoma field, that B cells could also be first infected and then undergo malignant transformation following differentiation (Campbell, Jenkins, & Rinaldo, 2014). Recently, it was shown that infection may drive alternate light chain expression in (from  $\kappa$  to  $\lambda$ ) for reasons that are still unclear (Totonchy J, 2018 ). It is worth noting that PEL and MCD are believed to arise from B cells of various stages of development (Chadburn A, 2008), (Du, et al., 2001). It is still unknown which type or types of B lymphocyte precursors are susceptible to KSHV. To this day, the potential range of B cells that may be critical for disease and the difficulty infecting them hinders the study of B cell infection (Dollery, 2019 ).

Taken together it can be concluded that the therapies that inhibit B cell infection may prove especially useful in KSHV infection prevention.

#### 1.1.4 Difficulties in KSHV Research

Despite the extensive body of work revolving around the role of individual KSHV factors in varying aspects of tumorigenesis, there is a lack of reliable models for KSHV infection *in vitro* as well as difficulty in *in vitro* viral particle production and challenges in production of recombinant virions (Zhou, 2002). All these factors together have coerced scientists to substitute non-relevant cell lines in models. This limits our knowledge of early events during *de novo* infection including, but not limited to, the cell types involved, viral and cellular factors influencing *de novo* infection, persistence, and the establishment of latency in disease-relevant cell types or how these factors might contribute to disease. Another challenge in the field of KSHV has been the lack of evidence for the viral transmission route, but recent data has indicated that there is a noticeable amount of viral shedding in saliva. Thus, establishing saliva as an important infectious reservoir and the most likely mode of KSHV transmission (Newton, et al., 2018). Furthermore, given the fact that this virus has lymphocyte tropism, we believe that the tonsil and oral lymphoid tissues represent the most relevant physiological niche in which to study the earliest stages of KSHV infection and spread.

#### **1.2 Rationale and Hypothesis**

Assuming that saliva is a primary route of KSHV spread and given the fact that this virus has tropism for B Lymphocytes and lymphatic endothelial cells, we

believe that the oral lymphoid tissues, such as the tonsil, represent the most relevant physiological niche to study the earliest stages of KSHV infection and spread.

Moreover, some of KSHV tegument proteins are specific to and highly conserved within the gamma herpesvirus family (Bai Z, 2014). These conserved factors could potentially be contributing to the gamma-herpesvirus family exclusive behaviors and characteristics (i.e., lymphocyte tropism). Therefore, identifying specific tegument proteins and further characterizing their specific roles in initiation, spread and persistence of infection will lead to valuable and critical knowledge that can help further the development of novel therapeutics, as well as discoveries about the human immune system.

As mentioned above, despite the many years of research on KSHV, the route of transmission is still not determined. However, in recent years there has been significant findings showcasing noticeable levels of virion shedding within the saliva of infected people. Thus, it is likely that transfer of the virion from infected patients to other subjects happens through exchange of saliva. In this scenario, one of the earliest points of contact between KSHV virions and susceptible target cells is going to occur in the subjects' tonsils (Non-keratinized stratified squamous tissues containing a considerable level of lymphocytes among other cells). Thus,

tonsil derived B lymphocytes are important cell type to study the initiation and establishment of KSHV infection in a new human host.

Given our labs previous experience with KSHV in development of molecular tools for the study of KSHV as well as establishment of a unique cellular model system for infection tonsil-derived B lymphocytes and mesenchymal cells (**Fig.1.4**); the research proposed herein will focus on the study of early infection events and the persistence of infection within the oral cavity.

We will identify and characterize virion-associated factors critical for the earliest stages of KSHV infection. We hypothesize that gamma-herpesvirus conserved tegument factors play critical but uncharacterized roles in the establishment of infection in B lymphocytes, and that utilizing our study model will provide us with the unique chance of observing related cells in this infection process at an early stage.

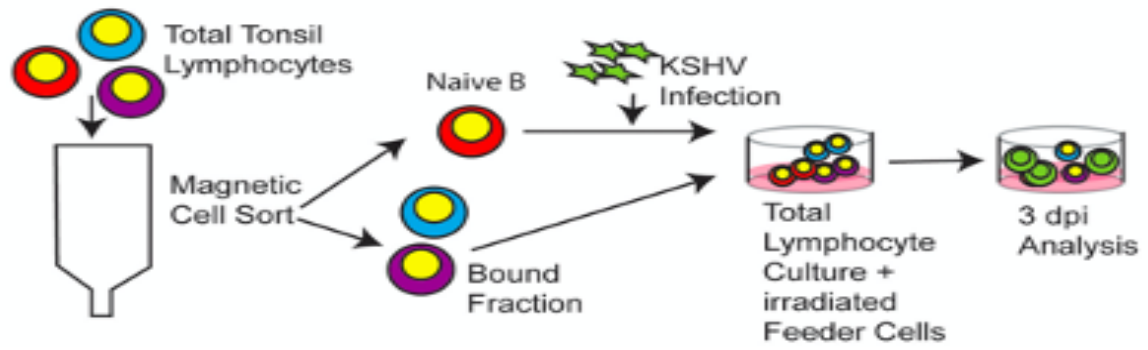


**Figure 1. 4 Scheme of the infection model used in our studies.** Lymphocytes are separated via magnetic sort, then Naïve B cells of different donors are used at the same density for infection, later on the other cells are also added back to the experimental condition well.

## 1.3 Specific Aims

### 1.3.1 Examining Host-Specific Differences in KSHV Infection of Tonsil-Derived B Lymphocytes

#### Hypothesis

From the time B Lymphocytes are produced in the bone marrow, they constantly undergo complex maturation and differentiation, especially within the secondary lymphoid tissues where they are exposed to signals introduced from other cells. This results in a robust mixed population of B lymphocyte subtypes coexisting within the tonsil and other lymphoid tissues. As KSHV interacts with B lymphocytes, different B lymphocyte subsets might respond differently to viral infection and persistence. To date, the susceptibility of different B lymphocyte lineages to KSHV infection has not been fully characterized.

Our lab previously developed an *in vitro* model system to determine phenotypic changes associated with KSHV-infection of primary B lymphocytes from human tonsil tissue over an elongated period. This model met two important criteria: (1) stable detectable infection of sufficient cell numbers and (2) maintenance of B cell immunophenotypes over time in culture. In this system, concentrated cell-free virions are used to infect a variety of B lymphocyte lineages in either bulk infection from total B cell fraction or isolated subsets sorted from human tonsil (Totonchy J, 2018 ) We have recently improved on this model system (**Fig.1.2**)

allowing us to examine infection of different B cell lineages while also providing a way to standardize infection of samples with different compositions to allow between samples comparisons.

### 1.3.2 Validating the Proteomic Composition of KSHV Virions

#### **Hypothesis**

KSHV virions package a substantial number of proteins in the tegument layer which interact with the host cells in the early stages of infection and affect the cellular tropism of virions. Tegument proteins affect changes to the host cell such as cell cycle modulation (De Oliveira, Ballon, & Cesarman, 2010), transcriptional activation of viral genes (Sathish N, 2012 ) inhibition of host gene expression activation (Zhu, Sathish, & Yuan, 2010) and translocation of the virion capsid within the nuclei (Bergson, et al., 2014 ). The composition of the tegument layer of KSHV has not been revisited in a decade. Thus, in order to understand how tegument proteins may be influencing the establishment of infection in human tonsil, we aim to independently validate and extend our understanding of the protein composition of KSHV virions.

This aim will ultimately serve as an establishment phase for the next specific aim which would be the study of selected viral tegument factors and their contribution to early events of infection in tonsil lymphocytes.

### 1.3.3 To Establish the Contribution of KSHV-ORF11 Tegument Protein in *de novo* Infection of B Lymphocytes.

#### **Hypothesis**

We hypothesize that systematic knockout of individual KSHV tegument factors will reveal that multiple tegument components are essential for KSHV infection, and that some of these factors may have cell type-specific effects. As mentioned previously, KSHV tegument proteins play a very crucial role in the establishment of infection, and only *de novo* infection systems can be used to determine which tegument proteins are essential for KSHV infection in disease-relevant cell types. One of these tegument factors is ORF11, a tegument protein of about 48kDa exclusive to KSHV virus only, which is poorly studied. But given the fact that only KSHV genome and virion contains this protein and considering that only KSHV, among the Rhadnoviral subfamily, has the B lymphocyte tropism previously mentioned. By combining gain-and loss-of-function study approaches, we will reveal previously uncharacterized functions of the KSHV tegument factor ORF11. We hypothesize that ORF11 has a role in early manipulation of KSHV infection specifically in B lymphocytes and thus may represent a therapeutic target for inhibiting KSHV infection and spread within the lymphocyte compartment.

## 1.4 Justification for and Significance of the Study

This study aims to address particularly important questions and increase the overall current knowledge of this field; using our unique in-house developed biological model, that closely represents MCD disease, we can classify the significance of the study in five categories.

### 1.4.1 Global Impact of KSHV on Public Health

In western countries, specifically, AIDS-KS has been a rising pandemic for the past 38 years (Gonçalves PH, 2017 ) Along with the rise of HIV infection there are reports of KS developing in up to 30% of AIDS patients. It has been reported that HIV-infected patients are almost 600 times more likely to develop KS (Rabkin CS, 1991 ), (Chaturvedi AK, 2008). It should be noted that unlike other KS forms, this form of KS is not only fast progressing but also uniformly fatal. Despite the invention of antiretroviral therapeutics (ART) that have been able to help control the incidence of KS in HIV+ people, the demand for targeted therapeutics is still present. Unfortunately, this need has not been answered in the last decade. One important reason for this could be the lack of a suitable animal model, as well as the limited number of patients which have made the clinical trials and *in vivo* studies difficult (Lukac DM, 2007. ). The goal of the current study here, is to provide novel druggable targets for KSHV. Furthermore, given our unique model we will be able to provide more information on early effects of *de novo* infection

with KSHV, as well as susceptibility of different B cell subsets to the infection, which will in serve to broaden the range of efficacy for the therapeutics.

#### 1.4.2. The Black Box of Basic KSHV Virology

We have extensive knowledge about some individual KSHV genes and their possible role in tumorigenesis and malignancies; however, the role of specific viral genes in *de novo* KSHV infection, particularly in disease-relevant cell types, has not been extensively explored.

Up to recent years, the common laboratory procedures were not able to produce high-titered cell-free infectious viral particles from mutant KSHV genomes (Brulois, et al., 2012). Thus, the contribution of viral factors, specifically in preliminary stages of the infection has been poorly studied, leading to lack of knowledge about the druggable targets responsible for viral spread. Our study focuses on the contribution of highly preserved viral factors exclusive to KSHV and their potential role in early stages of *de novo* infection of tonsil-derived B cells.

#### 1.4.3. Implementation of Tonsil Lymphatic Tissue as a Novel Study System

Although up to this day, the route of KSHV transmission has not been conclusively established. However, there is a convincing body of literature indicating that saliva may be the primary mode of transmission for KSHV (Minhas, 2014). These data

highlight the significance of oral cavity for establishment of KSHV infection, particularly given the fact that KSHV is a lymphotropic virus and lymphoid tissue is highly enriched with B cells. However, due to a lack of *de novo* infection models for KSHV, the oral biology of early KSHV infection and its contribution to KSHV-associated malignancy remains largely unexplored. The successful completion of the proposed project will provide critical insights and novel targets for therapeutic interventions in this important physiological niche.

#### 1.4.4. Targeting Tegument Factors as Potential Novel Druggable Targets

As previously stated, KSHV virions contain many of non-structural viral factors, some of which have been highly preserved during KSHV's evolution. Like in other herpesviruses, these viral factors assist the virus in establishment of infection and affect the host cell environment upon binding and entry of viral particles. Thus, making them strong candidates as targets for therapeutic interventions aimed at preventing viral spread. Such a study, if done on relevant host cells, can provide a better understanding for the role of these tegument proteins especially in early infection events, and could lead to development of novel therapeutics.

#### 1.4.5. Studying the Mechanism of Action and Effects of Specific Tegument Proteins

Old-world gamma-herpesviruses have some highly conserved genes, some of which have not been extensively studied, particularly in the context of their contribution to the establishment and progress of infection. This study therefore aims to address this lack of understanding in this field by approaching these poorly-studied factors through protein expression and further gain of function studies to not only discover the active contribution of these tegument proteins, but also discover new attributes of these novel proteins.

### **1.5 Innovations of the Study**

To date, the majority of the research done in KSHV virology has been done in one of the following three models:

1.5.1. Study of the KSHV virology in naturally infected lymphoma cell lines (Drexler, 1998 ).

1.5.2. Study of KSHV virology in cells infected with lymphoma-derived KSHV-WT (Friborg J Jr, 1998 ).

1.5.3. Study of KSHV virology in non-relevant cell lines like HEK-293 (Alkharsah KR, 2011 ).

These models are not ideal for answering questions about the early events in *de novo* infection. In the recent years there has been some innovative studies conducted focusing on tonsillar B cells, and infection of whole tonsil with KSHV, however the existing studies of KSHV infection in tonsil-derived B cells have explored a limited number of cell surface markers including IgM, immunoglobulin lambda light chains and activation markers on infected cells (Hassman:2011dj), (Nicol:2016ga), (Totonchy:2018ir). However, no studies to date have comprehensively explored the specific B lymphocyte lineages targeted by KSHV infection in human tonsil specimens. On the contrary, the studies conducted here will use a unique model developed to study *de novo* infection of multiple disease-relevant cell types, which also gives us the ability to study early events in the infection as well. This model will not only help us important biological questions and establish a solid foundation for extensive future research but will also provide a unique opportunity for developing therapeutic paradigms with broad efficacy and shed light on critical aspects of early KSHV infection in physiologically relevant contexts.

### **1.6 Scope of this study**

KSHV is a lymphotropic herpesvirus, but despite the many years of research in this field, the route of transmission however is still not determined. However, in recent years there has been significant findings demonstrating noticeable levels of virion

shedding within the saliva of infected people, so a possible mechanism of KSHV transmission is the transfer of the virion from infected patients to other subjects through exchange of saliva. In this context, one of the earliest points of contact for the newly introduced virions is going to be the subjects' tonsils (secondary lymphoid organs containing a considerable amount of B lymphocytes), making the tonsil derived B lymphocyte cells an important model to study the initiation and establishment of KSHV infection.

Given our labs previous experience with this virus in development of molecular tools for the study of KSHV as well as establishment of a unique cellular model system for infection tonsil-derived B lymphocytes, the research presented herein has focused on the study of early infection events and the persistence of infection within the oral cavity.

2 CHAPTER II: ANALYSIS OF KSHV B LYMPHOCYTE LINEAGE  
TROPISM IN HUMAN TONSIL REVEALS EFFICIENT INFECTION OF  
CD138+ PLASMA CELLS

**Authors:** Farizeh Aalam\*, Ramina Nabiee\*, Jesus Ramirez Castano and Jennifer  
Totonchy‡

School of Pharmacy, Chapman University, Irvine, California, USA

\*authors contributed equally to the manuscript and are listed alphabetically.

## Abstract

Despite 25 years of research, the basic virology of Kaposi Sarcoma Herpesviruses (KSHV) in B lymphocytes remains poorly understood. This study seeks to fill critical gaps in our understanding by characterizing the B lymphocyte lineage-specific tropism of KSHV. Here, we use lymphocytes derived from 40 human tonsil specimens to determine the B lymphocyte lineages targeted by KSHV early during *de novo* infection in our *ex vivo* model system. We characterize the immunological diversity of our tonsil specimens and determine that overall susceptibility of tonsil lymphocytes to KSHV infection varies substantially between donors. We demonstrate that a variety of B lymphocyte subtypes are susceptible to KSHV infection and identify CD138<sup>+</sup> plasma cells as a highly targeted cell type for *de novo* KSHV infection. We determine that infection of tonsil B cell lineages is primarily latent with few lineages contributing to lytic replication. We explore the use of CD138 and heparin sulfate proteoglycans as attachment factors for the infection of B lymphocytes and conclude that they do not play a substantial role. Finally, we determine that the host T cell microenvironment influences the course of *de novo* infection in B lymphocytes. These results improve our understanding of KSHV transmission and the biology of early KSHV infection in a naïve human host and lay a foundation for further characterization of KSHV molecular virology in B lymphocyte lineages.

## **Author summary**

KSHV infection is associated with cancer in B cells and endothelial cells, particularly in the context of immune suppression. Very little is known about how KSHV is transmitted and how it initially establishes infection in a new host. Saliva is thought to be the primary route of person-to-person transmission for KSHV, making the tonsil a likely first site for KSHV replication in a new human host. Our study examines KSHV infection in B cells extracted from the tonsils of 40 human donors in order to determine what types of B cells are initially targeted for infection and examine how the presence (or absence) of other immune cells influence the initial stages of KSHV infection. We found that a variety of B cell subtypes derived from tonsils can be infected with KSHV. Interestingly, plasma cells (mature antibody-secreting B cells) were a highly targeted cell type. These results lay the foundation for further studies into the specific biology of KSHV in different types of B cells, an effort that may help us ultimately discover how to prevent the establishment of infection in these cells or reveal new ways to halt the progression of B cell cancers associated with KSHV infection.

## 2.1 Introduction

Kaposi Sarcoma-associated Herpesvirus (KSHV/HHV-8) is a lymphotropic gamma-herpesvirus. In addition to its role in the pathogenesis of Kaposi Sarcoma (KS) (Chang, et al., 1994), KSHV infection is associated with two lymphoproliferative disorders, multicentric Castleman disease (MCD) and primary effusion lymphoma (PEL) (Cesarman E, 1995), (Soulier J, 1995), as well as a recently characterized inflammatory disorder KSHV inflammatory cytokine syndrome (KICS) (Uldrick TS, 2010 ). Although KSHV-associated lymphoproliferative disorders are rare, their incidence has not declined as HIV treatment has improved (Powles T, 2009 ), (Bhutani M, 2015 ) suggesting that, in contrast to KS, immune reconstitution is not sufficient to prevent KSHV-associated lymphoproliferative disease in people living with HIV/AIDS. Moreover, the KSHV-associated lymphoproliferative diseases are uniformly fatal with few effective treatment options (Carbone A V. E., 2014 ).

Despite the fact that KSHV is lymphotropic and causes pathological lymphoproliferation *in vivo*, study of *de novo* KSHV infection in B lymphocytes has historically been difficult (Kang S, 2017). Resting peripheral B cells and many established B cell-derived cell lines are refractory to KSHV infection but unstimulated tonsil-derived lymphocytes are susceptible to infection (Rappocciolo G, 2008 ) To date, several other groups, including our own, have been successful in infecting B lymphocytes derived from human tonsils (Hassman LM, 2011 ),

(Myoung J, 2011 ), (Myoung J, 2011), (Bekerman E, 2013 ), (Totonchy J, 2018 ), (Nicol SM, 2016 ). KSHV DNA is detectable in human saliva and salivary transmission is thought to be the primary route of person-to-person transmission for KSHV (Casper C K. E.-L., 2007 ), (Pauk J, 2000 ), (Casper C R. M.-L., 2004), (Vieira J, 1997 ) making the oral lymphoid tissues a likely site for the initial infection of B lymphocytes in a naïve human host. Thus, in addition to being susceptible to *ex vivo* infection, tonsil lymphocytes represent a highly relevant model for understanding early infection events in KSHV transmission.

The existing studies of KSHV infection in tonsil-derived B cells have explored a limited number of cell surface markers including IgM, immunoglobulin light chains and activation markers on infected cells (Hassman LM, 2011 ) (Totonchy J, 2018 ), (Nicol SM, 2016 ). One study using PBMC-derived B lymphocytes identified naïve, memory and plasma cell-like lineages as infection targets in both *in vitro* infection experiments and blood samples from KS patients (Knowlton ER, 2014 ). However, no studies to date have comprehensively explored the specific B lymphocyte lineages targeted by KSHV infection in human tonsil specimens.

In this study, we performed KSHV infection of 40 human tonsil specimens from diverse donors and utilized lineage-defining immunological markers by flow cytometry to establish the primary B cell lineage tropism of KSHV. Our results demonstrate that the susceptibility of tonsil-derived B lymphocytes to *ex vivo* KSHV

infection varies substantially from donor-to-donor, and that a variety of B cell lineages are susceptible to KSHV infection and that, at least at early stages post-infection KSHV is primarily latent in most cell types. In particular, CD138+ plasma cells are highly targeted by KSHV infection despite the fact that they are present at low frequencies in tonsil tissue. We demonstrate that high susceptibility of plasma cells to KSHV infection is not due to the presence of CD138 heparin sulfate proteoglycan as an attachment factor. Moreover, HSPG are not generally important for infection of primary B lymphocytes. Finally, we demonstrate that although the baseline T cell microenvironment does not seem to influence overall susceptibility of tonsil specimens to KSHV infection, the specific lineage distribution of KSHV infection is affected by the T cell microenvironment and manipulation of CD4/CD8 T cell ratios can alter the targeting of specific B cell lineages by KSHV. These results provide new insights into early events driving the establishment of KSHV infection in the human immune system and demonstrate that alterations in immunological status can affect the dynamics of KSHV infection in B lymphocytes.

## **2.2 Materials and Methods**

### **2.2.1 Ethics Statement.**

Human specimens used in this research were de-identified prior to receipt from NDRI and thus were not subject to IRB review as human subjects' research.

### 2.2.2 Reagents and Cell Lines.

CDw32 L cells (CRL-10680) were obtained from ATCC and were cultured in DMEM supplemented with 20% FBS (Sigma Aldrich) and Penicillin/Streptomycin/L-glutamine (PSG/Corning). For preparation of feeder cells CDw32 L cells were trypsinized and resuspended in 15 ml of media in a petri dish and irradiated with 45 Gy of X-ray radiation using a Rad-Source (RS200) irradiator. Irradiated cells were then counted and cryopreserved until needed for experiments. Cell-free KSHV.219 virus derived from iSLK cells (Myoung & Ganem, 2011 ) was a gift from Javier G. Ogembo (City of Hope). Human tonsil specimens were obtained from NDRI. Human fibroblasts were derived from primary human tonsil tissue and immortalized using HPV E6/E7 lentivirus derived from PA317 LXS<sup>N</sup> 16E6E7 cells (ATCC CRL-2203). Antibodies for flow cytometry were from BD Biosciences and Biolegend and are detailed below.

### 2.2.3 Isolation of primary lymphocytes from human tonsils.

De-identified human tonsil specimens were obtained after routine tonsillectomy by NDRI and shipped overnight on wet ice in DMEM+PSG. All specimens were received in the laboratory less than 24 hours post-surgery and were kept at 4°C throughout the collection and transportation process. Lymphocytes were extracted by dissection and maceration of the tissue in RPMI media. Lymphocyte-containing media was passed through a 40µm filter and pelleted at 1500rpm for 5 minutes. RBC

were lysed for 5 minutes in sterile RBC lysing solution (0.15M ammonium chloride, 10mM potassium bicarbonate, 0.1M EDTA). After dilution to 50ml with PBS, lymphocytes were counted, and pelleted. Aliquots of  $5 \times 10^7$  to  $1 \times 10^8$  cells were resuspended in 1ml of freezing media containing 90% FBS and 10% DMSO and cryopreserved until needed for experiments.

#### 2.2.4 Infection of primary lymphocytes with KSHV.

Lymphocytes were thawed rapidly at 37°C, diluted dropwise to 5ml with RPMI and pelleted. Pellets were resuspended in 1ml RPMI+20%FBS+100µg/ml DNase I+ Primocin 100µg/ml and allowed to recover in a low-binding 24 well plate for 2 hours at 37°C, 5% CO<sub>2</sub>. After recovery, total lymphocytes were counted, and Naïve B cells were isolated using MojoSort Naïve B cell isolation beads (Biolegend 480068) or Naïve B cell Isolation Kit II (Miltenyi 130-091-150) according to manufacturer instructions. Bound cells (non-naïve B and other lymphocytes) were retained and kept at 37°C in RPMI+20% FBS+ Primocin 100µg/ml during the initial infection process.  $1 \times 10^6$  Isolated naïve B cells were infected with iSLK-derived KSHV.219 (dose equivalent to the ID20 at 3dpi on human fibroblasts) or Mock infected in 400ul of total of virus + serum free RPMI in 12x75mm round bottom tubes via spinoculation at 1000rpm for 30 minutes at 4°C followed by incubation at 37°C for an additional 30 minutes. Following infection, cells were plated on irradiated CDW32 feeder cells in a 48 well plate,

reserved bound cell fractions were added back to the infected cell cultures, and FBS and Primocin (Invivogen) were added to final concentrations of 20% and 100µg/ml, respectively. Cultures were incubated at 37°C, 5% CO<sub>2</sub> for the duration of the experiment. At 3 days post-infection, cells were harvested for analysis by flow cytometry.

### 2.2.5 Flow cytometry staining and analysis of KSHV infected tonsil

lymphocytes.

A proportion of lymphocyte cultures at baseline or 3dpi representing ~500,000 cells were pelleted at 1400 rpm for 3 minutes into 96-well round bottom plates. Cells were resuspended in 100µl PBS containing (0.4ng/ml) fixable viability stain (BD 564406) and incubated on ice for 15 minutes. Cells were pelleted and resuspended in 100µl cold PBS without calcium and magnesium containing 2% FBS, 0.5% BSA (FACS Block) and incubated on ice for 10 minutes after which 100µl cold PBS containing 0.5% BSA and 0.1% Sodium Azide (FACS Wash) was added. Cells were pelleted and resuspended in FACS Wash containing B cell phenotype panel as follows for 15 minutes on ice: (volumes indicated were routinely used for up to  $0.5 \times 10^6$  cells and were based on titration of the individual antibodies on primary tonsil lymphocyte specimens) CD19-PerCPCy5.5 (2.5µl, BD 561295), CD20-PE-Cy7 (2.5µl, BD 560735), CD38-APC (10µl, BD 555462), IgD-APC-H7 (2.5µl, BD 561305), CD138-v450 (2.5µl, BD 562098), CD27-PE (10µl, BD 555441). After incubation,

150µl FACS Wash was added and pelleted lymphocytes were washed with a further 200µl of FACS Wash prior to being resuspended in 200µl FACS Wash for analysis. Data was acquired on a BD FACS VERSE Flow Cytometer and analyzed using FlowJo software. Readers should note that the BD FACS VERSE analysis instrument lacks a 561nm laser so RFP lytic reporter expression from the KSHV.219 genome is not detectable in the PE channel. For baseline T cell frequencies 0.5e6 cells from baseline uninfected total lymphocyte samples were stained and analyzed as above with phenotype antibody panel as follows: CD95-APC (2µl, Biolegend 305611), CCR7-PE (2µl, BD 566742), CD28-PE Cy7 (2µl, Biolegend 302925), CD45RO-FITC (3µl, Biolegend 304204), CD45RA-PerCP Cy5.5 (2µl, 304121), CD4-APC H7 (2µl, BD 560158), CD19-V510 (3µl, BD 562953), CD8-V450 (2.5µl, BD 561426)

#### 2.2.6 B lymphocyte lineage isolation by cell sorting.

At 3 days post-infection cells were collected and pelleted at 1400 rpm for 3 minutes into 12x75mm round bottom tubes. Cells were resuspended in 200µl PBS containing (0.4ng/ml) fixable viability stain (BD 565388) and incubated on ice for 15 minutes. Cells were pelleted and resuspended in 200µl cold MACS buffer containing 5% FBS (Sort Block) and incubated on ice for 10 minutes after which 200µl cold MACS buffer was added. Cells were pelleted and resuspended in MACS buffer containing B cell phenotype panel as follows for 15 minutes on ice: (volumes indicated are for

each  $1 \times 10^6$  cells and were scaled depending upon the number of cells being stained for sorting). For single cell sorting of plasma cells, the panel was follows: CD19-PerCPCy5.5 (5 $\mu$ l, BD 561295), CD20-PE-Cy7 (5 $\mu$ l, BD 560735), and CD138-APC (5 $\mu$ l, Biolegend 352307). For other lineages, the panel was as follows: CD19-PerCPCy5.5 (5 $\mu$ l, BD 561295), CD38-APC (20 $\mu$ l, BD 555462), IgD-PE-Cy7 (5, BD 561314), CD27-PE-Cy5 (5 $\mu$ l eBioscience 15-0279-42). After incubation, 500 $\mu$ l MACS buffer was added and pelleted lymphocytes were washed with a further 500 $\mu$ l of MACS buffer prior to being resuspended in 200 $\mu$ l MACS buffer and put through a cell strainer before sorting using the 70-micron nozzle on a BD FACSAria Fusion Cell Sorter.

### 2.2.7 RT-PCR.

At 3 days post infection, lymphocytes were harvested into Trizol or sorted into Trizol LS reagent 300 $\mu$ l Trizol was used for  $>1 \times 10^5$  cells and 100 $\mu$ l Trizol was used for  $<1 \times 10^5$  cells. An equal volume of DNA/RNA shield (Zymo Research R110-250) was added after collection and RNA extraction was performed using Zymo Directzol Microprep (Zymo Research R2060) according to manufacturer instructions. RNA was eluted in 10 $\mu$ l H<sub>2</sub>O containing 2U RNase inhibitors and a second DNase step was performed for 30 minutes using the Turbo DNA-Free kit (Invitrogen AM1907M) according to manufacturer instructions. One-step RT-PCR cDNA synthesis and preamplification of GAPDH, LANA and K8.1

transcripts was performed on 5 $\mu$ l of RNA using the Superscript III One-step RT-PCR kit (ThermoFisher 12574026) and 2 $\mu$ M outer primers for each target gene as follows: GAPDH outer forward (5'-TCGGAGTCAACGGATTTGGT-3'), GAPDH outer reverse (5'-GGGTCTTACTCCTTGGAGGC-3'), LANA outer forward (5'-AATGGGAGCCACCGGTAAAG-3'), LANA outer reverse (5'-CGCCCTTAACGAGAGGAAGT-3'), K8.1 outer forward (5'-ACCGTCGGTGTGTAGGGATA-3'), K8.1 outer reverse (5'-TCGTGGAACGCACAGGTAAA-3'). Duplicate no RT (NRT) control reactions were assembled for each lineage/sample containing only Platinum Taq DNA polymerase (Thermofisher 15966005) instead of the Superscript III RT/Taq DNA polymerase mix. After cDNA synthesis and 40 cycles of target pre-amplification, 0.002 $\mu$ l of pre-amplified cDNA or NRT control reaction was used as template for multiplexed real-time PCR reactions using TaqProbe 5x qPCR MasterMix - Multiplex (ABM MasterMix-5PM), 5% DMSO, primers at 900nM and probes at 250nM against target genes as follows: GAPDH forward (5'-TCGGAGTCAACGGATTTGGT-3'), GAPDH reverse (5'-GGGTCTTACTCCTTGGAGGC-3'), GAPDH probe (5'HEX-ACGCCACAGTTTCCCGGAGG-BHQ13') LANA forward (5'-AATGGGAGCCACCGGTAAAG-3'), LANA reverse (5'-CGCCCTTAACGAGAGGAAGT-3'), LANA probe (5' 6FAM-

ACACAAATGCTGGCAGCCCG-BHQ13'), K8.1 forward (5'-  
ACCGTCGGTGTGTAGGGATA-3'), K8.1 reverse (5'-  
TCGTGGAACGCACAGGTAAA-3'), K8.1 probe (5'FAM-  
TGCGCGTCTCTTCCTCTAGTCGTTG-TAMRA3') and analyzed using a 40  
cycle program on a ThermoFisher QuantStudio 3 real time thermocycler. Data is  
represented as quantitation cycle (Cq) and assays in which there was no  
detectable Cq value were set numerically as Cq=41 for analysis and data  
visualization.

#### 2.2.8 Single Cell RT-PCR.

At 3 days post-infection, cells were stained for sorting as described above. Single cells meeting lineage sort criteria were sorted into each well of a 0.2ml 96-well PCR plate containing 4µl of 0.5x PBS, 10mM DTT (Pierce no-weigh A39255), 1.2U RNase inhibitor (Lucigen 30281-2). After sorting, plates were sealed, centrifuged briefly to collect all material in the bottom of the well and stored at -80°C prior to analysis. Plates were thawed on ice and 2µl of DNase buffer (Invitrogen 18068-015) containing 0.5µl 10x buffer, 0.1U DNase, 0.4µl H<sub>2</sub>O) were added to each well. After incubation at room temperature for 15 minutes, EDTA (Thermofisher AM9260G) was added to a final concentration of 2mM and DNase was inactivated by incubation for 10 minutes at 65°C. One-Step RT-PCR reactions and no RT (NRT) controls were assembled using outer primers to GAPDH, LANA, and K8.1 as described above.

2µl of pre-amplified cDNA was used in the real time PCR reactions for GAPDH, K8.1, LANA as described above with the exception that the assay was multiplexed with all three targets using the same K8.1 probe sequence labeled with 5'Cy5 and 3'BHQ-2 quencher and analyzed on a BioRad CFX96 real time PCR thermocycler.

*KSHV neutralization via soluble CD138 Syndecan-1.* Infections were performed as described above except KSHV.219 virus was pre-incubated for 30 minutes on ice with serum free RPMI only or serum free RPMI containing recombinant human syndecan-1 protein (srCD138, Bio Vision, 7879-10) prior to being added to Naïve B lymphocytes. srCD138 concentrations noted in the text indicate the final concentration of recombinant syndecan-1 in the reconstituted total lymphocyte culture. Infection was analyzed at 3 days post-infection by flow cytometry for B cell lineages and KSHV infection as detailed above. For experiments involving human fibroblasts virus was added to cells in serum free media, cells were spinoculated for 30 minutes at 1000rpm, incubated at 37°C for 1 hour, then infection media was removed and replaced with complete media. At 3dpi cells were harvested via trypsinization and analyzed for infection by flow cytometry.

#### 2.2.9 Heparinase treatment of human fibroblasts and lymphocytes.

Total lymphocytes were thawed and recovered as described above and treated with Heparinase I and III Blend from *Flavobacterium heparinum* (Sigma-Aldrich # H3917) at 9U/25e6 of lymphocytes and incubated over irradiated CDW32 feeder

cells at 37°C, 5% CO<sub>2</sub> for 24 hours in complete media. E6/E7 transformed fibroblasts from human tonsil were treated at 4.5U/1e6 for 24hrs at 37°C, 5% CO<sub>2</sub>. To evaluate the effectiveness of the Heparinase treatment the samples were stained for flow cytometry, as described above, with Heparan Sulfate (10E4 epitope) (FITC) (United States Biological # H1890) at 2 µl/5e5 of the lymphocytes or E6/E7 transformed fibroblasts and analyzed with flow cytometry for loss of HSPG signal. Control untreated or Heparinase-treated samples were either Mock infected or infected with KSHV as described above. At 3 days post infection, fibroblasts were trypsinized and analyzed for GFP expression by flow cytometry and lymphocytes were harvested, stained for B cell lineages, and analyzed by flow cytometry as described above.

#### 2.2.10 T cell depletion studies.

Infections were performed as described above except a sub-population of total lymphocytes were depleted of either CD4 or CD8 T cells using positive selection magnetic beads (Biolegend MojoSort Human CD4 T Cell Isolation Kit 480009, MojoSort Human CD8 T Cell Isolation Kit 480011). The resulting depleted fractions or unmanipulated total lymphocytes were used to reconstitute naïve B lymphocytes following infection rather than bound lymphocyte fractions as described above.

### 2.2.11 Statistical Analysis.

Data plots and statistical analysis were performed in R software using ggplot2, ggcorrplot (ggcorrplot:2018tg) and RColorBrewer. Specific methods of statistical analysis and resulting values for significance and correlation are detailed in the corresponding figure legends.

## 2.3 Results

### 2.3.1 Variable immunological composition of human tonsil specimens.

In order to explore the B cell lineages targeted by KSHV infection in human tonsils, we procured a cohort of 40 de-identified human tonsil specimens from donors of diverse age, sex, and self-reported race (**Fig 2.1A and Table 2.1**).

Analysis of the baseline frequencies of B and T cell lineages by multi-color flow cytometry (**Appendix A.1, Appendix A.2 and Table 2.2**) revealed that the composition of individual human tonsil specimens is highly variable (**Fig 2.1B&D**). This variation was independent of donor age for many lineages.

However, overall B cell frequencies declined with age as did germinal center, plasmablast and transitional B cell populations while memory and naïve populations increased in frequency with donor age (**Fig 2.1C**). Similarly, most T cell lineages were not significantly correlated with donor age except for CD4+

transitional memory and CD8<sup>+</sup> terminal effector lineages which were both moderately, but significantly, negatively correlated with donor age (**Fig 2.1E**).

**Table 0.1 Donor demographics for the tonsil specimens used in the study (n = 40).**

Sex, n (%)	
Male	19 (47.5)
Female	21 (52.5)
Race, n (%)	
ND	6 (15)
White	17 (42.5)
Black	13 (32.5)
Hispanic	1 (2.5)
Asian	1 (2.5)
Other	2 (5)
Age, (years)	
(mean $\pm$ S.D.)	26.2 $\pm$ 16.47
Range	2–65

<https://doi.org/10.1371/journal.ppat.1008968.t001>

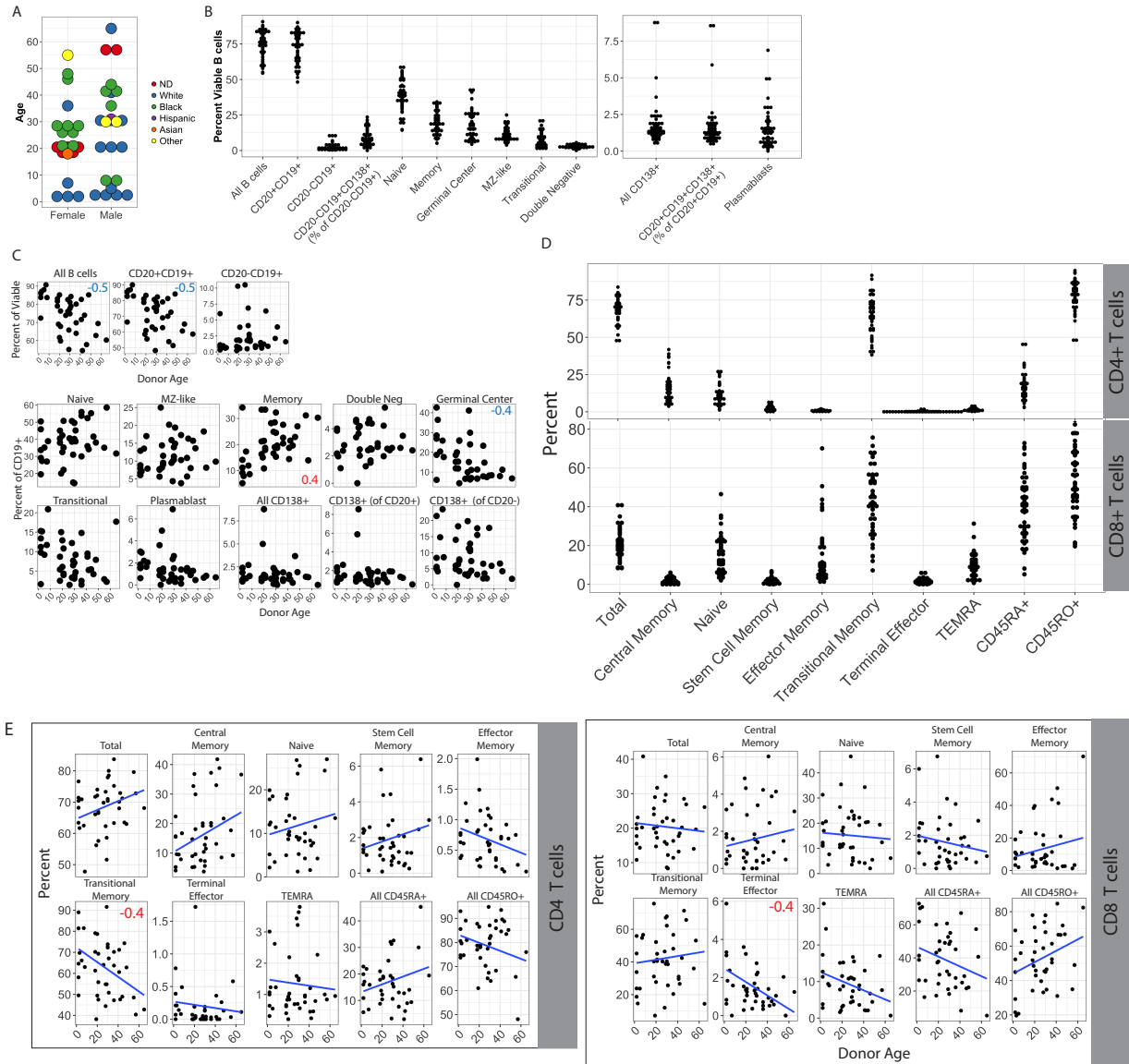


**Figure 2.2 Variability and age-dependence of B lymphocyte lineage distribution in human tonsils.** (A) Donor demographics for human tonsil specimens used in this study. Plotted by age (y-axis), sex (x-axis) and self-reported race (color) ND = not determined. (B) Frequency distributions of B cell lineages in tonsil specimens (see S1A Fig and Table 2 for lineage definitions). All B cells are shown as frequency of viable lymphocytes, other B cell subsets are shown as frequency of viable, CD19+ B cells unless otherwise specified in parenthesis. (C) Frequency of B cell lineages based on donor age. Pearson correlation coefficients ( $r$ ) with an absolute value greater than or equal to 0.4 are shown as red or blue inset text in the subset panels. (D) Frequency distributions of T cell lineages in tonsil specimens (see S1B Fig and Table 2 for lineage definitions). All T cells are shown as frequency of viable CD4+ (top) or CD8+ (bottom) T

cell except total CD4+ and total CD8+ (far left) which are shown as frequency of viable lymphocytes. (E) Frequency of CD4+ (left) and CD8+ (right) T cell lineages based on donor age. Pearson correlation coefficients (r) with an absolute value greater than or equal to 0.4 are shown as red or blue inset text in the subset panels.

**Table 0.2 Lineage definitions for lymphocyte subsets used in the study.**

<b>B Lymphocytes</b>	
<b>Subset</b>	<b>Molecular Markers</b>
Plasma	CD19 <sup>+</sup> , CD20 <sup>+/−</sup> , CD138 <sup>+(Mid to High)</sup> , CD38 <sup>−</sup>
Transitional	CD19 <sup>+</sup> , CD138 <sup>−</sup> , CD38 <sup>Mid</sup> , IgD <sup>+</sup> (Mid to High)
Plasmablast	CD19 <sup>+</sup> , CD138 <sup>−</sup> , CD38 <sup>High</sup> , IgD <sup>+/−</sup> (mostly −)
Germinal Center	CD19 <sup>+</sup> , CD138 <sup>−</sup> , CD38 <sup>Mid</sup> , IgD <sup>−</sup>
Naïve	CD19 <sup>+</sup> , CD138 <sup>−</sup> , CD38 <sup>Low</sup> , CD27 <sup>−</sup> , IgD <sup>+</sup> (Mid to High)
Marginal Zone Like (MZ-Like)	CD19 <sup>+</sup> , CD138 <sup>−</sup> , CD38 <sup>Low</sup> , CD27 <sup>+</sup> (Mid to High), IgD <sup>+</sup> (Mid to High)
Memory	CD19 <sup>+</sup> , CD138 <sup>−</sup> , CD38 <sup>Low</sup> , CD27 <sup>+</sup> (Mid to High), IgD <sup>−</sup>
Double Negative	CD19 <sup>+</sup> , CD138 <sup>−</sup> , CD38 <sup>Low</sup> , CD27 <sup>−</sup> , IgD <sup>−</sup>
<b>T lymphocytes</b>	
<b>Subset</b>	<b>Molecular Markers</b>
CD4+	CD19 <sup>−</sup> , CD4 <sup>+(Mid to High)</sup> , CD8 <sup>−</sup>
CD8+	CD19 <sup>−</sup> , CD4 <sup>−</sup> , CD8 <sup>+</sup> (Mid to High)
Naïve	CD19 <sup>−</sup> , CD4 <sup>+</sup> or CD8 <sup>+</sup> , CCR7 <sup>+(High)</sup> , CD45RA <sup>+(Mid to High)</sup> , CD45RO <sup>−</sup> , CD28 <sup>+</sup> , CD95 <sup>−</sup>
Stem Cell Memory	CD19 <sup>−</sup> , CD4 <sup>+</sup> or CD8 <sup>+</sup> , CCR7 <sup>+(High)</sup> , CD45RA <sup>+(Mid to High)</sup> , CD45RO <sup>−</sup> , CD28 <sup>+</sup> , CD95 <sup>+(Low to Mid)</sup>
Central Memory	CD19 <sup>−</sup> , CD4 <sup>+</sup> or CD8 <sup>+</sup> , CCR7 <sup>+</sup> , CD45RA <sup>−</sup> CD45RO <sup>+(Mid to High)</sup> , CD28 <sup>+(Mid to High)</sup>
Transitional Memory	CD19 <sup>−</sup> , CD4 <sup>+</sup> or CD8 <sup>+</sup> , CCR7 <sup>−</sup> , CD45RA <sup>−</sup> CD45RO <sup>+(Mid)</sup> , CD28 <sup>+(Mid to High)</sup>
Effector Memory	CD19 <sup>−</sup> , CD4 <sup>+</sup> or CD8 <sup>+</sup> , CCR7 <sup>−</sup> , CD45RA <sup>−</sup> CD45RO <sup>+(Mid)</sup> , CD28 <sup>−</sup>
Terminal Effector Memory	CD19 <sup>−</sup> , CD4 <sup>+</sup> or CD8 <sup>+</sup> , CCR7 <sup>−</sup> , CD45RA <sup>−</sup> CD45RO <sup>−</sup> , CD28 <sup>−</sup>
TEMRA CD4+ Cells	CD19 <sup>−</sup> , CD4 <sup>+</sup> or CD8 <sup>+</sup> , CCR7 <sup>−</sup> , CD45RA <sup>+(High)</sup> , CD45RO <sup>−</sup> , CD28 <sup>−</sup>

<https://doi.org/10.1371/journal.ppat.1008968.t002>

### 2.3.2 Variable susceptibility of tonsil-derived B cells to ex vivo KSHV infection.

Because of the heterogeneous nature of the tonsil samples, we predicted that each sample would also have variable levels of susceptible B cell subtypes. Therefore, we employed a method for normalizing infectious dose from donor-to-donor in order to obtain cross-sectional data that was directly comparable (**Fig 2.2A**). For each sample we used magnetic sorting to isolate untouched naïve B cells, which are a known susceptible cell type (Totonchy J, 2018 ), and infected 1 million naïve B cells with equivalent doses of cell-free KSHV.219 virus. After infection, bound lymphocytes from the magnetic separation were added back to each sample to reconstitute the total lymphocyte environment. Infected cultures were incubated for three days and analyzed for both B cell lineage markers and the GFP reporter present in the KSHV.219 genome to identify infected cells. We restricted our analysis to a single timepoint at 3 days post-infection in order to observe the establishment of infection in different lineages with minimal contribution of virus-mediated shifting of cellular immunophenotypes, which we observed in our previous study (Totonchy J, 2018 ), We first compared the overall lymphocyte populations between baseline (day 0 uninfected), Mock, and KSHV infected conditions to determine whether our infection and culture system and/or KSHV infection itself was causing significant shifts in the B lymphocyte composition of

the samples. These results demonstrate that most lineages were not substantially altered by our culture system or KSHV infection compared to the baseline samples (**Fig 2.2B, Appendix A.2, Appendix A.3**). However, naïve B cells were significantly reduced compared to baseline levels in both Mock and KSHV infected samples at 3 dpi, suggesting that the infection method may reduce naïve cell survival in this mixed model or that the culture model drives differentiation of naïve cells into a different immunophenotype. Interestingly, B cells with a transitional phenotype are significantly increased compared to baseline in both Mock and KSHV-infected cultures. Given that there is a relationship between transitional (IgD<sup>+</sup>, CD38<sup>mid</sup>) and naïve (IgD<sup>+</sup>, CD38<sup>low</sup>, CD27<sup>-</sup>) it is possible that naïve B cells are acquiring increased CD38 expression as a result of the infection and culture process and are thus falling into the transitional lineage gate at 3 dpi. Finally, this analysis shows that our culture system does not favor the survival of CD138<sup>+</sup> plasma cells indicated by a significant decrease comparing baseline and Mock at 3dpi. However, this effect was lower in the KSHV-infected cultures. This result suggests that KSHV infection is either providing a survival advantage for CD138<sup>+</sup> cells in the culture system or driving the differentiation of new CD138<sup>+</sup> cells during infection.

Overall, susceptibility of B cells to KSHV infection varied substantially within the cohort with the majority of samples showing between 1 and 2% GFP<sup>+</sup> B cells at 3

dpi and an overall range of 0.76-3.27% (**Fig 2.2C, Appendix A.2**). Analysis by point-biserial correlation revealed that susceptibility was not significantly correlated with sex ( $r_{pb}=0.17$ ). Kruskal-Wallis rank sum test showed no significant association of race and susceptibility ( $p=0.6$ ) and both Pearson ( $r=0.09$ ) and Spearman ( $r=0.01$ ) correlation tests indicated no linear or monotonic relationship between donor age and susceptibility in our data set. Thus, we can conclude that donor demographics do not substantially contribute to the variable susceptibility we observe in our tonsil lymphocyte samples.

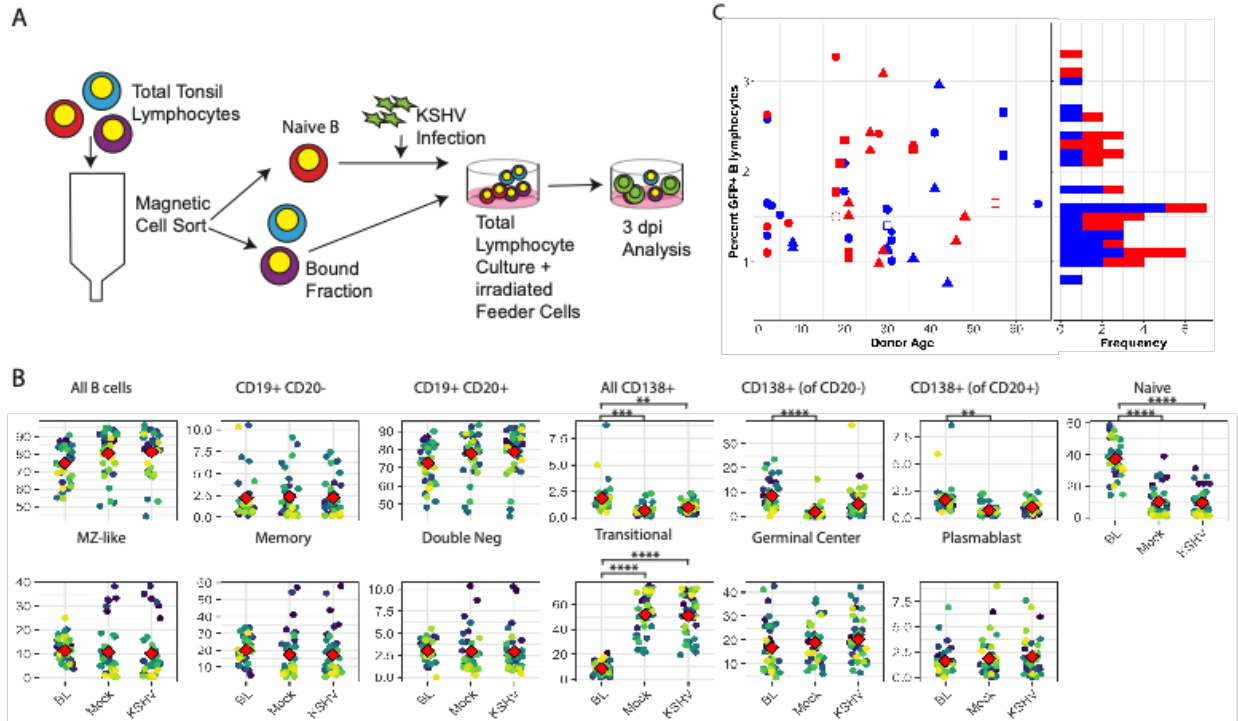


**Figure 2. 2 Tonsil-derived B lymphocytes from diverse donors display variable susceptibility to KSHV infection.** (A) Schematic of lymphocyte infection procedure.

Untouched naïve B cells are magnetically separated from total lymphocytes and 1e6 naïve B cells are infected per condition. Following infection, bound fractions are added back to reconstitute a total lymphocyte environment and cells are plated on X-ray irradiated CDw32 feeder cells.

Analysis is performed by flow cytometry at 3 days post-infection for B cell lineage markers as shown in S1 Fig and Table 2 and GFP reporter expression for KSHV infection. (B) The effect of KSHV infection and the culture system on overall B cell lineage frequency was examined by comparing the frequency of B cell lineages at baseline (BL, unmanipulated samples) and 3 days post infection in Mock infected and KSHV infected cultures. Student's T test was used to determine statistical significance for all comparisons \*\* $p < 0.004$ , \*\*\* $p < 0.0002$ , \*\*\*\* $p < 1e-6$  (C)

Infection frequency data for viable, CD19+GFP+ lymphocytes at 3 dpi  $n = 50$  from 40 tonsil specimens with biological replicates for 10 specimens displayed with respect to donor age (x-axis, left panel), sex (color), and self-reported race (shape, left panel). The histogram in the right panel is included to show the distribution of infection frequencies with the majority of infections resulting in 1–2% GFP+ B lymphocytes at 3 dpi.

### 2.3.3 Specific targeting of individual B cell lineages by KSHV infection

We next sought to establish the B lymphocyte tropism of KSHV in human tonsil lymphocytes by determining which B cell lineages are targeted for KSHV infection at early timepoints. Because levels of individual B cell lineages are highly variable between samples (**Fig 2.1B**), we have generally represented lineage-specific susceptibility data as the percentage of GFP<sup>+</sup> cells within each lineage so that data could be directly compared cross-sectionally within the sample cohort. Our analysis of specific B cell lineages targeted for infection by KSHV revealed that, although they represent a small proportion of the B cells within human tonsils (**Fig 2.1B**), CD138<sup>+</sup> plasma cells are infected at high frequencies at this early timepoint. Indeed, CD19<sup>+</sup> CD20<sup>-</sup> plasma cells displayed the highest within-lineage susceptibility of any cell type with several replicates showing 100% infection of this lineage at 3 dpi (**Fig 2.3A**). Other B cell lineages were susceptible to infection but were infected at relatively low within-population frequencies compared to plasma cells (**Fig 2.3A&B, Appendix A.2**). Most B cell lineages showed linear correlation between within-lineage infection and overall infection, while others like Plasmablast, double negative, and CD20<sup>-</sup> plasma cells showed no significant correlation between within-subset infection frequency and overall infection (**Fig 2.3B**).

The observation that plasma cells are highly targeted for infection is interesting given that we observed a decrease in overall plasma cell numbers in our cultures system that was somewhat abrogated in the KSHV-infected conditions (**Fig 2.2B**). Thus, we wanted to determine whether the apparent survival advantage for plasma cells in the KSHV-infected cultures was a direct result of infection. Interestingly, subset analysis for the plasma cells into total, CD20+ and CD20- plasma cells showed that the greatest survival effect (KSHV-Mock for the lineage) was within the CD20- population (**Fig 2.3C, left panel**), which was also the population with the highest level of infection among B lymphocytes (**Fig 2.3A**) When we plotted survival of each plasma cell sub-population against the percent of infection for that population, there was no significant correlation observed (**Fig 2.3C, right panels**). This data supports a conclusion of an indirect effect of KSHV infection on survival or differentiation of a different B cell lineage into CD138+ cells in our KSHV-infected tonsil lymphocyte cultures rather than KSHV conferring a survival advantage only to infected cells.

We next calculated within-subset frequency of infection for each lineage as a proportion of the total B lymphocytes (i.e. within-lineage % GFP x frequency of lineage within B lymphocytes) for each sample in order to determine the contribution of each lineage to the overall infection (**Fig 2.3D & E**). When shown on a per-sample basis, the data reveals high variability between donors with no

discernable contribution of the overall susceptibility (shown by the order of the samples on the x-axis) (**Fig 2.3D**). When shown on a per-lineage basis, the data reveals that germinal center, transitional and memory cells make the largest contributions to overall infection, plasma cells and MZ-like cells are intermediate contributors and double negative, naïve and plasmablast lineages make up a minor proportion of the infected cells (**Fig 2.3E**).

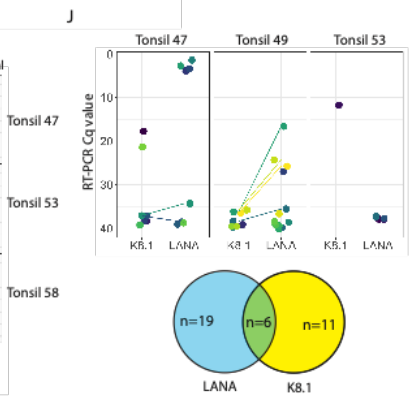
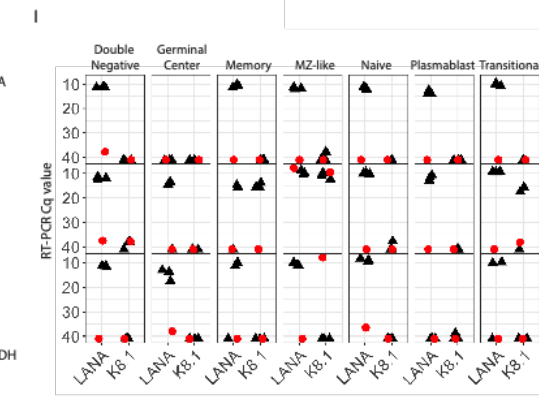
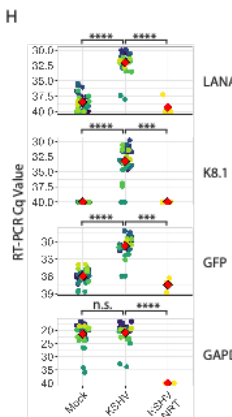
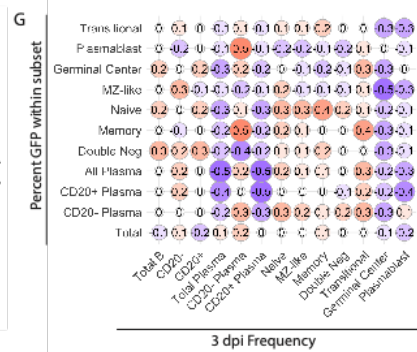
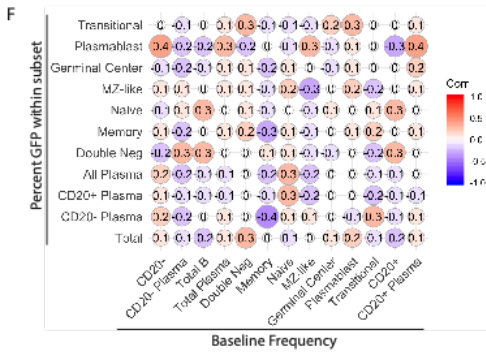
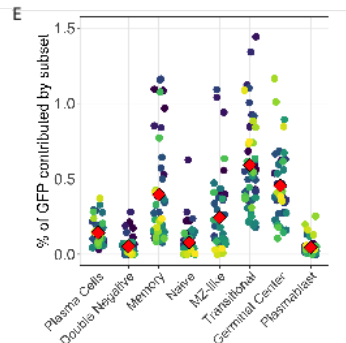
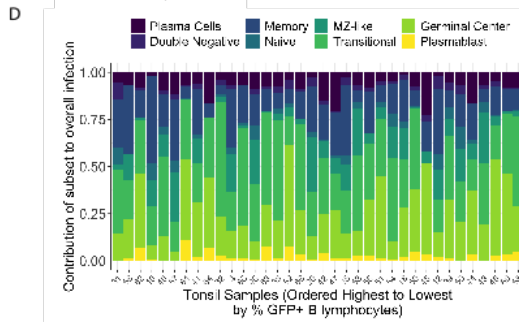
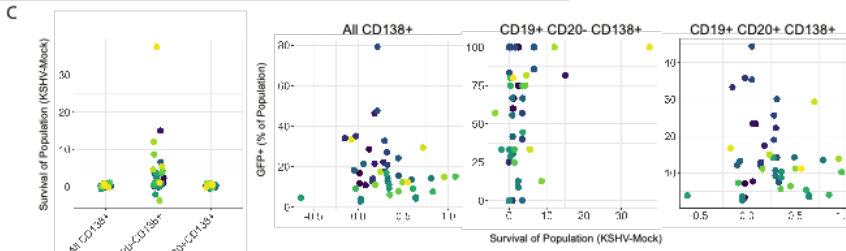
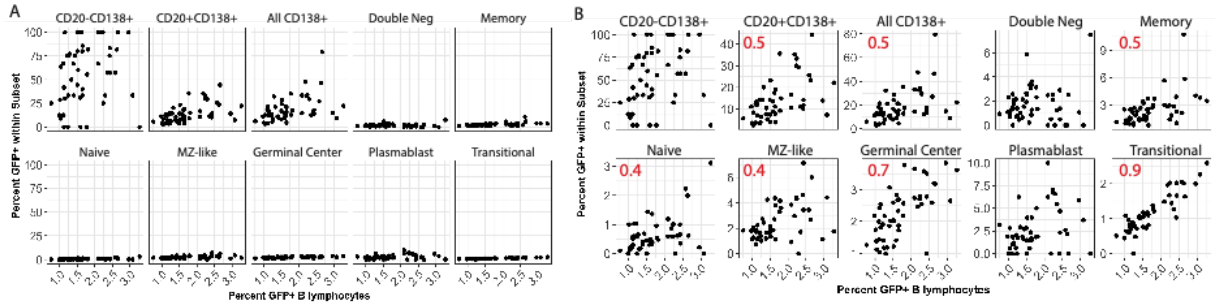


**Figure 2. 3 B lymphocyte lineage tropism of KSHV.** Naïve B lymphocytes from 40 individual human tonsil specimens (n = 50) were infected with KSHV.219 as in Fig 2A. Cells were collected at 3dpi, stained for B cell lineages as shown in S1A Fig and Table 2 and analyzed flow cytometry for B cell lineages and KSHV infection based on GFP reporter expression. The within-lineage infection frequency (y-axis) as a function of overall B cell infection frequency (x-axis) at 3dpi in for n = 50 infections from 40 individual tonsil specimens shown (A) normalized to 100% or (B) scaled to each individual lineage population. Pearson correlation coefficients (r) with an absolute value greater than or equal to 0.4 are shown in (B) as red inset text in the subset panels. (C) The survival of plasma cell lineages (frequency of viable B lymphocytes in KSHV-Mock samples at 3 dpi) was plotted for all CD138+, CD20-CD138+ and CD20+CD138+ lineages (left panel) and each lineage's frequency of KSHV infection was plotted against its survival (right three panels) with individual tonsil samples designated by color. Statistical analysis was performed for both linear (Pearson) and monotonic (Spearman) correlations. For all plasma cells  $r = 0.15$ ,  $\rho = 0.2$ ; for CD20- plasma cells  $r = 0.3$ ,  $\rho = 0.32$ , for CD20+ plasma cells  $r = 0.15$ ,  $\rho = 0.13$ . The contribution of specific B cell lineages to overall infection in each sample was calculated as % GFP within lineage \* % of lineage within viable B cells in each sample, and results are shown in (D) for each tonsil sample ordered from highest to lowest (right to left) based on overall GFP+ B lymphocytes (overall susceptibility) and (E) by lineage with individual samples designated by color and the mean infection frequency of each lineage shown as a red diamond. Correlation matrix analysis showing linear relationships (Pearson's correlation coefficient) between within-lineage infection frequency and (F) baseline (pre-infection) overall frequency or (G) 3 dpi overall frequency in KSHV-infected cultures for B lymphocytes and their subsets. Statistical power analysis indicates that this dataset can predict correlations at the level of  $r > |0.4|$  with alpha = 0.05 and power = 0.8. Thus, r values  $\geq 0.4$  can be considered a statistically significant correlation for this data. (H) KSHV transcripts LANA and K8.1 as well as GFP and GAPDH transcripts analyzed for n = 20 tonsil specimens by RT-PCR in bulk lymphocyte cultures at 3 dpi. Left panels show Ct values with individual Naïve B lymphocytes from 40 individual human tonsil specimens (n = 50) were infected with KSHV.219 as in Fig 2A. Cells were collected at 3dpi, stained for B cell lineages as shown in S1A Fig and Table 2 and analyzed flow cytometry for B cell lineages and KSHV infection based on GFP reporter expression. The within-lineage infection frequency (y-axis) as a function of overall B cell infection frequency (x-axis) at 3dpi in for n = 50 infections from 40 individual tonsil specimens shown (A) normalized to 100% or (B) scaled to each individual lineage population. Pearson correlation coefficients (r) with an absolute value greater than or equal to 0.4 are shown in (B) as red inset text in the subset panels. (C) The survival of plasma cell lineages (frequency of viable B lymphocytes in KSHV-Mock samples at 3 dpi) was plotted for all CD138+, CD20-CD138+ and CD20+CD138+ lineages (left panel) and each lineage's frequency of KSHV infection was plotted against its survival (right three panels) with individual tonsil samples designated by color.

Statistical analysis was performed for both linear (Pearson) and monotonic (Spearman) correlations. For all plasma cells  $r = 0.15$ ,  $\rho = 0.2$ ; for CD20- plasma cells  $r = 0.3$ ,  $\rho = 0.32$ , for CD20+ plasma cells  $r = 0.15$ ,  $\rho = 0.13$ . The contribution of specific B cell lineages to overall infection in each sample was calculated as % GFP within lineage \* % of lineage within viable B cells in each sample, and results are shown in (D) for each tonsil sample ordered from highest to lowest (right to left) based on overall GFP+ B lymphocytes (overall susceptibility) and (E) by lineage with individual samples designated by color and the mean infection frequency of each lineage shown as a red diamond. Correlation matrix analysis showing linear relationships (Pearson's correlation coefficient) between within-lineage infection frequency and (F) baseline (pre-infection) overall frequency or (G) 3 dpi overall frequency in KSHV-infected cultures for B lymphocytes and their subsets. Statistical power analysis indicates that this dataset can predict correlations at the level of  $r > |0.4|$  with  $\alpha = 0.05$  and power = 0.8. Thus,  $r$  values  $\geq 0.4$  can be considered a statistically significant correlation for this data. (H) KSHV transcripts LANA and K8.1 as well as GFP and GAPDH transcripts analyzed for  $n = 20$  tonsil specimens by RT-PCR in bulk lymphocyte cultures at 3 dpi. Left panels show Ct values with individual samples designated by color and the mean Ct values for each condition shown as a red diamond. Student's T-test was used to determine statistical significance for all comparisons \*\*\* $p < 1e-7$ , \*\*\*\* $p < 2e-10$ . (I) At 3 dpi, 10 million KSHV-infected lymphocytes from three tonsil specimens were stained for B lymphocyte surface markers and lineages were sorted into Trizol LS. RNA was extracted, reverse transcribed (black triangles) or amplified without reverse transcriptase (NRT, red circles) and analyzed by nested RT-PCR for viral transcripts in sorted B lymphocyte lineages. (J) At 3 days post-infection, 1 million KSHV-infected B cells from three tonsil specimens were stained for viability, CD19 and CD138. 187 single cells that were viable, CD19+, CD138+ were sorted into 96-well plates and analyzed by nested RT-PCR for viral transcripts. Colors indicate single plasma cells analyzed with RT-PCR (left) or control reactions including no reverse transcriptase (right) The bottom panel is a venn diagram quantitating the number of plasma cells in RT-PCR reactions which amplified for each and both viral transcripts.

Next, we wanted to determine whether the targeting of individual B cell lineages by KSHV infection is merely a function of the frequency of that lineage within the sample or dictated by the virus biology. Pairwise correlations between KSHV infection of specific lineages and the baseline (pre-infection) frequency of that lineage within the sample revealed no significant effect of the baseline frequency of any B cell lineage on the susceptibility of that lineage to KSHV infection, (Fig 3F). Interestingly, there were some significant correlations between baseline frequencies of specific lineages and infection of other lineages. Infection of plasmablasts was positively correlated with the baseline number of both CD20 negative B cells in the culture and the number of CD20+ plasma cells, and infection of CD20+ plasma cells was negatively correlated with the baseline frequency of memory B cells in the sample. Similarly, given that some populations shift in their frequency during the infection time course (**Fig 2.2B**), we wanted to determine whether KSHV infection of specific lineages was a result of the frequency of that population within the sample at 3 dpi. Pairwise correlations between KSHV infection of specific lineages and the frequency of that lineage at 3 dpi similarly revealed no direct correlations between lineage frequencies and infection frequencies (**Fig 2.3G**). These comparisons revealed more strong relationships between lineage frequencies and infection frequencies. Infection of

CD138<sup>+</sup> plasma cells and CD20<sup>+</sup> plasma cells (which are the more numerous of the two-plasma cell sub-populations as shown in **Fig 2.1B**) was negatively correlated with the total population of plasma cells and the CD20<sup>+</sup> sub-population of plasma cells. This result may indicate that infection of CD20<sup>+</sup> plasma cells results in significant toxicity for that lineage. Moreover, infection of many B cell lineages was negatively correlated with germinal center B cells at 3 dpi with MZ-like B cell infection being significantly associated. This observation could indicate that lymphocyte cultures with a microenvironment that favors the survival of germinal center cells establish a different subset distribution of B lymphocyte infection. Finally, the 3dpi level of CD20<sup>-</sup> plasma cells were positively correlated with infection of both Plasmablast and memory B cell lineages. This data could indicate that these lineages are differentiating into plasma cells upon infection. Taken together these data indicate that the B lymphocyte tropism of KSHV is broad and highly variable from donor to donor. Plasma cells are highly targeted as a lineage, but transitional, memory and germinal center lineages make up the bulk of the viral load in tonsil specimens. The distribution of KSHV infection among lineages is not simply a function of lineage population frequency within the sample and is likely dictated by cell-intrinsic factors as well as complex immunological interplay within the sample that remains to be fully characterized.

### 2.3.4 Viral gene expression in KSHV infected B lymphocytes

Our observation that KSHV targets diverse B cell lineages for infection is based on expression of the GFP reporter in the KSHV.219 genome, which is controlled by a non-viral EF1-alpha promoter. We wanted to validate that the GFP signal we observe by flow cytometry represents *bona fide* infection and not simply virus entry. In order to do this, we first examined total RNA extracted from mock or KSHV-infected lymphocyte cultures at 3 dpi and analyzed these samples by RT-PCR for viral transcripts (LANA and K8.1) as well as GFP as a marker for virus entry and GAPDH as a housekeeping gene for the efficacy of RNA extraction (Fig 3H). The data show that viral transcripts and GFP are absent in Mock samples but present in KSHV-infected samples with an average  $-\Delta\text{Ct}$  of 6.1 cycles for LANA, 6.6 cycles for K8.1 and 4 cycles for GFP. NRT controls were consistently negative, confirming that viral DNA was not the source of genetic material for these results. Both LANA and K8.1 were detected in the majority of samples, suggesting a mix of lytic and latent infection programs in B lymphocytes. This data demonstrates *bona fide* infection, with the production of viral transcripts, is present in tonsil lymphocyte samples at 3 dpi.

Given that the bulk RT-PCR data showed mixed lytic and latent transcripts present in our tonsil lymphocyte cultures, we wanted to determine whether B lymphocyte lineages preferentially undergo a particular viral replication program. To

accomplish this, we performed large-scale lymphocyte infections, as above, for three unique tonsil specimens, stained for B cell lineage markers, and sorted individual lineages using our FACS Aria Fusion cell sorter. We were able to obtain between 10,000 and 200,000 cells for each lineage from the cell sorting. Total RNA was extracted from sorted samples and subjected to nested RT-PCR analysis for GAPDH, LANA and K8.1. These results show that LANA transcripts are present in all lineages for at least 2/3 tonsil samples analyzed. Transcription of the K8.1 late lytic gene was observed in memory cells and transitional cells for 1/3 tonsil samples along with LANA transcripts indicating that in this sample there was a mixture of lytic and latent cells within the lineage populations. NRT negative controls (red circles) for most lineages were negative or amplified >10 cycles later than the matched RT positive samples indicating that viral DNA was not the source of genetic material for these results. However, the MZ-like lineage had positive amplifications in NRT controls for 2/3 tonsil samples. This result may indicate that in some samples there is a high load of KSHV DNA present in this lineage so that even the extensive DNase digestion used in our protocol failed to remove it sufficiently (**Fig 2.3I**). Because plasma cells are a low abundance cell type in our tonsil samples, we were uncertain whether bulk sorting would result in sufficient cells to successfully extract RNA for RT-PCR analysis. Thus, in order to determine the viral transcription program in plasma cells we gated

viable/CD19+/CD138+ cells and sorted single cells directly into 96-well plates containing a hypotonic lysis buffer. We performed single cell nested RT-PCR analysis without RNA extraction for LANA, K8.1 and GAPDH on 187 plasma cells from three unique tonsil samples (**Fig 2.3J, left panel**). NRT controls were consistently negative confirming that viral DNA was not the source of genetic material for these results (**Fig 2.3J, right panel**). We observed 19 plasma cells expressing LANA transcripts only, 11 plasma cells expressing K8.1 only and 6 plasma cells expressing both viral transcripts (**Fig 2.3J, bottom**).

Our gene expression data validates the lineage-specific tropism observed in our flow cytometry data, showing that each lineage identified as susceptible by GFP expression also contains viral transcripts, indicating *bona fide* KSHV infection. Moreover, these results demonstrate that most B cell lineages express latent transcripts only, with few lineages including plasma cell, memory, transitional and possibly MZ-like lineages contributing to lytic replication. Given that transitional and memory cells represent a high proportion of the per-sample viral load in our analysis (**Fig 2.3D & E**) it is not surprising to find that they are competent for lytic replication. However, germinal center cells are uniformly latent in this data, but were a highly represented cell type in our analysis of lineage contributions to overall infection. This may indicate that germinal center B cells are another highly targeted cell type. Finally, differences in this data between tonsil samples indicates

that lytic replication in our system may be more dependent upon host factors than lineage-specific factors.

### 2.3.5 KSHV infection of B lymphocytes does not rely on heparin sulfate proteoglycans

Previous studies have shown that heparin sulfate proteoglycans (HSPG) of the syndecan family can serve as an attachment factor facilitating KSHV entry via interaction with the gH/gL glycoprotein complex (Hahn A, 2009). In order to test whether the high susceptibility of tonsil-derived plasma cells was due to increased attachment via CD138 (syndecan-1), we attempted to selectively neutralize KSHV entry by pre-treating cell-free virus particles with soluble recombinant CD138 (srCD138) protein prior to infection. We utilized recombinant CD138 for these experiments rather than a neutralizing antibody against CD138 because the biochemistry of the putative interaction between CD138 and gH has not been established. Thus, the soluble protein will contain all of the protein sequences that might be bound by gH while an antibody blocks only specific epitopes which may or may not be part of the interaction domain. Pre-treating KSHV virions with 12.5µg/ml of srCD138 showed a small decrease in overall KSHV infection of B lymphocytes in 6 of 7 tonsil samples tested (**Fig 2.4A**). However, the inhibition was not dose-dependent for any sample. B cell lineage analysis revealed decreased infection of plasma cell lineages in 3 of 7 samples, but again the effect was

inconsistent within the data set and was not dose-dependent for any sample. KSHV infection of other B cell lineages was similarly inconsistently affected by srCD138 treatment of virus particles (**Fig 2.4B**). Next, we used srCD138 pre-treated virions to infect human fibroblasts to determine whether srCD138 was able to neutralize gH on another cell type. In these experiments we observed a slight decrease in infection in 4 of 6 replicates (**Fig 2.4C**). Taken together, these results suggest that, although srCD138 treatment seems to weakly neutralize KSHV viral particles, the effect is not B cell specific. As a way of confirming these results with a cell-directed method as opposed to a virus neutralization approach, we used heparinase treatment to remove all HSPG prior to KSHV infection. Treatment of human fibroblasts with a heparinase I/III blend resulted in decreased cell surface heparin sulfate by flow cytometry analysis (**Fig 2.4D**) and, as demonstrated previously in human fibroblasts (Akula SM, 2001 ), consistently reduced KSHV infection of treated target cells compared to untreated controls (**Fig 2.4E**). Lymphocytes had lower steady-state HSPG levels compared to fibroblasts, which was further reduced by heparinase treatment (**Fig 2.4F**). Interestingly, heparinase treatment of lymphocytes did not result in a reproducible decrease in KSHV infection (**Fig 2.4G**). We next wanted to determine whether there was any effect of heparinase treatment on KSHV infection of particular B cell lineages. Because the most reliable cell surface marker for plasma cells is the CD138 HSPG,

which would be removed by heparinase treatment, we first confirmed that plasma cells recovered CD138 expression before our 3 dpi analysis timepoint (**Fig 2.4H**). Subset analysis revealed no significant differences in KSHV infection between control and heparinase treated populations for any B lymphocyte lineage (**Fig 2.4I**). Taken together these data do not support the conclusion that plasma cell expressed CD138 is used as an attachment factor for KSHV entry and, indeed, indicates that HSPG are not a significant factor in KSHV attachment to B primary lymphocytes.

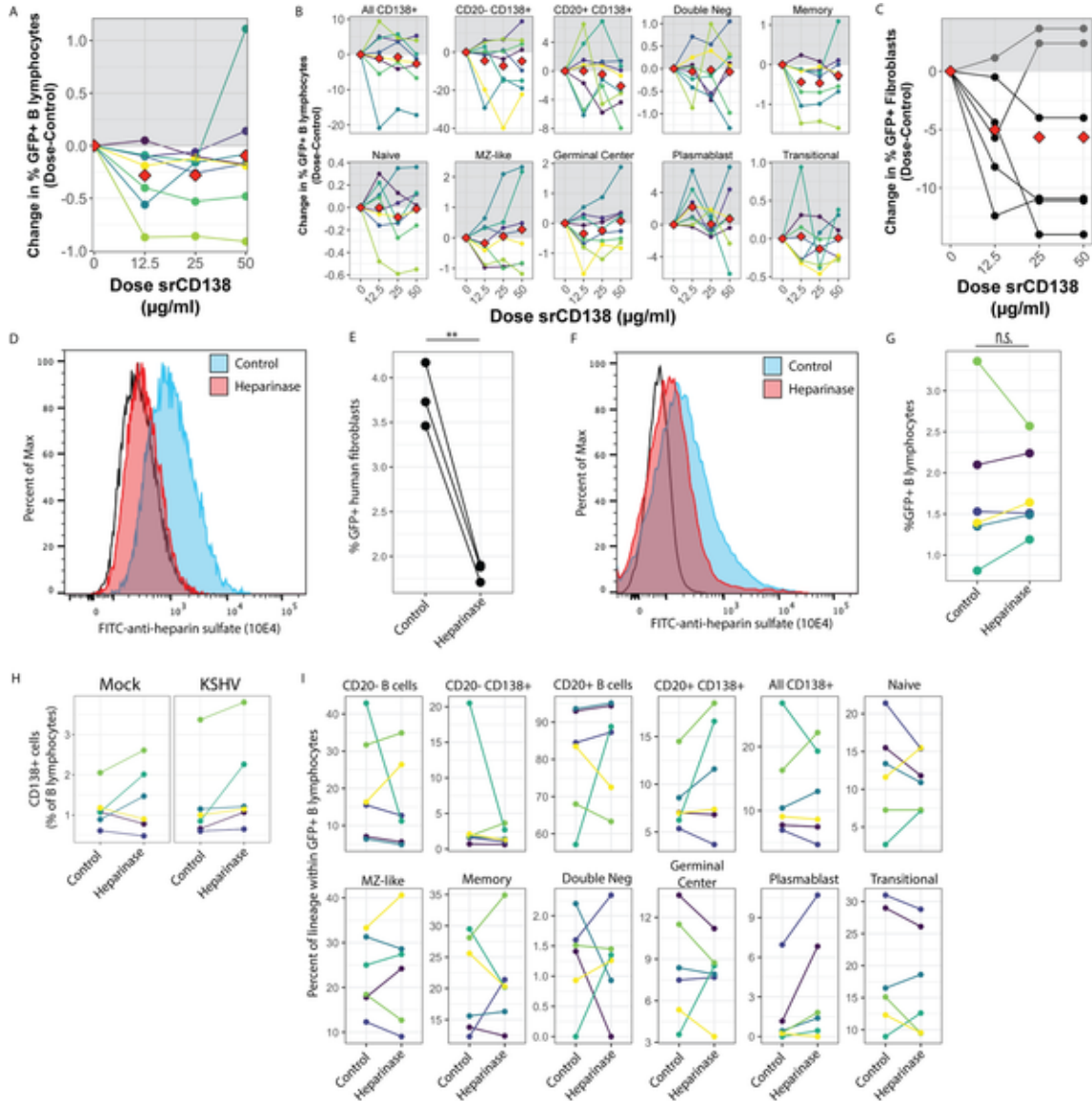


**Figure 2.4 CD138 and heparin sulfate proteoglycans as attachment factors for KSHV in B**

**lymphocytes.** Purified KSHV virions were pre-treated with srCD138 protein at indicated concentrations (x-axis) and used for infection of B lymphocytes. Cells were collected at 3dpi, stained for B cell lineages as shown in S1A Fig and Table 2 and analyzed by flow cytometry for lineage frequencies and KSHV infection by GFP reporter expression. 8 experimental replicates of 5 unique tonsil specimens are shown where the average infection rate was  $1.8 \pm 0.5\%$  in untreated controls. Data is represented as change in GFP+ cells at each dose of srCD138 compared to untreated control. Colors denote individual experimental replicates and red diamonds are the mean change at each dose for all replicates. (B) Data as in (A) for within-subset GFP quantitation. (C) Similar experiments were performed in E6/E7 transformed fibroblasts derived from human tonsils. 6 experimental replicates are

shown where the average infection rate was  $25.5 \pm 16\%$  in untreated controls. Data is represented as change in GFP+ cells as in (A). (D) 1 million E6/E7 transformed human tonsil fibroblasts were treated with 4.5 units of heparinase I/III blend for 24 hours and removal of heparin sulfate proteoglycans was verified by flow cytometry using a heparin sulfate-FITC antibody. Black line indicates no antibody control. (E) Control (untreated) or heparinase-treated fibroblasts were infected with KSHV.219 and analyzed for infection by GFP reporter expression at 3 dpi. Student's T-test was used to compare control and heparinase-treated cultures for  $n = 3$  experimental replicates  $p = 0.007$ . (F) 25 million human tonsil lymphocytes were treated with 9U of heparinase I/III blend and plated on X-ray irradiated CDW32 feeder cells for 24 hours. After incubation removal of heparin sulfate proteoglycans was verified by flow cytometry as in (D). (G) After heparinase treatment lymphocytes were fractionated and infected as shown in Fig 2A and viable, GFP+ B lymphocytes were quantitated by flow cytometry at 3 days post-infection. 6 experimental replicates with 6 tonsil specimens were performed and colors designate unique samples and can be compared between this panel, panel H and panel I. Student's t-test was performed to compare infection of control and heparinase treated lymphocytes  $p = 0.969$ . (H) the recovery of cell surface CD138 HSPG after 3 days of culture was examined by comparing CD138+ cells as a percent of viable B cells in control and heparinase treated samples for both mock and KSHV-infected conditions. Colors indicate unique tonsil specimens. Student's T-test was performed to compare control vs. heparinase conditions for mock  $p = 0.57$ , for KSHV  $p = 0.52$  (I) Data for KSHV-infected cultures at 3dpi with or without heparinase pre-treatment as in (G) showing the level of KSHV infection for specific B cell lineages. Student's T-test indicates no significant difference comparing control and heparinase treated samples for any lineage.

### 2.3.6 Immune status alters KSHV infection of B lymphocytes

KSHV lymphoproliferative disorders occur primarily in the context of immunosuppression, and other studies have shown interactions between T cells and KSHV infected B cells in tonsil lymphocyte cultures affecting the frequency of lytic reactivation (Myoung J, 2011 ). Therefore, we wanted to determine whether the immunological composition of the tonsil lymphocyte environment would affect the establishment of KSHV infection in B lymphocytes and specifically whether overall susceptibility or targeting of particular B cell lineages is influenced by the presence or absence of T cells. Like B cell lineages, levels of CD4<sup>+</sup> and CD8<sup>+</sup> T cell lineages vary considerably between tonsil donors (Fig 1D). However, unlike B lymphocyte subsets, the distribution of T cell subsets are not generally correlated with donor age (**Fig 2.1E**). Examination of whether the ratio of CD4/CD8 T cells in individual tonsil specimens was correlated with the susceptibility of B lymphocytes to KSHV infection revealed no significant correlation (**Fig 2.5A**). Next, we examined correlations between B cell infections and baseline levels of various CD4 and CD8<sup>+</sup> T cell subsets to determine whether any T cell lineages affected the tropism of KSHV for particular B cell lineages (**Fig 2.5B**). Interestingly, levels of naïve and stem cell memory CD4<sup>+</sup> T cells was positively correlated with infection of plasma cells (**Fig 2.5B and Fig 2.5C, left panels**) with a greater effect on CD20<sup>+</sup> plasma cells than CD20<sup>-</sup> plasma cells, while overall

levels of CD45RO<sup>+</sup> activated memory T cells were negatively correlated with KSHV infection of plasma cells (**Fig 2.5C, right panel**). In addition, although the correlations were too weak to be significant in this data set, nearly every B cell lineage and overall KSHV infection was negatively correlated with the presence of CD4<sup>+</sup> T cells expressing a TEMRA phenotype (**Fig 2.5B**). Baseline levels of CD8<sup>+</sup> T cells had less effect on KSHV infection with only one significant positive correlation observed in our dataset between CD8<sup>+</sup> terminal effector cells and KSHV infection of naïve B cells (**Fig 2.5B**).

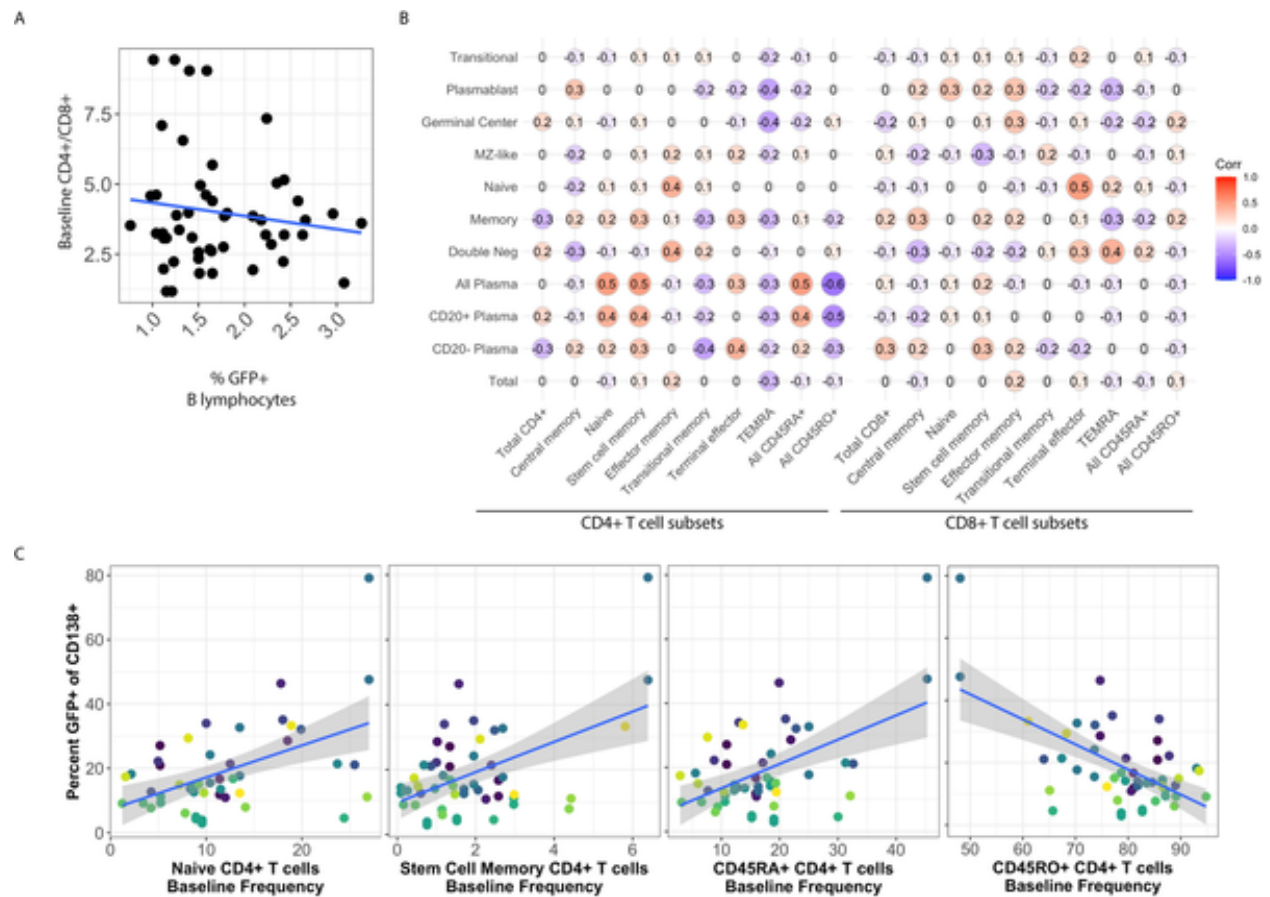


**Figure 2. 5 The donor specific CD4+ T cell microenvironment influences infection of CD138+ plasma cells.** For each donor, baseline levels of CD4+ T cells/CD8+ T cells is plotted against the overall susceptibility of the specimen based on the percent of GFP+ B lymphocytes at 3 dpi. Blue line indicates least means linear regression. Correlation analysis reveals no significant linear or monotonic relationship between the variables. (B) Pairwise linear correlations (Pearson method) were performed for overall (Total) and lineage specific KSHV infection at 3 dpi (vertical axis) and baseline T cell subsets as defined in S1 Fig and Table 2. Power analysis reveals that the data set can predict significant correlations at the level of  $p > |0.4|$  with  $\alpha = 0.05$  and power = 0.8. (C) Scatter plots of significant correlations from (B) between the baseline frequency of CD4+ T cell subsets (x-axis) and KSHV infection of CD138+ plasma cells (y-axis). Blue lines indicate least means linear regression and grey shading is standard error. Colors indicate unique tonsil specimens and can be compared across panels within the figure.

To determine whether manipulating the T cell environment would affect KSHV infection in individual tonsil samples, we performed T cell depletion experiments. Based on the correlation data shown in Figure 5B, we hypothesized that depletion of CD4<sup>+</sup> T cells would have a greater effect on KSHV infection. We performed KSHV infections in which total lymphocytes, CD4-depleted total lymphocytes or CD8-depleted total lymphocytes were added back following infection of sorted naïve B cells. At 3dpi, we validated T cell depletions (**Fig 2.6A**) and analyzed KSHV infection of B lymphocytes. The effect of T cell depletion varied substantially from sample to sample and neither CD4 nor CD8 depletion significantly altered overall KSHV infection in tonsil-derived B cells when data from 11 tonsil samples were aggregated (**Fig 2.6 B**). However, due to the heterogeneous nature of our tonsil samples (**Fig 2.1B & D**), we hypothesized that the baseline T cell composition of each sample might influence the effect of T cell depletion on KSHV infection. Indeed, when the change in KSHV infection in depleted fractions is plotted against the baseline CD4/CD8 T cell ratio, we observe that KSHV infection increased when depletions were performed in samples with high baseline levels of CD4<sup>+</sup> T cells (**Fig 2.6 C**). We next analyzed the effect of T cell depletion on KSHV infection of specific B cell lineages (**Fig 2.6 D**). These data reveal that depletion of CD4<sup>+</sup> T cells increases infection of plasma cells as well as MZ-like and Transitional B cell lineages and that the effect is dependent

upon the baseline CD4/CD8 T cell ratio in the sample with CD4<sup>+</sup> T cell-rich samples showing the greatest effect. Interestingly, CD8 depletions altered infection of different lineages compared to CD4 depletions but showed a similar dependence on the baseline level of CD4<sup>+</sup> T cells. Power analysis indicates that only the effect on CD138<sup>+</sup> cells and MZ-like lineages in the CD4-depleted condition and plasmablast lineage in the CD8-depleted condition can be considered statistically significant based on the sample size. Taken together, these data support the conclusion that the T cell microenvironment influences the lineages targeted by KSHV infection in the B lymphocyte compartment.

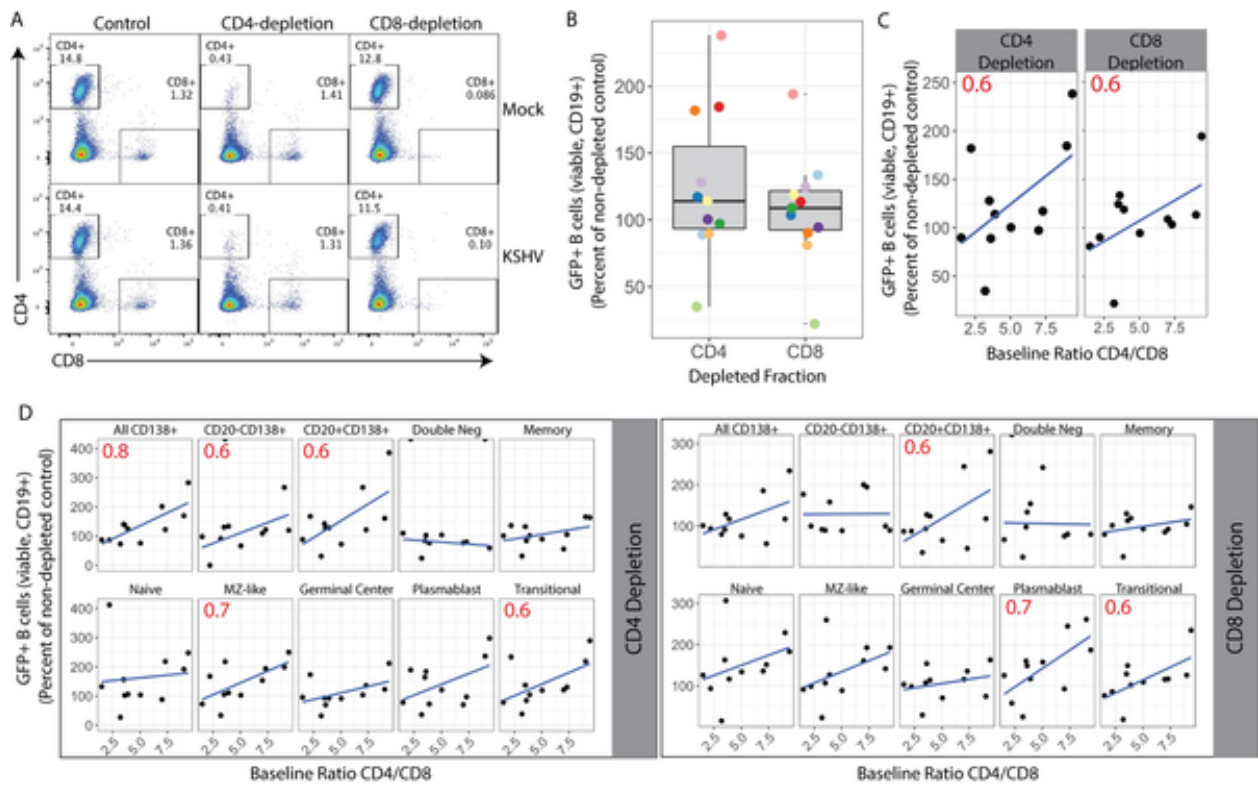


**Figure 2.6 Manipulation of T cell microenvironment alters KSHV tropism for B cell lineages.** Naïve B lymphocytes from 11 human tonsil specimens were infected with KSHV.219 as in Fig 2A, total lymphocytes added back following infection were either untreated or depleted of CD4+ or CD8+ T cells. At 3 days post-infection cells were collected. (A) T cell depletions were validated by flow cytometry and (B) Cells were stained for B cell lineages as shown in S1A Fig and Table 2 and analyzed flow cytometry for lineage frequencies and KSHV infection by GFP reporter expression to determine the change in GFP+ B lymphocytes (viable, CD19+) in CD4 or CD8 depleted samples compared to non-depleted controls. Colors indicate individual tonsil specimens (n = 11). Student's T test reveals no statistically significant change in GFP+ B cell frequency between either CD4-depleted or CD8-depleted and non-depleted controls. (C) infection data for T cell depletion studies as in (A) plotted against the baseline (pre-infection) CD4/CD8 T cell ratio in the sample. (D) within-lineage infection frequency plotted against baseline (pre-infection) CD4/CD8 T cell ratio. For B and C linear regression of the data is shown as a blue line and Pearson correlation coefficients (r) are shown as red text within panels only for r with an absolute value  $\geq 0.6$ . Statistical power analysis indicates that this

dataset can predict correlations at the level of  $r > |0.7|$  with  $\alpha = 0.05$  and power = 0.8. Thus,  $r$  values  $\geq 0.7$  can be considered a statistically significant correlation for this data.

## 2.4 Discussions

*Ex vivo* infection of tonsil lymphocytes is emerging as a viable strategy for studying early infection events for KSHV infection in B lymphocytes. However, the existing literature on KSHV infection of tonsil lymphocytes is highly varied in both approach and outcome. Hassman et. al. used cell free wild-type BCBL-1 derived KSHV virions to infect total CD19+ B lymphocytes from tonsil specimens and used staining for LANA as the only marker for infection, thus limiting their analysis to latently infected cells (Hassman LM, 2011 ). Bekerman et. al. also used isolated CD19+ B cells as infection targets but employed a co-culture infection procedure using iSLK cells infected with the recombinant KSHV.219 strain employing the GFP reporter as a marker for infection. Nicol et. al. also employed a co-culture method to infect tonsil lymphocytes with KSHV.219 but used Vero cells as producers and did not isolate CD19+ B cells prior to infection. In two studies, Myoung et. al. used cell free KSHV.219 produced from Vero cells to infect mixed lymphocyte cultures. With the exception of Bekerman et. al, all of the above-mentioned studies employed some kind of activating agent (PHA stimulation or CD40L stimulation) to manipulate the activation and/or proliferation of cells *in vitro*. For our studies, we used cell-free, iSLK-derived KSHV.219 to infect naïve B lymphocytes followed by reconstitution of the total lymphocyte environment. We also avoided activation of lymphocytes in both the isolation and culture procedures

using our previously characterized CDw32 feeder cell system (Totonchy J, 2018 ).To date, no consensus has yet emerged on how to perform tonsil lymphocyte infection studies with KSHV, and how differences in infection and culture procedure influences the resulting data remains to be established.

Although previous studies in mixed lymphocyte cultures have explored limited surface markers including immunoglobulins and activation markers (Hassman LM, 2011 ), (Nicol SM, 2016 ) and NK cell ligands (Bekerman E, 2013 ),these studies essentially treated all B cells as one population. Targeting of specific lineages including naïve, memory and CD138+ plasma cell-like B lymphocytes was explored by Knowlton et. al. using B cells derived from peripheral blood, but their detection method for infected cells was immunostaining for ORF59 protein and thus their enumeration of infection was biased towards cells undergoing lytic replication (Knowlton ER, 2014 ). Our current study is the first to use a comprehensive panel of lineage-defining cell surface markers to carefully explore the lineage-specificity of KSHV infection in B lymphocytes.

Although previous studies of KSHV infection in tonsil-derived B lymphocytes have shown the acquisition of plasmablast-like features at later timepoints post-infection (Hassman LM, 2011 ), (Kang S, 2017), the CD38 high plasmablast lineage is a minor proportion of our infected cultures at 3 dpi. Based upon these studies, we might expect to see the emergence of more plasmablast-like cells over time and it

will be interesting to determine whether this is a result of infected plasmablasts expanding or trans-differentiation from other lineages. Our observation that KSHV-infected B cells are primarily latent in our mixed tonsil lymphocyte cultures is consistent with previous observations that T lymphocytes control lytic reactivation of KSHV in tonsil-derived B cells (Myoung J, 2011 ).

For the gamma-herpesviruses EBV and MHV68, the current consensus is that naïve B cells are the primary infection target and infected cells transit the germinal center as a way of increasing viral load without resorting to lytic replication and lifelong latent infection is established in memory B cells while plasma cells are a source of lytic replication constantly replenishing the viral reservoir by producing virus which infects more naïve B cells (Johnson KE, 2020 ). Here, we show that multiple lineages from human tonsils, including terminally differentiated CD138+ plasma cells, can be targeted by KSHV for *de novo* infection. In our data, plasma cells are not primarily lytic as in EBV models, but instead are a mix of lytic and latent transcription programs with latency slightly predominating (**Fig. 2.3J**). This result is not surprising given that KSHV-associated lymphoproliferative diseases are characterized by primarily latent infection in cells with plasma-like features but PEL derived cell lines are competent for KSHV replication given the proper stimulus. In future studies, it will be interesting to examine what factors influence the lytic/latent balance for KSHV in primary plasma cells. Additionally, our data indicate that

memory cells are competent for lytic replication (**Fig 2.3I**), which is also different from the current model for EBV. However, the studies upon which the EBV models are based are primarily examination of cells from previously infected human hosts, representing EBV distribution in an established infection. We are unaware of any study of EBV infection in human tonsil that recapitulates the early infection timepoint and the level of detail in characterizing B cell lineages that is used here, thus it is difficult to place our data in the context of EBV infection. Given that recombinant EBV molecular genetics systems and ex vivo tonsil lymphocyte culture systems are now well established, perhaps a second look at the early-stage B lymphocyte tropism of EBV is warranted.

Our finding that KSHV efficiently targets CD138<sup>+</sup> plasma cells early in infection of tonsil B lymphocytes is particularly intriguing and relevant in the context of KSHV-mediated lymphoproliferative diseases, which often have a plasma cell or plasmablast-like phenotype (Chadburn A, 2008), (Carbone A V. E., 2014 ). Particularly for PEL, which uniformly presents as a clonal CD138<sup>+</sup> neoplasm, these results suggest that the pathological cells may not be derived from KSHV-driven differentiation from less mature lineages, but instead could be the result of modifications of differentiated plasma cells by direct infection. Recent studies have revealed that XBP-1, a critical cellular mediator of the unfolded protein response (UPR) which is essential for the differentiation of plasma cells (Iwakoshi NN,

2003), can activate expression of KSHV vIL-6 without inducing ORF45 or other lytic genes (Hu D, 2016 ). The fact that the UPR and XBP-1 are uniformly active in immunoglobulin-producing cells, like plasma cells, suggests that these cells may provide a unique niche for KSHV persistence where vIL-6 can be produced to support infected plasma cell survival in the absence of KSHV lytic replication. Future studies will examine whether vIL-6 is responsible for the survival advantage we observed for plasma cells in the KSHV-infected conditions in this study (**Fig 2.2B**).

Current models of human plasma cell maturation suggest that CD20 expression is lost on plasma cells as they mature and migrate from peripheral lymphoid organs (such as the tonsil) to the blood and finally the bone marrow (Medina F, 2002). Thus, CD138+CD20- plasma cells in tonsil that are highly targeted by KSHV in our analysis may represent a population of cells that is ready to leave the tonsil and migrate to the bone marrow. A few studies have shown KSHV infection in bone marrow from patients with MCD (Bacon CM, 2004 ), (Ibrahim HAH, 2016 ) and HIV positive patients without MCD (Meggetto F, 2001 ), and it would be interesting to pursue the idea that KSHV uses plasma cells to disseminate to the bone marrow early in infection. Certainly, our results highlight the virology of KSHV in primary plasma cells as an area urgently requiring further study.

In this study, we were unable to establish that targeting of plasma cells was due to enhanced virion binding via gH/gL interaction with the CD138 HSPG molecule, as was suggested by a previous study (Hahn A, 2009 ). However, we acknowledge that selectively blocking virion binding to a specific HSPG in a primary cell system is technically difficult, and we have no way to directly verify that our neutralization of gH/gL binding sites using soluble CD138 was effective. Our data using heparinase treatment to remove HSPG from B lymphocytes prior to infection supports the conclusion that CD138 is not used as an attachment factor for plasma cells, and indeed, HSPG are generally dispensable for infection of B cells in our system (**Fig. 2.4G-I**). These results are consistent with a previous study that shows low HSPG levels on the KSHV-susceptible MC116 lymphoma cell line (Dollery SJ, 2018) and another study showing that ectopic HS expression enhanced binding but was not sufficient to allow efficient KSHV infection of the BJAB lymphoma cell line (Jarousse N, 2011 ). Thus, the mechanisms underlying KSHV targeting of plasma cells and other B lymphocyte lineages for infection remains to be established. Additional studies in lymphoma cell lines have identified Ephrin receptors as critical factors in KSHV entry (Großkopf AK, 2019), (Muniraju M, 2019) Thus, our future studies in this area will and Ephrin family receptors in KSHV infection of tonsillar B lymphocyte lineages.

Our characterization of immunological diversity of a large cohort of human tonsil specimens will be of interest to the general immunology community. Although a few studies have examined T cell (Petra D, 2015) or B cell (Varon LS, 2017) subsets in tonsils associated with particular disease states. To our knowledge, only one other study has used multicolor flow cytometry to examine the immunological composition of both B cells and T cells in a large cohort of human tonsil samples (Stanisce L, 2018), and this study was focused on comparing the microenvironments present in matched tonsils and adenoids rather than comparison between donors based upon demographic data as we have done here.

In this study, we make the observation that manipulating the T cell composition has a more profound effect on KSHV infection in tonsil specimens that were CD4<sup>+</sup> T cell rich at baseline. Moreover, although the specific B cell lineages affected by depletion was different depending on whether CD4<sup>+</sup> or CD8<sup>+</sup> T cells were experimentally depleted, the greater effect in CD4<sup>+</sup> T cell rich samples was consistent. This data in combination with the viral transcript data shown in Figure 3H-J reveals that KSHV infection of B cells and the lytic/latent balance is sensitive to the host-specific overall immunological microenvironment and highlight that there is complexity to this relationship that cannot be adequately understood in the context of the current study. It will be interesting in future studies to explore the

contribution of donor-specific and context-specific immunology to KSHV lytic reactivation in tonsillar B lymphocyte lineages.

3 CHAPTER III: An Update of the Virion Proteome of Kaposi Sarcoma-  
Associated Herpesvirus

Authors: Ramina Nabiee, Basir Syed, Jesus Ramirez Castano, Rukhsana Lalani  
and Jennifer E. Totonchy

Biomedical and Pharmaceutical Sciences Department, Chapman University School  
of Pharmacy, Irvine, CA 92618, USA;

## **Abstract**

The virion proteins of Kaposi sarcoma-associated herpesvirus (KSHV) were initially characterized in 2005 in two separate studies that combined the detection of 24 viral proteins and a few cellular components via LC-MS/MS or MALDI-TOF. Despite considerable advances in the sensitivity and specificity of mass spectrometry instrumentation in recent years, leading to significantly higher yields in detections, the KSHV virion proteome has not been revisited. In this study, we have re-examined the protein composition of purified KSHV virions via ultra-high resolution Qq time-of-flight mass spectrometry (UHR-QqTOF). Our results confirm the detection of all previously reported virion proteins, in addition to 17 other viral proteins, some of which have been characterized as virion-associated using other methods, and 10 novel proteins identified as virion-associated for the first time in this study. These results add KSHV ORF9, ORF23, ORF35, ORF48, ORF58, ORF72/vCyclin, K3, K9/vIRF1, K10/vIRF4, and K10.5/vIRF3 to the list of KSHV proteins that can be incorporated into virions. The addition of these proteins to the KSHV virion proteome provides novel and important insight into early events in KSHV infection mediated by virion-associated proteins. Data are available via ProteomeXchange with identifier PXD022626.

Keywords: KSHV virion proteome; viral proteomics; bottom-up shotgun proteomics; UHR-QqTOF

### **3.1 Introduction**

Kaposi's sarcoma herpes virus (KSHV) was first discovered about twenty-five years ago through the use of representational difference analysis by Chang et al. (Chang, et al., 1994) and about a year later, Moore et al. (Moore, et al., 1996) looked into similarities of this novel virus with other known gammaherpesviruses and were able to identify it as the most similar with herpesvirus saimiri (HVS) through gene alignment and amino acid sequencing alignments on Open Reading Frames (ORFs) suitable for phylogenetic analysis; however, they noted that the divergence between the viruses is ancient. They, furthermore, classified this virus as the first human gamma-2 herpesvirus. To this day, KSHV is the only viral agent of the rhadinoviral subfamily capable of infecting human B cells **1**. In the context of immunosuppression, KSHV infection causes Kaposi's sarcoma, an endothelial cell neoplasm, the B cell lymphoproliferative disorders primary effusion lymphoma (PEL) and multicentric Castleman's disease (MCD), as well as a recently discovered KSHV inflammatory cytokine syndrome disease (KICS) (Karass M. e., 2017).

As with all herpesviruses, KSHV undergoes either latent or lytic infection programs. New virions are produced during the lytic phase, and latency is used for

long-term maintenance of viral genomes as extra-chromosomal episomes (Speck & Ganem, 2010). Although different environmental and physiological signals, such as viral coinfections (Vieira, O’Hearn, Kimball, Chandran, & Corey, 2001), hypoxia (Davis, et al., 2001), oxidative stress (Ye, et al., 2011); cellular factors and cellular signaling (Yu, et al., 2007), such as histone deacetylases (Shin, Decotiis, Giron, Palmeri, & Lukac, 2013), and even dietary supplements (Dyson, Walker, Whitehouse, Cook, & Akula, 2012) can cause KSHV lytic reactivation, latency is thought to be the predominant mode of KSHV infection in human hosts. However, there is convincing evidence that lytic replication plays a significant role in KSHV-associated pathology (Grundhoff & Ganem, 2004 ). Despite the substantial body of work on KSHV, early infection events in disease-relevant cell types and the role of individual virion-associated tegument factors in the establishment of infection remain poorly studied (Naranatt, et al., 2004).

The tegument layer is a dense proteinaceous layer sandwiched between the nucleocapsid and the virion envelope that can critically affect the host’s cellular and viral biology immediately following viral entry (Roizman, et al., 1981 ). These proteins make up a large proportion of the virion’s overall protein composition, and they serve as prepackaged factors capable of influencing the host cell physiology immediately upon the fusion of the viral envelope with the host cell membrane. Early infection functions of tegument proteins include cell cycle modulation (De Oliveira,

Ballon, & Cesarman, 2010), transcriptional activation of viral genes (Sathish N, 2012 ), inhibition of host gene expression activation (Zhu, Sathish, & Yuan, 2010), translocation of the virion capsid to the nucleus (Bergson, et al., 2014 ), and evasion of the innate immune response. Thus, identification and functional analysis of the virion proteins of KSHV is a critical step in understanding the early stages of KSHV infection.

In 2005, two research groups independently characterized the virion proteins of KSHV derived from lytic induction of latently infected BCBL-1 PEL cells. These studies both utilized a bottom-up proteomics approach to characterize virion-associated proteins by extracting individual protein bands visible on SDS-PAGE gels of purified virions, using either MALDI-TOF (Bechtel, Winant, & Ganem, 2005) or LC, MS/MS (Zhu, 2005) to identify the individual proteins after tryptic digestion. These studies together identified 24 viral and a few cellular proteins as virion associated. Additional proteins have since been detected in KSHV virions via other methods (Dai, Gong, Wu, Sun, & Zhou, 2014 ), (Wu, et al., 2015), (Gong, et al., 2014), (Butnaru & Gaglia, 2019), (Dünn-Kittenplon, Kalt, Lellouche, & Sarid, 2019), (Sander, et al., 2007 ), (Majerciak, Yamanegi, & Zheng, 2006 ), (Chow, He, Snow, Rose-John, & Garcia, 2001 ); however, despite significant advances in proteomics methods and instrumentation in recent years, the KSHV virion proteome has not been revisited.

Advances in proteomics technology have given rise to de novo sequencing in shotgun proteomics (den Ridder, Daran-Lapujade, & Pabst, 2020 ), which combines high-resolution spectrum data from modern mass spectrometry instruments with automated de novo peptide sequencing algorithms. These technological advances, combined with enhancements in sample preparation, have revolutionized proteomics in the last ten years.

In this study, we have taken advantage of advanced instrumentation and analysis methods; to reanalyze the KSHV virion proteome using a bottom-up shotgun method (Yates, 1998 ), combined with de novo sequencing on highly purified KSHV virions produced from the iSLK the epithelial cell line as well as dual digestion with trypsin/lys-c and chymotrypsin. Our method's improved sensitivity has allowed us to validate all of the 24 previously reported virion-associated proteins and add seventeen other proteins to the KSHV virion proteome. Seven of our novel proteomic hits have been identified as virion-associated by non-proteomic methods, and we report ten proteins in our analysis that have never previously been identified as virion-associated.

## 3.2 Materials and methods

### 3.2.1. Purification of Cell-Free KSHV Virions

Latently infected iSLK producer cells stably infected with BAC16 recombinant KSHV WT were grown to 70–75% confluency in DMEM (Caisson Labs, Smithfield, UT, United States Catalog#: DML10—500 ML) supplemented with 10% cosmic calf serum (Sigma-Aldrich, St. Louis, MO, United States Catalog#: C8056—500 ML), 250  $\mu\text{g}/\text{mL}$  geneticin (Goldbio, St. Louis, MO, United States Catalog#: G-418-1), 1  $\mu\text{M}$  puromycin (Bio Basic, Markham, ON, Canada Catalog#: PJ593), and 1.2  $\text{mg}/\text{mL}$  hygromycin B (A.G. Scientific, San Diego, CA, United States Catalog#: H-1012-PBS). Then induced for 72 h with 3  $\text{mM}$  sodium butyrate (Sigma-Aldrich, St. Louis, MO, United States Catalog#: B5887-1G) and 2  $\mu\text{M}$  doxycycline (Tocris, Minneapolis, MN, United States Catalog#: 4090—50 mg). Culture supernatants were clarified by centrifugation at 500 g for 12 min and passed through a 0.45  $\mu\text{m}$  filter placed on ice. The virus was then pelleted out of clarified supernatants over a 50% Opti-prep (Iodixanol) (Ford, Graham, & Rickwood, 1994) cushion prepared in TNE buffer at pH 7.40 by ultracentrifugation at 41,000 g for 120 min using an SW28 rotor. Immediately after (adapting a previously reported purification method used for mass spectrometry of virions), the concentrated virus particles were centrifuged through a 10–50% Iodixanol density step gradient prepared in TNE buffer (Garrigues,

Rubinchikova, DiPersio, & Rose, 2008 ) at 45,000 g for 2 h. The virus band at the gradient junctions of 22–24% was collected and kept at –80 °C for further processing. Iodixanol fractions were also collected and the viral DNA was extracted from them using the Zymo Quick DNA/RNA Viral kit (Zymo Research, Irvine, CA, United States Catalog#: D7020). Endpoint RFU qPCR assay was then performed on DNA fractions using probes and primers against LANA (LANA forward (5'-AATGGGAGCCACCGGTAAAG-3'), LANA reverse (5'-CGCCCTTAACGAGAGGAAGT-3'), LANA probe (5' 6FAM-ACACAAATGCTGGCAGCCCG-BHQ13')) using TaqProbe 5x qPCR MasterMix-Multiplex (ABM MasterMix-5PM), 5% DMSO, primers at 900 nM and probes at 250 nM on BioRad(Hercules, CA, United States ) CFX qPCR machine in 40 cycles.

### 3.2.2. Trypsin and Detergent Treatment of Purified Virions

The purified virion sample was then divided into two fractions. One fraction was treated with 0.25% trypsin- 2.21 mM EDTA for 60 min at 37 °C, while shaking at 300 rpm, to cleave and strip external envelope proteins and non-viral proteins and debris from virion preparations followed by virion lysis. This fraction is herein referred to as VTT fraction. The second fraction was kept untreated and is herein referred to as VT fraction. Both fractions were then treated with Pierce protease inhibitor (Thermo Scientific, Waltham, MA, United States Catalog#: A32963).

Proteins were extracted and lipids removed using ReadyPrep 2D-Cleanup Kit (BioRad, Hercules, CA, United States Catalog#: 1632130). Protein concentration was then quantified using a Qubit 3.0 fluorometer (Invitrogen, Waltham, MA, United States). The sample concentration was adjusted to a minimum of 0.5 mg/mL and pH as adjusted to (pH 7.5). The purified proteome samples were reduced and alkylated, using ThermoFisher EasyPep™ Mini MS Sample Prep Kit (Thermo Fisher Scientific, Waltham, MA, United States Catalog#: A40006).

The samples were then either tryptic digested for 6–8 h at 37 °C in Tris-HCl buffer with final protease to a protein ratio of 1:100 w/w of Pierce Trypsin/Lys-C to protease mix (Thermo Scientific, Waltham, MA, United States Catalog#:1863467) or digested with Pierce Chymotrypsin Protease (TLCK-treated) (Thermo Fisher Scientific, Waltham, MA, United States Catalog#: 90056) with final protease to protein ratio of 1:100 w/w, for 12–14 h at 37 °C in 1 mM HCl, while shaking at 300 rpm. The digestion was stopped using the digestion stop reagent of the EasyPep™ Mini MS Sample Prep Kit, and the samples were further cleaned and filtered following the kit's protocol. The samples were then extracted in 0.1% formic acid in diH<sub>2</sub>O and kept at –80°C until analysis.

### 3.2.3. Mass Spectrometry Analysis

The samples were thawed on ice, and 50 uL of the peptide digest fraction was then injected onto a reverse-phase C18 Acclaim RSLC 120 column

(Thermo Scientific, Waltham, MA, United States Catalog#:074812) at 2.2  $\mu\text{m}$  and 120°C 2.1  $\times$  250 mm connected to an ultra-high performance liquid chromatography (UHPLC) coupled to an electrospray ionization source of an ion trap mass spectrometer (Bruker Impact II UHR-QqTOF LC/MS). The sample was separated within 75 min with 0.2 mL/minute flow rate. A gradient method started at 99% buffer A (0.1% Formic acid in water) and 1% buffer B (0.1% Formic acid in Acetonitrile) and held at 1% B for 5 min. The gradient was changed linearly to 55% B in 60 min, and then changed to 90% B in 10 min. Finally, it was held for 5 min to equilibrate back to 1% B initial condition. The column oven set at 37 °C.

QTOF parameters for electrospray capillary at 4.5 V dry gas was set to 8 L/min. Dry temperature was set to 200 °C. Nebulizer was set to 1.8 Bar. Target mass range was set from 300 to 1600 m/z. Collision cell energy was set to 8 e (De Oliveira, Ballon, & Cesarman, NF- $\kappa$ B signaling modulation by EBV and KSHV. , 2010 ) (De Oliveira, Ballon, & Cesarman, NF- $\kappa$ B signaling modulation by EBV and KSHV. , 2010) Transfer time was set to 90  $\mu\text{s}$ , and pre-pulse storage was set to 10  $\mu\text{s}$ . Spectra rate was set to 2 Hz with Auto MS/MS Spectra rate upper limit of 30 and lower limit of 4 and only the most intense precursor ions were selected for fragmentation and cycle time of 3 s. Dynamic exclusion duration was 0.3 min and exclude singly charged m/z. Precursor ions isolation was m/z dependent window of 2–5. The collision energy was adjusted, as a function of m/z value, between 23–65 eV, the

system was calibrated using 10 mM sodium formate solution, and the accepted range was set to 250–1600 m/z.

Utilizing PEAKS DB, PEAKS PTM, and SPIDER search tools from PEAKS Studio (software version 10), the mzxml files were analyzed against a sequence database with the HHV8 protein database's customized library pulled from Uniprot (Swiss-prot)

(<https://www.uniprot.org/uniprot/?query=reviewed:yes%20taxonomy:37296#>)

downloaded on 07/01/2020 containing 86 sequences. Trypsin (for trypsin digested samples) and chymotrypsin (for samples digested with chymotrypsin) were selected with a maximum of three missed cleavages permitted; the search parameters were set to fixed modification of Carbamidomethyl and variable modification of methionine oxidation. Additional criteria used in the search were peptide mass tolerance of  $\pm 20.0$  ppm, and fragment mass tolerance of  $\pm 0.05$  Da followed with the peptide score *p*-value of less than 0.00316. Using the Spider search feature, a special feature in PEAKS software, a single amino acid mutation and up to three additional modifications per peptide were automatically detected with PTM\_Ascore of 20 and mutation ion intensity of 5%. All of reported peptides (Appendix **B1.-B.6**(Tables S1–S6)) have a score ( $-10\lg P$ ) greater than 25 and corresponding to a statistically significant ( $p < 0.00316$ ) confident identification; moreover, from our positive matches, only proteins identified with more than at least 3 peptide

sequences with a mass tolerance of <0.05 Da were reported. An exception was made for the two previously reported ORF53 and ORF28, which are exceedingly small in size and contain a limited number of trypsin cleavage sites when using trypsin. However, using chymotrypsin, we were able to report more hits for both proteins. Additionally, we queried a common contaminants database to ensure the overall quality of the samples. The mass spectrometry proteomics data have been deposited to the ProteomeXchange Consortium via the PRIDE (Perez-Riverol, et al., 2019 ) partner repository with the dataset identifier PXD022626 and 10.6019/PXD022626 (Deutsch, et al., 2020), (Perez-Riverol, et al., 2016).

#### 3.2.4. Antibodies and Western Blotting

Purified virion proteome equivalent to 1:50 of the final yield was mixed 1:1 with 5× Laemmli buffer (0.5M Tris-HCl PH6.8, Glycerin, S.D.S., 0.25%Bromophenol blue, B-mercaptoethanol) boiled for 10 min at 95 °C and then run on Mini-Protean T.G.X. Stain Free 4–15% Bis-Tris PAGE gels (BioRad, Hercules, CA, United States, Catalog#:4561081), then transferred to chemiluminescence Polyvinylidene difluoride(PVDF) membranes (Amersham, Buckinghamshire, United British Kingdom, Catalog#:88585). The membranes were dry-blocked overnight and rehydrated with 2% dried milk in T.B.S. buffer and then incubated with diluted primary antibodies against ORF8 (gB) (Invitrogen, Waltham, MA, United States, Catalog#:PA5-19852) or B-actin (Cell Signaling technology, Danvers, MA,

United States, Catalog#8H10D10) as the housekeeping control for four h at room temperature or 4 °C overnight. Anti-rabbit or anti-mouse immunoglobulin G antibody conjugated to horseradish peroxidase (Invitrogen, Waltham, MA, United States) was used as the secondary antibody. The enhanced chemiluminescence system (BioRad, Hercules, CA, United States, Catalog#: 1705060S) was used to detect antibody–antigen complexes using the BioRad Universal Hood II gel imager.

For the iodixanol fractions each fraction was collected then mixed 1:1 with 5x Laemmli buffer (0.5M Tris-HCl PH6.8, Glycerin, S.D.S., 0.25% Bromophenol blue, B-mercaptoethanol) boiled for 10 min at 95 °C and then run on two similar Mini-Protean T.G.X. Stain Free 4–15% Bis-Tris PAGE gels (BioRad, Hercules, CA, United States, Catalog#:4561081), post run one of the gels were stained with Coomassie blue (0.05% Coomassie brilliant blue, 50% methanol, 10% acetic acid) for 1 h, and destained (50% methanol, 10% acetic acid) for 3 h. The second gel was then transferred to chemiluminescence PVDF membranes (Amersham, Buckinghamshire, United British Kingdom, Catalog#:88585). The membrane was dry-blocked overnight and rehydrated with 2% dried milk in T.B.S. buffer and then incubated with diluted primary antibody against ORF8 (gB) (Invitrogen, Waltham, MA, United States, Catalog#:PA5-19852) four hours at room temperature or 4 °C overnight. Anti-rabbit G antibody conjugated to horseradish peroxidase (Invitrogen, Waltham, MA, United States) was used as the secondary

antibody. The enhanced chemiluminescence system (BioRad, Hercules, CA, United States, Catalog#: 1705060S) was used to detect antibody–antigen complexes using C-DiGit Blot Scanner (Li Cor Biosciences, Lincoln, NE, United States).

### **3.3 Results**

#### **3.3.1. Purification of Cell Free KSHV Virions and Virion Protein Fractions**

One of the significant limitations of the original KSHV proteomics studies was the production of high-yield purified virions from BCBL1 cells sufficient to obtain a high protein concentration for analysis. In this study, we employed the more recent and highly productive iSLK producer cell line to produce KSHV virions from the recombinant BAC16 KSHV genome for our studies (Myoung & Ganem, 2011 ). iSLK cells were induced at confluency with doxycycline and sodium butyrate, and at 72 h post-induction, virions were purified from 2 L of filtered culture supernatants for further processing. Adopting a method previously reported for KSHV virion purification for mass spectrometry (Garrigues, Rubinchikova, DiPersio, & Rose, 2008 ), the supernatant was then ultracentrifuged over a 50% Iodixanol (Opti prep) (Ford, Graham, & Rickwood, 1994 ) cushion, the cell free virions in 50% iodixanol were collected and further purified by ultracentrifugation on a 10–50% Opti-Prep in TNE buffer density step gradient to ensure further cleanup of the sample. Virus was quantitated by real-time qPCR using LANA as a genomic target. A genome peak

was obtained at the 22–24% Opti-Prep interface (**Figure 3.1a**). Fractions were then used in Coomassie blue staining and Western blotting against the ORF8(gB) antibody to determine the purity and concentration of virions in these fractions (similar to methodology used in Bechtel et al. (Bechtel, Winant, & Ganem, 2005)), respectively, (**Figure 3.1b**), and only the fractions around 22–24% iodixanol were collected and labeled as V fraction and kept at –80 °C for further processing.

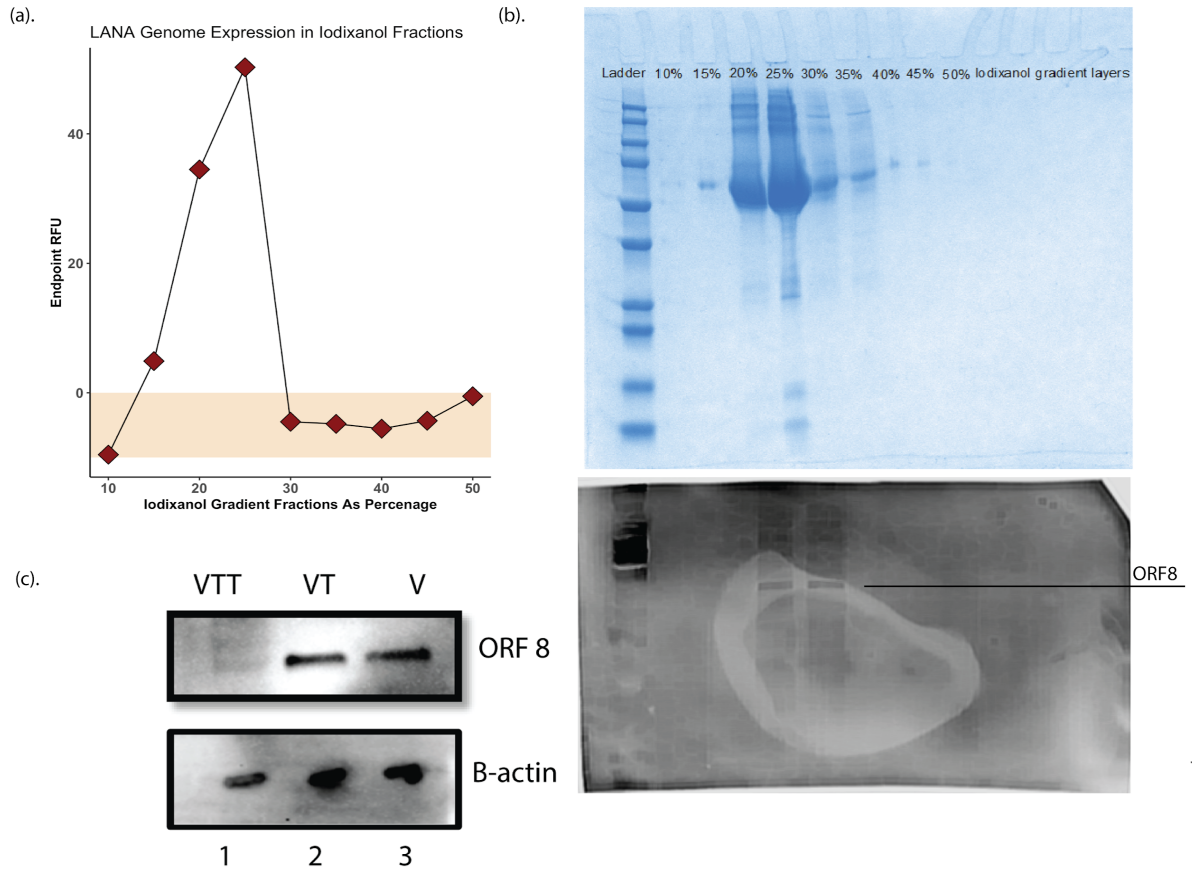


**Figure 3. 2 (a) Endpoint RFU qPCR using LANA genome on Iodixanol fractions. (b) Top Coomassie blue staining of the Iodixanol gradient fractions. (b) Bottom Western blot using gB/ORF8 antibody on different iodixanol gradient fractions to ensure the quality of the virion purification, based on the data, only fractions of 22–24% Iodixanol containing virions was used for further processing. This fraction was labeled as fraction V. (c) Western blot for gB/ORF8 on proteins from trypsin digested (VTT) and purified (VT) fractions as well as virions.**

The V fraction was then divided into two equal fractions, one where the proteins were extracted and then digested with either trypsin/LysC or chymotrypsin, referred to as VT fraction. The second was exposed to 0.25% trypsin- 2.21 mM EDTA for 60 min at 37 °C, while shaking at 300 rpm to strip the envelope layer and possible cellular debris before protein extraction and purification using labeled as the VTT fraction. The quality and purity of these fractions and the efficacy of external trypsin treatment was validated by Western blotting for ORF8/gB and B-actin (**Figure 3.1c**).

### 3.3.2. Mass Spectrometry Quality Control

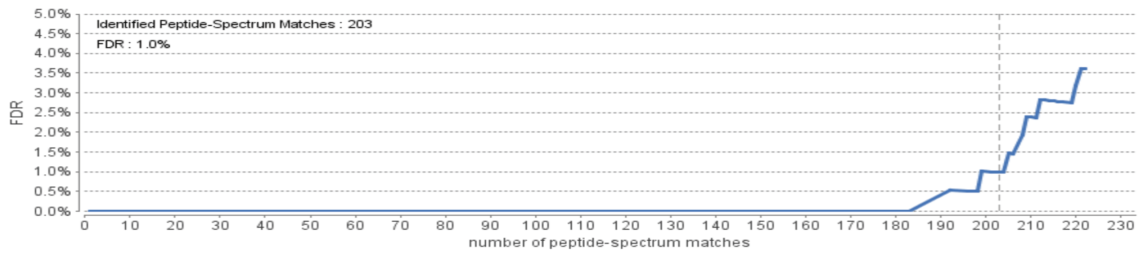
As the VT fraction contains both glycoproteins as well as envelope contained proteins, it was used for the initial mass spectrometry analysis of probing for previously reported virion proteins. PEAKS Studio software (Version 10) (Zhang, et al., 2012) was used for all of the data analysis presented herein. Using the database search approach, the raw datafiles were analyzed against a customized library of HHV8 protein database pulled from Uniprot (Swissprot)(<https://www.uniprot.org/uniprot/?query=reviewed:yes%20taxonomy:37296#>) downloaded on 07/01/2020 containing 86 sequences). Trypsin (for trypsin digested samples) and chymotrypsin (for samples digested with chymotrypsin) were selected with a maximum of three missed cleavages permitted; the search parameters were set to fixed modification of carbamidomethyl and

variable modification of methionine oxidation. Additional criteria used in the search were peptide mass tolerance of  $\pm 20.0$  ppm, and fragment mass tolerance of  $\pm 0.05$  Da followed with the peptide score  $p$ -value of less than 0.00316. Using the Spider search feature, a special feature in PEAKS software, a single amino acid mutation and up to three additional modifications per peptide were automatically detected with PTM, a score of above 20 and mutation ion intensity of 5%. All of the reported peptides (included in **Appendix B.1-B.6(Tables S1–S6)**) have a score ( $-10\log P$ ) greater than 25, corresponding to a statistically significant ( $p < 0.00316$ ) confident identification. Moreover, from our positive matches, only proteins identified with more than at least three peptide sequences with a peptide mass tolerance of  $< 20$  ppm detected in triplicate runs were reported. It should be noted that similar to Zhu et al. (Zhu, 2005), for the previously reported ORFs 28 and 53, due to the smaller size of the proteins, and limited trypsin cleavage sites, an exception was made where two and one peptide hits with trypsin were also accepted; however, using chymotrypsin, we detected three and two unique peptide hits, respectively.

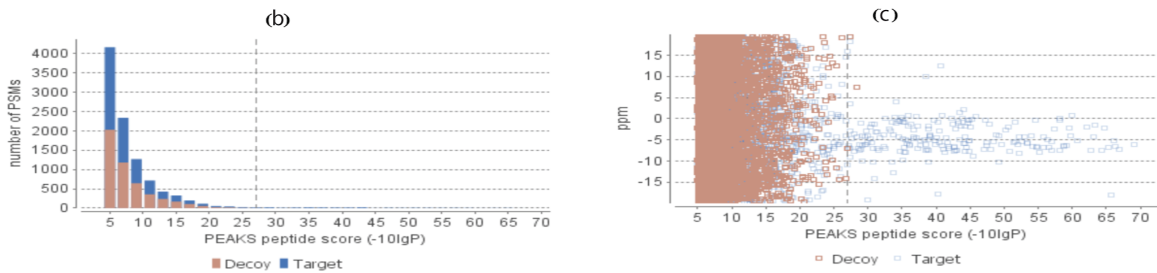
An example of the quality control statistics and our applied methodology is shown in **Figure 3.2**. At an false discovery rate (FDR) = 1.0% (**Figure 3.2a**), 203 peptide matches were accepted following the other criteria including the  $-\log p$ , which is set at 25 (**Figure 3.2b**) corresponding to the  $p$ -value of less than 0.01, demonstrating our sacrifice in reduction in the decoy hits in exchange for

increase in true peptide match score. This decrease of  $p$ -value indicating the ppm peptide error is demonstrated and the blue dots are the high-quality hits (**Figure 3.2c**). Although the PEAKS DB database search feature was mainly used for our analysis, the PEAKS de novo sequencing feature was also used and Table S8 shows a few examples of some of our sequences with the ALC% cut-off of 75%. Figure **2d, e** respectively show the distribution of our detected peptide features as well as the increasing trend in the accuracy of the de novo peptide match sequencing with a tight error tolerance.

(a). False discovery rate (FDR) curve. X axis is the number of peptide-spectrum matches (PSM) being kept. Y axis is the corresponding FDR.



(b). and (c). PSM score distribution. (b) Distribution of PEAKS peptide score; (C) Scatterplot of PEAKS peptide score versus precursor mass error.



(d). and (e). Distribution of identified peptide features. (d) Feature abundance distribution (e) *De novo* sequencing validation.

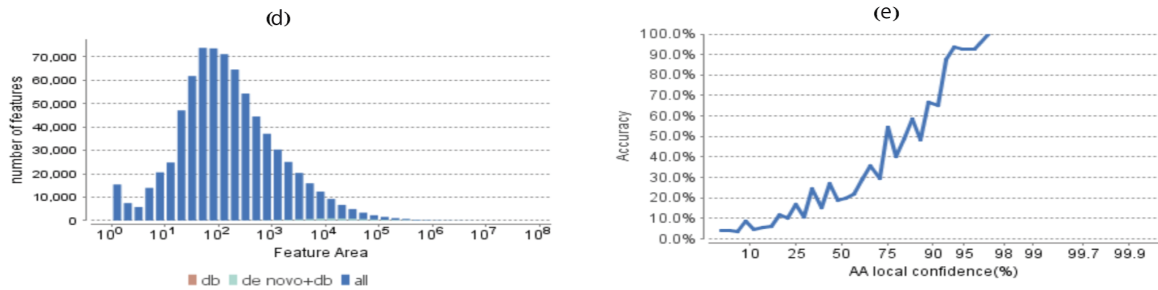


**Figure 3. 2** Statistical data presented from PEAKS analysis on the 17 proteins found uniquely in our study, with false discovery rate (FDR) set at 1%. (a) The false discovery rate (FDR) curve. The X-axis is the number of peptides-spectrum matches (PSM) being kept. The Y-axis is the corresponding FDR for the unique hits of our study.

(b) Peptide-spectrum matches (PSM) score distribution, showing the distribution of the PEAKS peptide score. (c) The precursor mass error in ppm vs.  $-10\lg P$  peptide score for all the PSMs. (d) Distribution of abundance of identified peptides. (e) The *de novo* sequencing validation and accuracy level (ALC).

### 3.3.3. KSHV Virion Protein Identification

Using the MS methodology mentioned above, we detected all 25 previously reported virion proteins that were identified by Bechtel et al. (Bechtel, Winant, & Ganem, 2005) and Zhu et al. (Zhu, 2005) (**Table 3.1 Appendix B.1-B.6 (and Tables S1 and S4)**). We detected ORFs 18, 32, 38, 42, 43, 56, and K2, which were not identified as virion-associated in the first proteomic studies but have since been identified as virion proteins by other methods 20–27 (**Table 3.2 and Appendix B.1-B.6 (Tables S2 and S5)**). Finally, we detected 10 KSHV proteins that have not been previously reported as virion associated. These novel virion proteins are ORFs 9, 23, 35, 48, 58, 72, K3, K9, K10, K10.5 (**Table 3.3 and Appendix B.1-B.6 (Tables S3 and S6)**). **Figure 3.3** shows an example of the protein coverage in our study (**Figure 3.3**) where a detected peptide sequence hit of ORF52 (DRPLTATEK) with  $-10\lg p$  of 44.48 with an  $m/z$  of 515.7792,  $z = 2$  using Collision-Induced Dissociation (CID) activation mode on qTOF detected Via PEAKS Studio software.

<b>Gene</b>	<b>Protein</b>	<b>aa Size</b>	<b>Previous Report by MS</b>	<b>Number of Unique Peptide Hits via Trypsin Digest</b>	<b>Number of Unique Peptide Hits via Chymotrypsin Digest</b>
<b>ORF6</b>	<b>Major DNA-binding protein (MBP)</b>	<b>1133</b>	<b>Zhu et al. 19</b>	<b>7</b>	<b>6</b>
<b>ORF7</b>	<b>Tripartite terminase subunit 1 (TRM1)</b>	<b>695</b>	<b>Zhu et al. 19</b>	<b>6</b>	<b>3</b>
<b>ORF8</b>	<b>Envelope glycoprotein B (gB)</b>	<b>845</b>	<b>Zhu et al. 19, Bechtel et al.18</b>	<b>10</b>	<b>20</b>
<b>ORF11</b>	<b>ORF11</b>	<b>407</b>	<b>Zhu et al. 19</b>	<b>9</b>	<b>5</b>
<b>ORF17</b>	<b>Capsid Scaffolding protein</b>	<b>534</b>	<b>Zhu et al. 19</b>	<b>3</b>	<b>3</b>
<b>ORF21</b>	<b>Thymidine kinase</b>	<b>580</b>	<b>Zhu et al. 19, Bechtel et al.18</b>	<b>8</b>	<b>3</b>
<b>ORF22</b>	<b>Envelope glycoprotein H (gH)</b>	<b>730</b>	<b>Zhu et al. 19,</b>	<b>7</b>	<b>5</b>

			<b>Bechtel et al. 18</b>		
<b>ORF24</b>	<b>ORF24</b>	<b>752</b>	<b>Bechtel et al. 18</b>	<b>4</b>	<b>7</b>
			<b>Zhu et al. 19, Bechtel et al.18</b>	<b>5</b>	<b>6</b>
<b>ORF25</b>	<b>Major capsid protein (MCP)</b>	<b>1376</b>			
			<b>Zhu et al. 19, Bechtel et al.18</b>	<b>5</b>	<b>6</b>
			<b>Zhu et al. 19, Bechtel et al.18</b>	<b>5</b>	<b>3</b>
<b>ORF26</b>	<b>Triplex capsid protein 2 (TRX-2)</b>	<b>305</b>			
			<b>Zhu et al. 19</b>	<b>6</b>	<b>4</b>
<b>ORF27</b>	<b>ORF27</b>	<b>290</b>	<b>Zhu et al. 19</b>	<b>6</b>	<b>4</b>
			<b>Zhu et al. 19</b>	<b>2</b>	<b>3</b>
<b>ORF28</b>	<b>ORF28</b>	<b>102</b>			
			<b>Zhu et al. 19, Bechtel et al. 18</b>	<b>7</b>	<b>7</b>
<b>ORF33</b>	<b>Cytoplasmic envelopment protein 2 (CEP-2)</b>	<b>334</b>			
			<b>Zhu et al. 19</b>	<b>6</b>	<b>3</b>
<b>ORF39</b>	<b>Envelope glycoprotein M (gM)</b>	<b>400</b>			
			<b>Zhu et al. 19</b>	<b>6</b>	<b>3</b>

<b>ORF45</b>	<b>ORF45</b>	<b>407</b>	<b>Zhu et al. 19</b>	<b>5</b>	<b>4</b>
<b>ORF47</b>	<b>Envelope glycoprotein L (gL)</b>	<b>528</b>	<b>Zhu et al. 19</b>	<b>5</b>	<b>3</b>
<b>ORF52</b>	<b>ORF52</b>	<b>131</b>	<b>Zhu et al. 19</b>	<b>9</b>	<b>5</b>
<b>ORF53</b>	<b>Envelope glycoprotein N (gN)</b>	<b>110</b>	<b>Zhu et al. 19</b>	<b>1</b>	<b>2</b>
<b>ORF62</b>	<b>Triplex capsid protein 1 (TRX-1)</b>	<b>331</b>	<b>Zhu et al. 19, Bechtel et al. 18</b>	<b>4</b>	<b>3</b>
<b>ORF63</b>	<b>Inner tegument protein</b>	<b>927</b>	<b>Zhu et al. 19, Bechtel et al. 18</b>	<b>7</b>	<b>5</b>
<b>ORF64</b>	<b>Large tegument protein deneddylase</b>	<b>2635</b>	<b>Zhu et al. 19</b>	<b>6</b>	<b>12</b>
<b>ORF65</b>	<b>Small capsomere- interacting protein (SCP)</b>	<b>170</b>	<b>Zhu et al. 19</b>	<b>4</b>	<b>3</b>
<b>ORF68</b>	<b>Packaging protein UL32 homolog</b>	<b>545</b>	<b>Zhu et al. 19</b>	<b>3</b>	<b>4</b>

<b>ORF75</b>	<b>ORF75</b>	<b>1296</b>	<b>Zhu et al. 19, Bechtel et al.18</b>	<b>8</b>	<b>6</b>
<b>ORF K8.1</b>	<b>gp35/37</b>	<b>228</b>	<b>Zhu et al. 19</b>	<b>4</b>	<b>4</b>

**Table 3.1. Proteins identified in the VT fraction in our study that were previously reported by mass spectrometry.**

Proteins identified in VT fraction of our study that were previously reported by mass spectrometry. All peptides have a score ( $-10\lg P$ ) greater than 25 and correspond to a statistical significance of  $p < 0.00316$ ; moreover, from our positive matches, only proteins identified with more than at least 3 peptide sequences with a mass tolerance of  $<0.05$  Da were reported.

<b>Gene</b>	<b>Protein</b>	<b>aa Size</b>	<b>Previous Report by MS</b>	<b>Unique Peptide Hits via Trypsin Digest</b>	<b>Unique Peptide Hits via Chymotrypsin Digest</b>
<b>ORF18</b>	<b>Protein UL79 homolog</b>	<b>257</b>	<b>Gong et al. 22</b>	<b>4</b>	<b>4</b>
<b>Capsid vertex</b>					
<b>ORF32</b>	<b>component 1 (CVC- 1)</b>	<b>454</b>	<b>Dai et al. 20</b>	<b>7</b>	<b>4</b>
<b>Cytoplasmic</b>					
<b>ORF38</b>	<b>envelopment protein 3 (CEP-3)</b>	<b>61</b>	<b>Wu et al.21</b>	<b>4</b>	<b>3</b>
<b>Cytoplasmic</b>					
<b>ORF42</b>	<b>envelopment protein 1 (CEP-1)</b>	<b>278</b>	<b>Butnaru et al. 23</b>	<b>3</b>	<b>3</b>
<b>Dünn-</b>					
<b>ORF43</b>	<b>Portal Protein</b>	<b>605</b>	<b>Kittenplon et al.24</b>	<b>6</b>	<b>5</b>
<b>ORF48</b>	<b>ORF48</b>	<b>402</b>	<b>Sander et al. 25</b>	<b>6</b>	<b>3</b>
<b>ORF56</b>	<b>DNA primase</b>	<b>843</b>	<b>Majerciak. 26</b>	<b>6</b>	<b>4</b>

<b>ORF</b>	<b>Viral Interleukin 6</b>	<b>204</b>	<b>Katano, H. et</b>	<b>12</b>	<b>7</b>
<b>K2</b>	<b>Homolog</b>		<b>al.37</b>		

---

**Table 3.2. Proteins identified by mass spectrometry in our study that were previously reported by other methods.**

Proteins identified in VTT fraction of our study that were previously reported by non-mass spectrometry methods. All peptides have a score ( $-10\lg P$ ) greater than 25 and correspond to a statistical significance of  $p < 0.00316$ ; moreover, from our positive matches, only proteins identified with more than at least 2 peptide sequences with a mass tolerance of  $<0.05$  Da were reported.

Gene	Protein	aa Size	Unique Peptide		Unique Peptide	
			Hits via Trypsin Digest	-10lgP (Trypsin)	Hits via Chymotrypsin Digest	-10lgP (Chymotrypsin)
ORF9	DPOL	1012	6	45.15	4	34.08
ORF23	ORF23	404	6	26.45	4	32.21
ORF35	ORF35	150	4	26.23	3	37.48
ORF58	ORF58	357	5	42.45	4	41.66
ORF72	viral cyclin homolog	257	4	42.46	4	45.19
E3						
ORF K3	ubiquitin- protein ligase MIR1	333	5	35.01	3	32.7
Viral IRF-						
vIRF-1 like protein 1		449	5	39.12	4	26.26
Viral IRF-						
vIRF-3 like protein 3		566	7	27.51	3	26.50

<b>Viral IRF-</b>					
<b>vIRF-4 like protein</b>	<b>911</b>	<b>11</b>	<b>37.95</b>	<b>5</b>	<b>30.02</b>
	<b>4</b>				
<hr/>					
<b>DNA</b>					
<b>ORF44 Replication</b>	<b>788</b>	<b>0</b>	<b>N/A</b>	<b>5</b>	<b>35.06</b>
<hr/>					
<b>helicase</b>					

**Table 3.3 Virion-associated proteins identified that have not previously been reported by any method.**

Novel proteins identified in VTT fraction. All peptides have a score ( $-10\lg P$ ) greater than 25 and correspond to a statistical significance of  $p < 0.00316$ ; moreover, from our positive matches, only proteins identified with more than at least 2 peptide sequences with a mass tolerance of  $<0.05$  Da were reported.

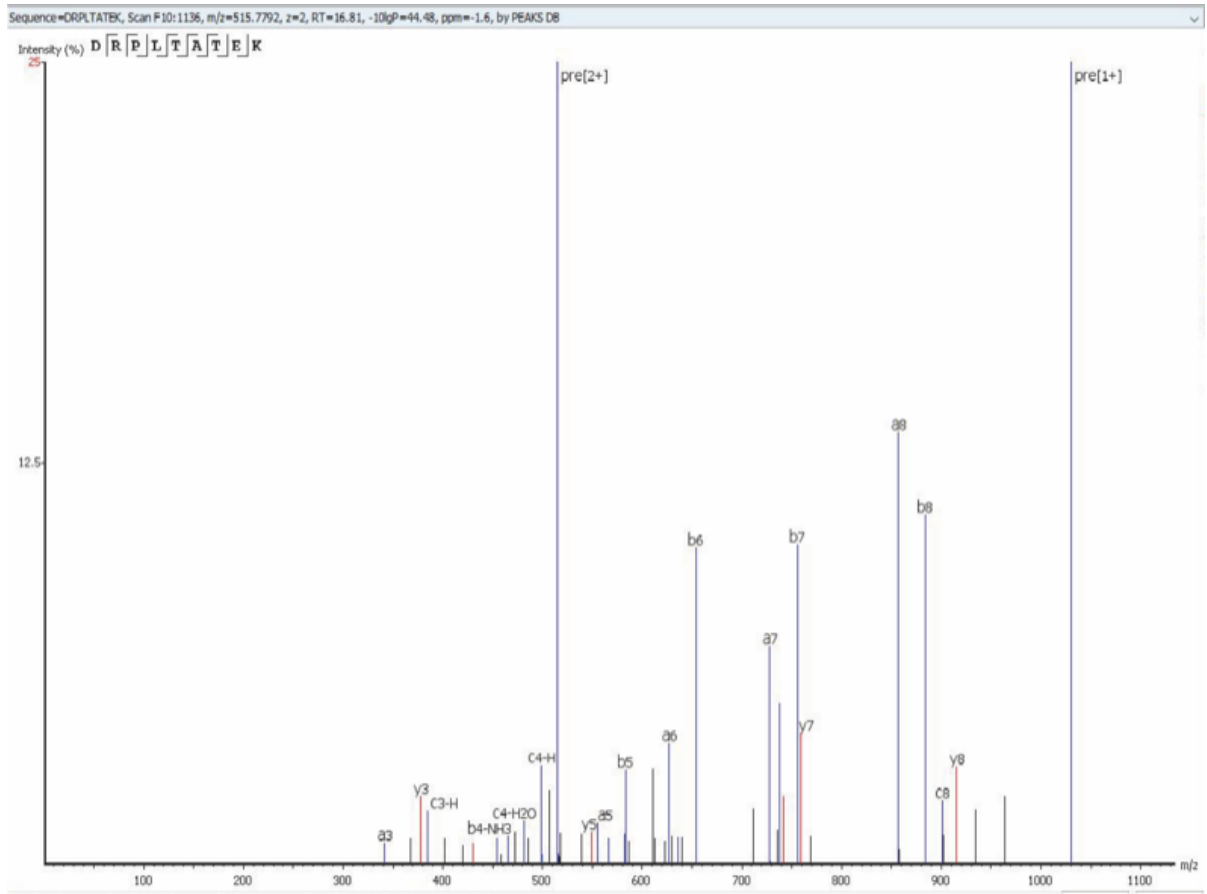


**Figure 3. 3** CID spectrum of the precursor ion at  $m/z$ 7792 ( $z = 2$ ) corresponding to the peptide sequence (DRPLTATEK) of an ORF52 ( $-10\lg P$  of 44.48 and  $-1.6\text{ppm}$ ), from F10:1136 detected by using the Bruker Impact II UHR-QqTOF 125 LC/MS system identified with PEAKS Studio software.

For some of the previously reported hits like ORF6 and ORF7, we were able to detect more unique peptide fragments than were reported initially; however, for some other proteins such as ORF25, the number of peptide hits we found was less than what was previously reported; Bechtel et al. (Bechtel, Winant, & Ganem, 2005) explain that one reason for having so many peptides for ORF25 in their study could be that virions were damaged during the purification and processing of their sample. Our reduced detection of ORF25 peptides could indicate that our altered sample preparation approach resulted in less damage to virions prior to protein extraction.

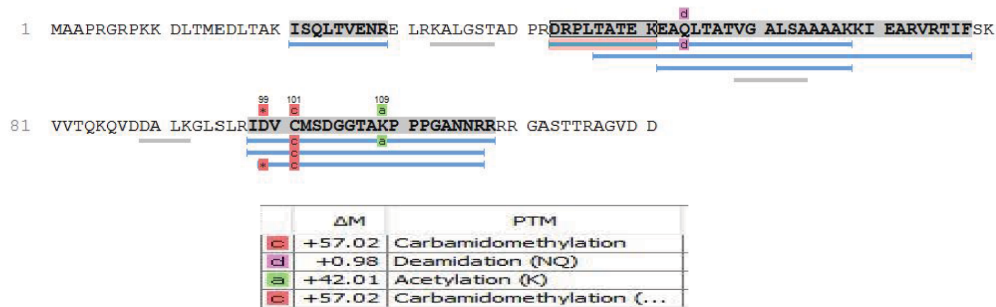


**Figure 3. 4** Example of post-translational modifications (PTMs) detected via PEAKS DB analysis for ORF52.

Additionally, we detected ORF44 peptides only with chymotrypsin digestion and not with trypsin digestion, the peptide hits for this protein also followed our tight criteria of peptide mass tolerance of 20 ppm and fragment mass tolerance of 0.01; in addition to that, they all have  $-10\lg P > 25$ . The identified peptides are included in Table S7.

It is important to note that we analyzed our dataset using a database containing only KSHV protein sequences, so our analysis does not include any host proteins associated with the virion. Next, we wanted to confirm that our novel hits (Table 3) were actually encapsulated within the virions and not due to debris that might have been coincidentally co-purified with the virion fraction. To accomplish this, we pre-treated intact, purified virions with 0.25% trypsin-EDTA to eliminate any proteins not being protected by the virion envelope before performing protein extraction and MS analysis (VTT protein fraction). We used a Western blot for gB to validate the trypsin pre-treatment's efficacy in stripping the envelope layer (**Figure 3.1c**). Both original virion proteomic studies (Bechtel, Winant, & Ganem, 2005), (Zhu, 2005) identified beta-actin as a cellular protein incorporated into KSHV virions, so we utilized this marker as a loading control for this analysis. As expected, MS analysis of the digested pre-treated (VTT) protein fractions included all of the protein hits shown in **Tables 3.1–3.3** except for 10 proteins, including the eight known glycoproteins ORFs 8, 22, 28, 39, 47, 53, 68, and K8.1, as well as

ORF27 and one of our novel detected proteins, ORF58. Thus, we can conclude confidently that nine of our novel virion proteins, ORFs 9, 23, 35, 48, 72, K3, K9, K10, K10.5, are contained within the virion envelope and are not present in the sample due to contamination of the virion preparation with free proteins that are not indeed virion encapsulated. These results also support the prevailing hypothesis that ORFs 27 and 58 are glycoproteins (Russo, et al., 1996 ), (Chandran, et al., 1998), (Quiceno, 2010).

Moreover, these data reconfirm Zhu et al.'s (Zhu, 2005) speculation that ORF28 is an envelope glycoprotein, based on only its similarity in homology to EBV BDLF3 protein. Of the proteins mentioned in **Table 3.2**, that have been introduced as tegument proteins of KSHV, ORF18 was reported by Gong et al. (Gong, et al., 2014) to be essential for de novo lytic activity and viral reactivation, which is in line with our observation of this protein within the newly formed virions. Dai et al. (Dai, Gong, Wu, Sun, & Zhou, 2014 ) in 2014 reported ORF32 as a tegument assembly mediator. ORF42 has been reported to be an essential post-translational regulator, and the loss of it would result in the formation of fewer virion particles. ORF43 has been shown to function as a gate for the packaging of viral DNA into procapsids and a further injection of it to the host nucleus (Sander, et al., 2007 ). ORF56 plays a vital role in DNA replication and viral DNA synthesis and is reported to be a primary lytic gene. Interestingly, its protein expression levels have

been reported to be dependent on ORF57 (Majerciak, Yamanegi, & Zheng, Gene structure and expression of Kaposi's sarcoma-associated herpesvirus ORF56, ORF57, ORF58, and ORF59. , 2006 ), (Jenner, Albà, Boshoff, & Kellam, 2001 ), (Majerciak, Pripuzova, McCoy, Gao, & Zheng, 2007 ). In our analysis, we also observed post-translational modifications including, but not limited to, oxidation, carbamidomethylation, deamidation, and acetylation. These modifications, where present, are indicated in the peptide sequences reported in **Supplemental Tables S1–S6(Appendix B.1-B.6)**. An example of some PTMs observed in the ORF52 protein are shown in Figure 4. It should be noted that, although our analysis was able to detect some PTMs and they are reported in our data, sample preparation for bottom-up proteomics often introduces modifications during sample preparation. Observation of the true spectrum of PTMs in KSHV virion proteins would require further studies using specialized methodologies that were not employed here.

### **3.4 Discussion**

Since the emergence of system-wide protein analysis three decades ago, a common approach to proteomics has been the 2D separation of proteins followed by in-gel trypsinization of individual bands before sequencing and identification (Shevchenko, Tomas, Havlis, Olsen, & Mann, 2006 ). Despite its ease of use and flexibility, this technique has some significant drawbacks, including incomplete

digestion, loss of sample, failure to detect low abundance proteins, and limited dynamic range for proteins. These limitations have resulted in a recent shift towards in-solution, gel-free, or “shotgun” proteomics (Zhang, Fonslow, Shan, Baek, & Yates, 2013 ). Moreover, the development of ultra-high-pressure LC systems in conjunction with smaller inner diameter columns and particle size and development of algorithms and software for de novo sequencing has enabled the detection of thousands of proteins in single LC-MS runs (den Ridder, Daran-Lapujade, & Pabst, 2020 ), (Thakur, et al., 2011). Our study has taken advantage of these advances in proteomics technology to take a fresh look at the KSHV virion proteome.

The current study benefits majorly from a few advancements in KSHV research, some of which were not accessible at the time of the original studies done by Bechtel et al. (Bechtel, Winant, & Ganem, 2005) and Zhu et al. (Zhu, 2005). In particular, the iSLK cell producer cell line has greatly improved KSHV virion yields compared to previous systems isolating WT KSHV from PEL cell lines (Brulois, et al., 2012), (Myoung & Ganem, 2011 ). We believe this increased virion yield, combined with modern instrumentation and analysis software, contributed substantially to the increased sensitivity of our analysis.

EBV systems have shown that gamma-herpesvirus virions can have altered protein composition based upon the producer cell type (Borza & Hutt-Fletcher, 2002 ). However, differences in KSHV virion protein composition from different cell types have not been examined. Given that both original mass spectrometry studies analyzed KSHV virions from PEL cell lines, we cannot determine whether our novel proteins are a result of the increased sensitivity of our methods or the fact that these proteins are only incorporated into virions when they are produced in iSLK or possibly generally from cells of epithelial origin. Since the iSLK system has become increasingly prevalent in the field for the production of KSHV, these results provide critical insight into the protein composition of the iSLK-derived virions, which are commonly used for both in vitro and in vivo experimental studies of KSHV virology.

In addition to validating all of the previously reported proteins packaged within KSHV virions, we report 10 novel virion-associated proteins. ORF58 encodes a homolog of EBV BMRF2 protein with unknown functions (Nishimura, Watanabe, Yagi, Yamanaka, & Fujimuro, 2017 ), but together with ORF27, it has long been speculated to be a glycoprotein (Russo, et al., 1996 ), (Chandran, et al., 1998), (Quiceno, 2010). Our data that ORF58 is removed from the virion by pre-treatment of intact viral particles with trypsin support the conclusion that this ORF58 is a glycoprotein. Similarly, although ORF27 was not novel in our study, we showed

that trypsin pre-treatment removed ORF27 from our virion proteome, thus confirming Zhu et al. (Zhu, 2005) primary classification of ORF27 as a glycoprotein.

Three additional novel virion proteins detected here are highly conserved among gamma herpesviruses (ORF 23, 35, and 48). ORF23 binds to ORF34, and its specific function is still unknown (Ohno, Steer, Sattler, & Adler, 2012). However, a study in MHV68 has shown that its ortholog is not essential for in vitro and in vivo infection (Bergson, et al., 2016). ORF35 encodes a poorly characterized protein that is essential for viral reactivation (Hikita, Yanagi, & Ohno, 2015). A study of MHV68 ORF35 has shown that it is essential for efficient lytic replication and latency (Qi, et al., 2015 ). ORF48 is also poorly studied in KSHV, but a study on the homologous protein in MHV68 has determined that this gamma-herpesvirus-conserved ORF is RTA-responsive and functions in both viral lytic replication and latency during in vivo infections (Wu, et al., 2001). Future studies into the functions of these proteins are needed to establish the implications of their presence in the virus particle.

ORF9 encodes the viral DNA polymerase (Holzerlandt, Orengo, Kellam, & Albà, 2002) and interacts with K10/vIRF4 (Sander, et al., 2007 ). There is evidence of ORF9 gene expression as early as 0–10 hours post-infection (Jenner, Albà,

Boshoff, & Kellam, 2001 ), implying that genome replication is an important a crucial step establishment of infection. ORF72 is the viral cyclin homolog, which shares 54% sequence homology with the cellular Cyclin D2 (Holzerlandt, Orengo, Kellam, & Albà, 2002), (Chang, et al., 1996 ), (Li, et al., 1997 ), (Moore, Boshoff, Weiss, & Chang, 1996 ), (Jones, et al., 2014 ) and binds to a number of cellular cyclin-dependent kinases to promote proliferation of KSHV-infected cells (Godden-Kent, et al., 1997 ), (Swanton, et al., 1997 ), (Chang & Li, 2008 ) Packaging ORF9 and ORF72 into the virus particle implies that early genome replication and manipulation of the host cell cycle are critically important for the initial establishment of KSHV infection in a new host cell.

Our remaining novel virion proteins can broadly be classified as immunomodulatory and immune evasion genes. K2 expresses the viral IL-6 homolog (Neipel, et al., 1997 ), which has significant immunomodulatory effects during KSHV infection and KSHV-associated disease (Sakakibara S. &, 2011). Although vIL-6 is known to signal intracellularly in the endoplasmic reticulum to manipulate host cell processes in an autocrine manner (Meads & Medveczky, 2004 ), (Giffin, West, & Damania, 2015 ), we are unsure of the specific implications of the protein being contained in the virus particle where it would presumably be released into the cytoplasm upon infection. K3 is a membrane-associated ubiquitin ligase, which, along with K5, inhibits antigen presentation on

Major Histocompatibility Complex Class I ( MHC Class I) (Lorenzo, Jung, & Ploegh, 2002 ) and cell surface expression of receptors such as DC-SIGN (Lang, Bynoe, Karki, Tartell, & Means, 2013 ). Despite clear data from overexpression studies showing that K3 can reduce MHC-I expression at the cell surface (Coscoy & Ganem, 2000 ), previous studies using K3 knockout viruses have led to the prevailing theory that K3 does not function in this way during lytic reactivation or early infection (Brulois, et al., 2012), (Brulois, et al., 2014 ). Importantly, however, the earliest timepoint examined by Brulois et al. in their 2012 study of de novo infection with a K3 knockout virus was 36 h post-infection, which is well past the window we would expect to see an effect of K3 as a virion-incorporated factor. Our data that K3 is virion incorporated establish a new context in which K3 may function very early in the viral life cycle (exceedingly early of infection) and may provide an explanation for the previous negative data for K3 function in the context of viral infection.

Finally, we observed three viral interferon regulatory factor (vIRF) proteins as novel virion-associated proteins in our analysis. K9/vIRF-1 suppresses both type I and type II interferon responses (Pozharskaya, et al., 2004 ), (Gao, et al., 1997). Similarly, K10.5/vIRF-3 interferes with both type I and type II interferon responses and additionally can alter CIITA and MHC II expression (Wies, et al., 2008 ), (Schmidt, Wies, & Neipel, 2011 ). In 2014, Lee et al. reported that K10/vIRF4 is a

lytic protein capable of suppression of c-IRF4 and c-Myc, thus manipulating the host gene expression profiles to facilitate viral lytic replication (Lee, et al., 2014 ). In 2017, the same group characterized novel immune evasion strategies of vIRF4 to inhibit the IRF7-mediated IFN- $\alpha$  production (Hwang, Kim, Jung, & Lee, 2017 ), (Zhu, King, Smith, Levy, & Yuan, 2002). It is not the first time that an immunomodulatory protein has been reported to be prepackaged within KSHV virion in order to have a quick response against immune recognition; ORF45, as reported by Zhu et al. (Zhu, 2005), (Paulose-Murphy, et al., 2001 ), is not only packaged within the virion but is also known to interact with IRF7. Our data that three additional vIRFs are encapsulated within the virion necessitate further study into how these proteins may participate in immune evasion very early in KSHV infection.

## 4 CHAPTER IV: KSHV ORF11 Tegument Protein Suppresses Plasmablast And Plasma Cell Proliferation

**Authors:** Ramina Nabiee, Jesus R. Castano, Sarah Barr, Jennifer E. Totonchy

Biomedical and Pharmaceutical Sciences Department, Chapman University School  
of Pharmacy, Irvine, CA 92618, USA;

**This manuscript is under preparation for submission to a scientific journal.**

## **Abstract**

KSHV is the etiologic agent of the lymphoproliferative disorder Multicentric Castleman Disease (MCD). However, not much is known about how KSHV establishes infection in B lymphocytes. KSHV infected cells with plasmablast characteristics are frequently found in the lymph nodes and spleens of MCD patients. Reports have shown that these plasmablasts increase in number and coalesce to form variably sized cellular aggregates both within and outside of the germinal centers of infected lymph nodes and spleens. Thus, it is possible that KSHV gene products contribute directly to plasmablast proliferation and/or differentiation during early infection in B lymphocytes.

The majority of virion proteins reside within the tegument layer of herpesviruses. Some of these proteins play a crucial role in virus life cycle and early stages of infection. ORF11 is one of the few tegument proteins that is only found in the gamma-herpesvirus family. This conservation has led us to hypothesize that ORF11 has B cell-specific functions, which have not been characterized. Here, we utilize both gain-of-function and loss-of-function approaches to determine the role of ORF11 in early KSHV infection of B lymphocytes. For loss of function studies, we have made a recombinant virus lacking ORF11 tegument factor and used it to perform *de novo* infections on primary B cells. We show that ORF11 affects the

proliferation of plasmablasts during early KSHV infection. Our gain of function studies also reveals that, ORF11 has a transmembrane domain. Taken together our results demonstrate that ORF11 participates in the establishment or maintenance of KSHV latency in B lymphocytes. And further suggests that plasmablast differentiation during KSHV infection is regulated both positively and negatively by KSHV gene products, and these gene products may alternately influence disease progression in KSHV-associated lymphoproliferative disorders.

#### **4.1 Introduction**

KSHV is a rhadinoviral gamma herpesvirus, capable of both lytic and latent life cycles (G. Miller L. H., 1997). However, in *in vivo* endothelial and B cell infection with KSHV, infection is primarily latent, accompanied by the expression of a few viral genes including LANA, viral cyclin, vFLIP and vIRF3 (Chen, 2007), (K.A. Staskus, 1997 ), (B. Lubyova, 2000 ). This state of infection is very dynamic and can shift towards lytic reactivation, via poorly-characterized processes which lead to RTA (replication and transcription activator) protein expression (R. Renne, 1996 ), (R. Sun, 1998 ). In the lytic phase, a significant level of viral gene expression through a cascade of signaling occurs (R. Sarid, 1998 ) leading to structural protein production and packaging of the virion.

KSHV shares a series of highly conserved genes, some of which have been known to have enzymatic regulatory roles in different host interactions such as nucleic

acid metabolism, DNA production, and protein expression and modification (K. Borchers, 1994 ). One of these genes is KSHV open reading frame 11 (ORF11), a highly conserved gene common to majority of the gamma herpesviruses subfamily (M.M. Alba, 2001).

In the KSHV genome, the ORF11 gene is located adjacent and in the opposite orientation to the significantly characterized ORFK2 (vIL-6) (H. Deng, 2002 ), and it was detected for the first time by Russo et al. (Russo, et al., 1996 ) using BC-1 genomic libraries for its mapping. Later, two other groups were able to demonstrate detection of ORF11's activity post chemical stimulation, or RTA expression, thus establishing it as a lytic gene (R.G. Jenner, 2001), (H. Nakamura, 2003). Davidson and Stow later applied computational analysis to ORF11's sequence and speculated that the ORF11 coding sequence contains a dUTPase domain (A.J. Davison, 2005). Two years later, Chen and Lagunoff reported that ORF11 is not significantly involved in the regulation of other viral genes in BJAB cells (Chen, 2007). The ORF11 protein is associated with purified KSHV virions (Zhu, 2005), (Nabiee R., 2020). Investigations on virion-wide protein–protein interactions have revealed that ORF11 interacts with other tegument proteins such as ORF45, ORF64 and ORF63, suggesting a potential role in primary KSHV infection (R. Rozen, 2008). This association suggests that ORF11 may function in KSHV virion morphology, latency establishment, or host interactions (Zhu, 2005).

Chen et al., in two consecutive studies (Chen L., 2009), (Chen L. M. S., 2011), further explored how ORF11 gene transcription is regulated in KSHV lytic replication. They showed that ORF11 expression is not directly regulated by RTA, which indicates other viral or cellular factors may be involved in the regulation of ORF11 gene expression. They also detected a silencer region within the ORF11 sequence, suggesting a novel mechanism of gene regulation utilized by KSHV to precisely control ORF11 gene expression.

Due to its conservation exclusively in gamma-herpesviruses, we hypothesized that ORF11 may have a B cell-specific function. In the current manuscript, we have utilized gain of function and loss of function assays to reveal previously uncharacterized functions of ORF11. Our gain of function studies demonstrate that ORF11 localizes to the plasma membrane in HEK293 cells we also show that ORF11 has a transmembrane domain. In our loss of function studies, we demonstrate that ORF11 is not an essential protein for viral production, but has a suppressive role in proliferation and differentiation of particular subsets of B lymphocytes.

## **4.2 Materials and Methods**

### **4.2.1 Tissue Culture**

Different tissue culture techniques were used in this study, details have been highlighted in the proper sections of methodology. Overall maintenance immortalized cell flasks were always maintained up to 80-85% confluency and passaged weekly; primary cells were cryopreserved and thawed before seeding for specific experiments, with an emphasis on passage number consistency between samples and/or replicates.

### **4.2.2 X-ray Irradiation**

CDw32 L cells (CRL-10680) were obtained from ATCC and were cultured in DMEM supplemented with 20% FBS (Sigma Aldrich) and Penicillin/Streptomycin/L-glutamine (PSG/Corning). For preparation of feeder cells, CDw32 L cells were trypsinized and resuspended in 15 ml of media in a petri dish and irradiated with 45 Gy of X-ray radiation using a Rad-Source (RS200) irradiator. Irradiated cells were then counted and cryopreserved until needed for experiments.

#### 4.2.3 Tonsil Tissue Dissociation and Isolation of Primary Lymphocytes

De-identified human tonsil specimens were obtained after routine tonsillectomy by NDRI and shipped overnight on wet ice in DMEM+PSG. All specimens were received in the laboratory less than 24 hours post-surgery and were kept on ice, throughout the collection and transportation process. Lymphocytes were extracted by dissection and maceration of the tissue in RPMI media. Lymphocyte-containing media was passed through a 40 $\mu$ m filter and pelleted at 1700rpm (Heraeus Megafuge Centrifuge by Thermo Fisher Scientific) for 5 minutes. RBC were lysed for 5 minutes in sterile RBC lysing solution (0.15M ammonium chloride, 10mM potassium bicarbonate, 0.1M EDTA). After dilution to 50ml with PBS, lymphocytes were counted, and pelleted. Aliquots of 5E7 to 1E8 cells were resuspended in 1ml of freezing media containing 90% Serum (FBS or CCS) and 10% DMSO and cryopreserved until needed for experiments.

#### 4.2.4 Generation of KSHV- $\Delta$ ORF11 using BAC16

KSHV- $\Delta$ ORF11 was constructed by seamless two-step Red recombination (Tischer et al., 2010) in GS1783 E. coli containing the BAC16 KSHV genome (Brulois et al., 2012). Primers containing sequences from the N-terminal coding region of ORF11 containing two consecutive stop codons (Fig 4.2) were used to amplify the Kanamycin selection cassette from pepKanS plasmid and en passant

mutagenesis was performed to introduce the stop codons seamlessly into the ORF11 gene. Mutant strains were verified by Sanger sequencing of the region of interest, pulse field electrophoresis to validate maintenance of the LTR packaging sequences and next generation sequencing of the entire genome using an Illumina miSeq to verify that mutagenesis did not produce any second site mutations.

BAC16 contains a constitutive GFP reporter under an EF1alpha promoter and hygromycin resistance for selection of infected cells in mammalian culture. iSLK producer cell lines were made by first transfecting BAC16 genomic DNA into 293T and selecting 293T for 2 days with 50 µg/ml hygromycin B. Thereafter, infected 293T lines were co-cultured with iSLK. The selective media for iSLK (detailed below) was used to remove 293T from these cultures once the infection was transferred to the iSLK. Pure iSLK producer lines were made by selection with hygromycin B at 1.2 mg/ml.

#### 4.2.5 Preparation of Cell Free Recombinant KSHV Particles

iSLK (Brulois, et al., 2012) stably infected with BAC16 (Plancoulaine S, 2000) recombinant KSHV were grown in DMEM supplemented with 10% CCS, 50µg/ml gentamicin, 250µg/ml G418, 1µM Puromycin, and 1.2mg/ml Hygromycin B. Twelve confluent T175 flasks were induced at 70% confluency for 72 hours with 3mM Sodium Butyrate and 2µM Doxycycline. Culture supernatants were

clarified by centrifugation at 1500rpm for 12 minutes and passed through a 0.45  $\mu$ M filter placed on ice. Virus was pelleted out of clarified supernatants over a 25% sucrose cushion prepared in TNE buffer at PH 7.40 by ultracentrifugation at 22,000 rpm for 120 minutes. Virus pellets were resuspended in a total of 2mL TNE buffer and stored in smaller quantities to avoid freeze thaw at -80°C.

#### 4.2.6 Viral Titering

To determine the Multiplicity of Infection (MOI), Human fibroblasts were derived from primary human tonsil tissue and immortalized using HPV E6/E7 lentivirus derived from PA317 LXS<sup>N</sup> 16E6E7 cells (ATCC CRL-2203). These E6/E7 transformed fibroblasts were seeded at 100,000 cell/well in 6-well culture plates. 24 hours post-seeding increasing doses of cell free KSHV was added in serum free DMEM. Infected cultures were spinoculated at 1000rpm, 4°C, 30 minutes followed by incubation for 1 hour at 37°C. Cultures were then fed with complete media (DMEM+10% FBS+ PSG) and maintained at 37°C for 3 days. At 72 hours post infection, viral titers were assessed using flow cytometry with eGFP expression as a marker for virus-positive cells, using a FACSV<sup>ERSE</sup> flow cytometer (BD Biosciences, San Jose, CA), and data were analyzed using FlowJo cytometry analysis software (FlowJo, LLC, Ashland, OR). as well as quantitative PCR (qPCR) of genomic DNA copy number in virus stock. For qPCR, DNA was

extracted from the virus stock (pretreated with DNase) using zymo viral DNA/RNA extraction kit (Zymo Research, Inc., Irvine, CA). Viral genomes were quantified using TaqMan Fast advanced master mix (Applied Biosystems, Foster City, CA) utilizing thermo fisher scientific primers and probes targeting the BAC16 eGFP cassette (Thermo Fisher Scientific, Waltham, MA)(Fwd: TGACCCTGAAGTTCATCTGC, Rev: GAAGTCGTGCTGCTTCATGT, Probe: CCCACCCTCGTGACCACCCT). Samples were analyzed in duplicates. An eight-series of 10-fold dilutions of plasmid pCAGGS-eGFP(17) was used as a standard for absolute quantification of viral genome copies.

The data was then compared to make sure that in primary infections we are reaching TCID<sub>20</sub> as well as ensuring that for different viruses the genome copy number of virus compared to cells (gCPC) were similar.

#### 4.2.7 Infection of Primary Lymphocytes with KSHV

Lymphocytes were thawed rapidly at 37°C, diluted dropwise to 5ml with RPMI and pelleted at 1500 rpm for 5 minutes. Pellets were resuspended in 1ml RPMI+20%FBS+100µg/ml DNase I+ Primocin 100µg/ml and allowed to recover in a low-binding 24 well plate for 2 hours at 37°C, 5% CO<sub>2</sub>. After recovery, total lymphocytes were counted, and Naïve B cells were isolated using Mojosort™ Naïve B cell isolation beads (Biolegend 480068) or Naïve B cell Isolation Kit II

(Miltenyi 130-091-150) according to manufacturer's instructions. Bound cell fraction (non-naïve B and other lymphocytes) were retained and kept at 37°C in RPMI+20% FBS+ Primocin 100µg/ml during the initial infection process. 1E6 Isolated naïve B lymphocyte were infected with iSLK-derived Bac16-KSHV (WT and/or mutant) (dose equivalent to the ID20 at 3dpi on human fibroblasts) or Mock infected; in 400ul of total of virus + serum free RPMI in 12x75mm round bottom tubes via spinoculation at 1000rpm (Eppendorf centrifuge 5840r) for 30 minutes at 4°C followed by incubation at 37°C for an additional 30 minutes. Following infection, cells were plated on irradiated CDW32 feeder cells in a 48 well plate, reserved bound cell fractions were added back to the infected cell cultures at the density of 1E6, and FBS and Primocin (Invivogen) were added to final concentrations of 20% and 100µg/ml, respectively. Cultures were incubated at 37°C, 5% CO<sub>2</sub> for the duration of the experiment. Followed by intermittent feeding every 72 hours by replacing 200uL of the media with fresh media.

#### 4.2.8 Multicolor Flow cytometry

A proportion of lymphocyte cultures equivalent to ~500,000 cells were acquired by aseptic technique at certain time points such as: at baseline, 3,6, and 10 days post infection(dpi) these representing cells were pelleted at 1500 rpm (using Eppendorf centrifuge 5840 (Eppendorf AG, Hamburg, Germany) for 5 minutes into 96-well

round bottom plates. The supernatant for some experiments' would be collected and frozen at -80°C (Eppendorf AG, Hamburg, Germany) for further analysis and cells were then resuspended in 100µl PBS (calcium and magnesium free) containing (0.4ng/ml) fixable viability stain (BD Biosciences, Franklin Lakes, NJ) light protected and incubated on ice for 15 minutes. Cells were pelleted and resuspended in 100µl cold PBS (without calcium and magnesium) containing 2% FBS, 0.5% BSA and 0.1% Sodium Azide (FACS Block) and incubated on ice for 10 minutes after which 100µl cold PBS (without calcium and magnesium) containing 0.5% BSA and 0.1% Sodium Azide (FACS Wash) was added. Cells were pelleted and resuspended in FACS Wash containing B lymphocyte and T lymphocyte specific phenotype panel (including but not limited to, and depending on the time point and purpose of analysis) as follows for 15 minutes on ice: (volumes indicated were routinely used for up to  $0.5(10)^6$  cells and were based on titration of the individual antibodies on primary tonsil lymphocyte specimens(FMO)) CD19-PerCPCy5.5 (2.5µl, BD 561295), CD20-PE-Cy7 (2.5ul, BD 560735), CD38-APC (10µl, BD 555462), IgD-APC-H7 (2.5µl, BD 561305), CD138-v450 (2.5µl, BD 562098), CD27-PE (10µl BD 555441). After incubation, 150µl FACS Wash was added and pellet lymphocytes were washed with a further 200µl of FACS Wash prior to being resuspended in 200µl FACS Wash for analysis. Data was acquired on a BD FACSVERSE Flow Cytometer or a BD

Fortessa X20 Special Order Flow Cytometer, and analyzed using FlowJo software.

Table 4.1 shows which B cell subset express particular surface markers.

<b>B Lymphocytes</b>	
<b>Subset</b>	<b>Molecular Markers</b>
Plasma	CD19 <sup>+</sup> , CD20 <sup>+/-</sup> , CD138 <sup>(Mid to High)</sup> , CD38 <sup>-</sup>
Transitional	CD19 <sup>+</sup> , CD138 <sup>-</sup> , CD38 <sup>Mid</sup> , IgD <sup>(Mid to High)</sup>
Plasmablast	CD19 <sup>+</sup> , CD138 <sup>-</sup> , CD38 <sup>High</sup> , IgD <sup>+/- (mostly -)</sup>
Germinal Center	CD19 <sup>+</sup> , CD138 <sup>-</sup> , CD38 <sup>Mid</sup> , IgD <sup>-</sup>
Naïve	CD19 <sup>+</sup> , CD138 <sup>-</sup> , CD38 <sup>Low</sup> , CD27 <sup>-</sup> , IgD <sup>(Mid to High)</sup>
Marginal Zone Like (MZ-Like)	CD19 <sup>+</sup> , CD138 <sup>-</sup> , CD38 <sup>Low</sup> , CD27 <sup>(Mid to High)</sup> , IgD <sup>(Mid to High)</sup>
Memory	CD19 <sup>+</sup> , CD138 <sup>-</sup> , CD38 <sup>Low</sup> , CD27 <sup>(Mid to High)</sup> , IgD <sup>-</sup>
Double Negative	CD19 <sup>+</sup> , CD138 <sup>-</sup> , CD38 <sup>Low</sup> , CD27 <sup>-</sup> , IgD <sup>-</sup>

**Table 4.1 B cell lineages used in this study**

**4.2.9 RT-PCR for Viral Gene Expression**

For viral gene expression assays, primary naïve lymphocytes 1E6 cells were harvested at indicated time points and total RNA was extracted using DirectZol RNA Miniprep Kit (Zymo Research, Inc., Irvine, CA) according to manufacturer instructions. A second DNase step was performed using Ambion DNA free Kit (Cat #AM1906) and cDNA was synthesized from 50ng total RNA using Thermo High-Capacity cDNA synthesis kit. 3µl of cDNA was used for duplicate RT-PCR reactions with TaqMan Fast Advanced Mastermix (Cat #: 4444556). Primer and probe (FAM/BGH) sequences were as follows (5' to 3') in the Table 4.2.

Primer / Probe Name	Primer / Probe Sequence
LANA Forward	GCCTATACCAGGAAGTCCCA
LANA Reverse	GAGCCACCGGTAAAGTAGGA
LANA Probe	ACACAAATGCTGGCAGCCCG

K8.1 Forward	TGCTAGTAACCGTGTGCCAT
K8.1 Reverse	AGATGGGTCCGTATTTCTGC
K8.1 Probe	TGCGCGTCTCTTCCTCTAGTCGTTG
ORF59 Forward	TTAAGTAGGAATGCACCCGTT
ORF59 Reverse	GGAAGCCGGTGGTAGGAT
ORF59 Probe	CCAGGCTTCTCCTCTGTGGCAA

**Table 4.2 : Primer and Probe Sequences used for qPCR Assays.**

#### 4.2.10 Immunofluorescence assays (IFA)

Cells were fixed for 15 minutes at RT using 4% formaldehyde, washed with Sterile PBS, and labeled using traditional IFA methods incorporating 4% PFA solution in PBS for fixation followed by incubation at RT for 15 minutes, 3X PBS washes, and permeabilization using Perm Buffer (BD Catalog#: 554723). These steps were then followed by 1 hour RT incubation with Primary Antibody (Anti- C-MYC Antibody, Catalog#: 626801 Biolegend) and 3X PBS washes. Finally the secondary Antibody ( Alexa flour 488, Thermofisher Catalog#: A1134) and DAPI (ThermoFisher Scientific Catalog #: 28718-90-3) were added for 30 minutes at RT, the samples were washed 3X times with PBS and covered with PBS for further

analysis. For high intensity signaling the Tyramide IFA kit ( ThermoFisher Scientific, Catalog#: B40922) was used following its protocol, ( (Scientific, 2020)). Cells were washed and then fixed on the slides or kept in the vessels depending on whether they are adherent or non-adherent cells, until examined using a Nikon A1R high-definition resonant scanning confocal microscope and a NIS- Elements software (AR 4.30.02, 64bit).

It is worth mentioning that for some procedures the methanol fixation method will be used as the antibody and protein reaction post fixation might vary. For which the cells will be washed and then pure (100%) methanol that has been chilled prior at -20°C will be added on top of them and incubated at -20°C for 5 minutes and from there the rest of the procedure was similar to 4%PFA IFA method.

#### 4.2.11 Construction of ORF11-myc-pCDNA

Utilizing a C-myc tag for the studies and the following primers (ORF11\_P1: AGTGTGGTGGGAATTCTGCatggcgcaggagtcagagc, ORF11\_VR: tctgactcctgcgccatGCAGAATTCCACCACACTGG ; and ORF11\_P3: ttgccaccggacgcagtGAACAAAACTCATCTCAGAAGAGG) in a pCDNA plasmid backbone, DNA was produced, and verified via running on agarose gel as well as PCR, then purified via ZYMO DNA purification kits, and HEK293T cells were then transiently transfected with the DNA using 0.1mM MgCL<sub>2</sub> and HEPES

1x for DNA delivery, cells were then antibiotic screened using Zeocin. The cells were also kept under antibiotic selection for the duration of studies, the cells were treated with 10ug of MG132, in order to increase the stability of expressed protein upon inhibition of proteasomal degradation for 3 hours before IFA staining for confocal microscopy. For the codon optimized studies the following P1, P3 and VR primers were used in the same pCDNA (ORF11CO\_P1: AGTGTGGTGGGAATTCTGCatggccaagagtccgagcagtgc , ORF11CO11\_P2: TGAGATGAGTTTTTGTTCGCTTCTGCCGGTGGCCACG, ORF11CO\_VR: tcggactcttgggcatGCAGAATTCCACCACACTGG).

#### 4.2.12 Cell Proliferation assays

BrdU tagging kit in APC channel was obtained from BD(Catalog #:557892 BrdU APC Staining Kit Component A) and cells were treated and plated with 7.5 uL of 10mM BrdU post infection and on 3- and 6-days post infection they were stained and analyzed on BD LSR-Fortessa II with a panel consisting of 15 markers as described above.

#### 4.2.13 UV inactivation studies

Purified cell free virions were freshly thawed on ice and the UV inactivated for 10 minutes prior to B cell infection, BrdU was added to the wells post infection and

cells were similarly analyzed on 3- and 6-days post infection they were stained and analyzed on BD LSR-Fortessa II with a channel consisting of 15 markers.

## 4.3 Results

### 4.3.1 ORF11 Protein Localizes to Plasma Membrane and has a Transmembrane Domain.

Cloning the ORF11 open reading frame from the KSHV genome into pCDNA2.1-myc resulted in very low expression levels upon transfection that were not improved by inhibiting proteasomal degradation with MG132 (data not shown). However, codon optimization of ORF11 significantly improved the expression level. Our microscopy analysis reveals that ORF11 is localized within the plasma membrane (**Fig.4.1**). To investigate whether ORF11 resides fully within the plasma membrane and determine its topology, cells were induced and stained for the C-terminal myc tag either unpermeabilized or permeabilized with Triton X-100 at 0.1%. We observed the signal in both fractions, demonstrating that the C-terminus of ORF11 is outside the cell. We further verified this observation through topology prediction modeling utilizing TMHMM topology prediction modeler

from university of Denmark (A. Krogh, 2001), which predicts an 18 amino acid transmembrane helix domain in the ORF11 protein. Based on these results we are proposing a schematic model for ORF11 localization within the plasma membrane (**Fig 4.2**).

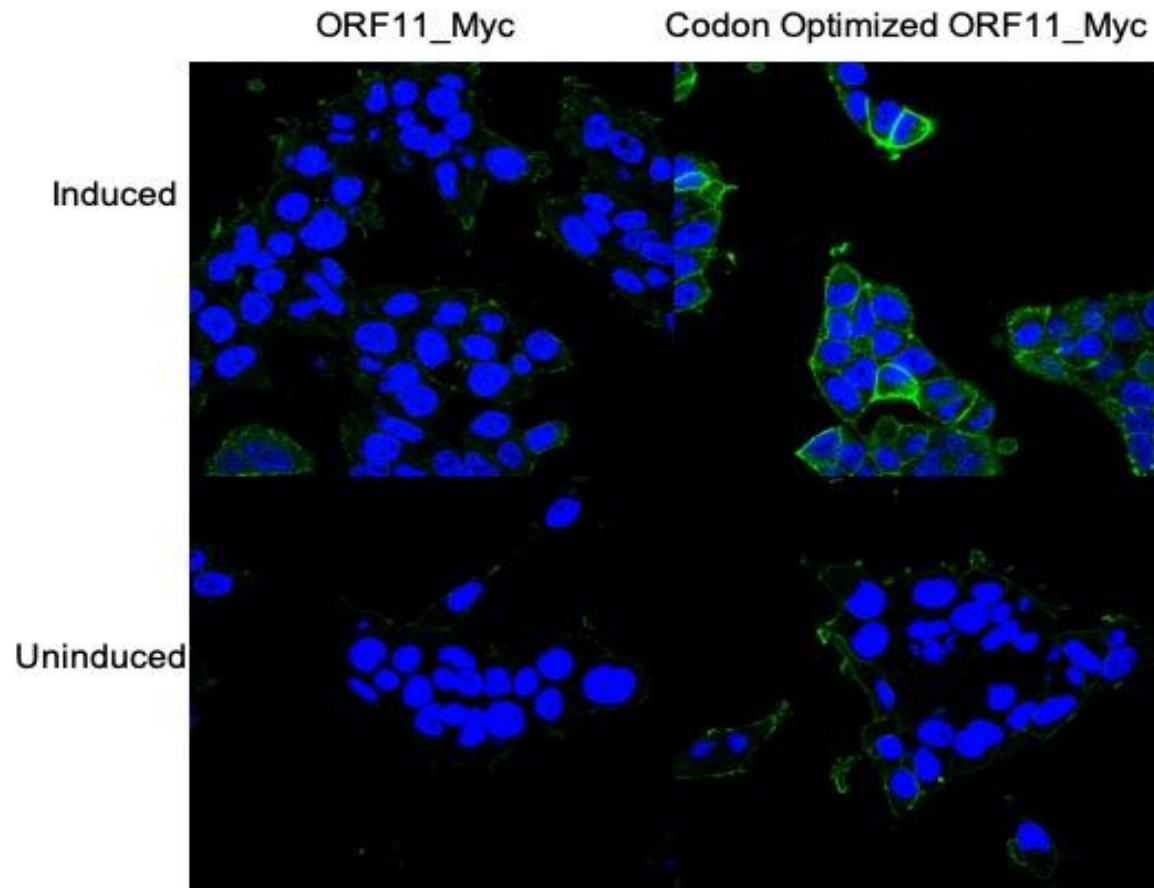


**Figure 4. 1** ORF11 expression is localized to plasma membrane and the expression level is significantly improved by codon optimization. the top panels show HEK293T cells transfected with ORF11 pCDNA constructs, post 24 hours of induction using Doxycycline, the nuclei are stained using DAPI and the green signal is from the C-myc tagged ORF11 protein expressing GFP marker.

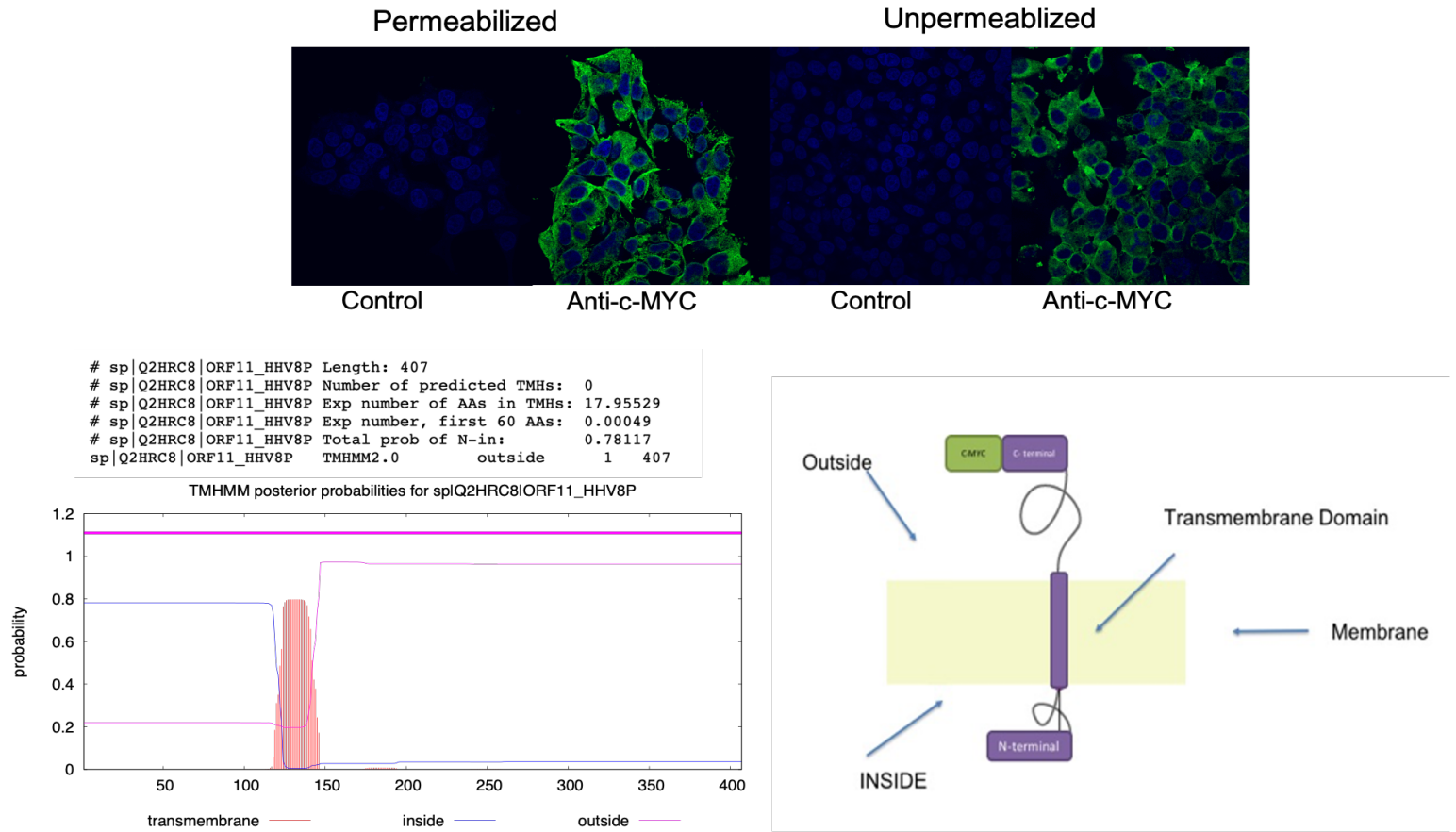


**Figure 4. 2** ORF11 protein Has A Transmembrane Domain. (A)The top panel is confocal microscopy analysis of the HEK293T cells expressing ORF11 pCDNA, samples on the left are permeabilized using 0.1% Tritonx-100 while the samples on the right are not permeabilized, demonstrating the transmembrane domain. (B) demonstrates the results of TMHMM topology prediction for KSHV ORF11. (C) shows our proposed scheme for the localization of ORF11 protein within the cells.

### 4.3.2 KSHV ORF11KO, Mutant Development, And Preliminary Studies

#### Confirm That ORF11 Is Not Essential for Viral Production

Next, we designed loss of function approaches to study the events occurring in *de novo* infection of B lymphocytes with a knockout ORF11 mutant (KSHV- $\Delta$ ORF11) compared to KSHV-WT. A BAC16 mutant was produced through the introduction of two sequential stop codons within the ORF11 sequence, the entire BAC genome was further sequenced, and no other alterations were observed within the genome. (**Fig4.3**)

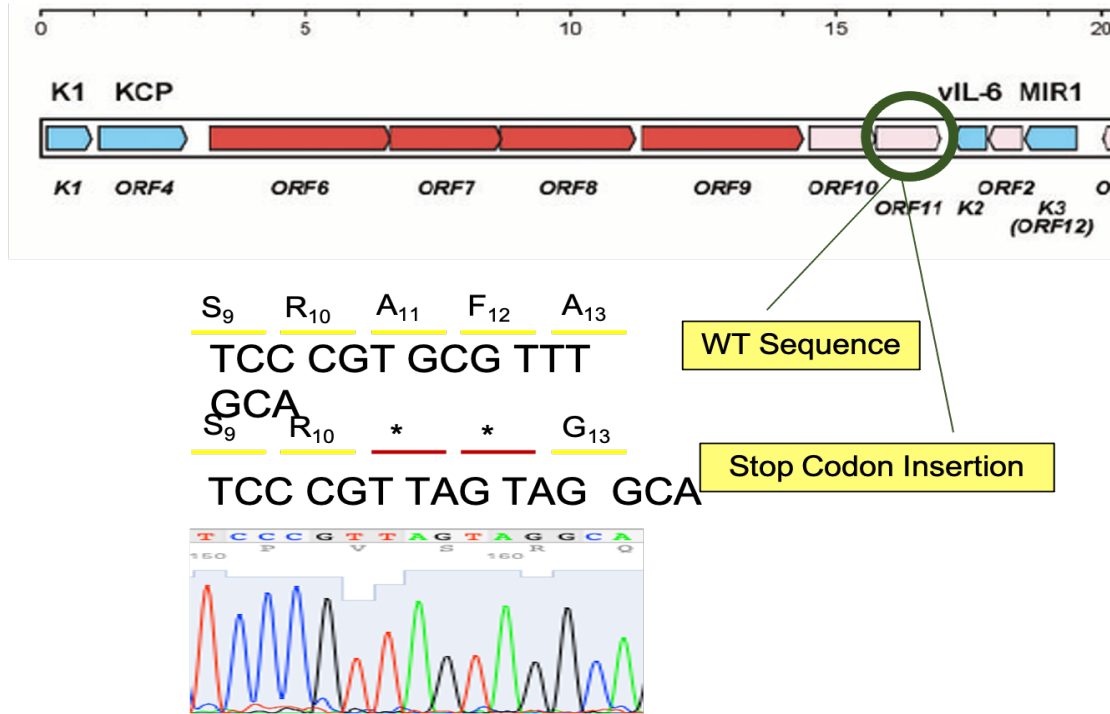


**Figure 4. 2** KSHV ORF11 Mutant development. As demonstrated two amino acids genetic codons (11 and 12) have been mutated to DNA stop codons thus rendering an ORF11 Knockout construct. The bottom panel is the sequencing results confirming that the only change introduced in the backbone has been the insertion of the stop codons

KSHV- $\Delta$ ORF11 virions were efficiently produced from iSLK producer cell lines, demonstrating that ORF11 is not essential for viral production and packaging. Once cell free virions were prepared, we used E6/E7 fibroblast cells for viral titering, higher GFP expression within the  $\Delta$ ORF11 infected samples is observed with similar number of viral particles (based on qPCR genome titering). **(Fig4.4)**

## E6/E7 Fibroblasts infected with BAC16 Virus

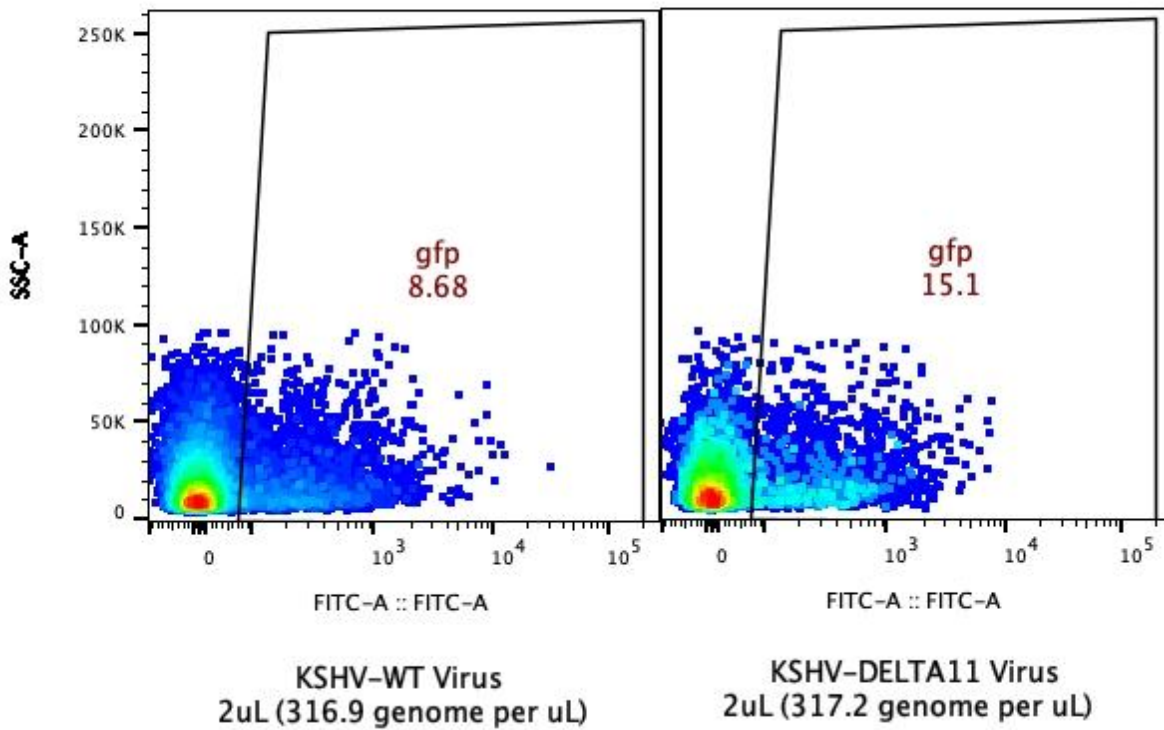


**Figure 4. 4** Higher GFP Expression Within The  $\Delta$ ORF11 Infected Samples Is Observed Within Similar Doses, With Similar Number of Viral Particles (Based On (PCR genome Titering) in E6/E7 Fibroblasts, results are acquired at 3 days post infection.

### 4.3.3 Increased Infection with ORF11KO Is Observed in B lymphocytes

However, There Is No Significant Viral Particle Production Change.

Equivalent TCID<sub>20</sub> doses of WT and  $\Delta$ ORF11 virus were used for *de novo* infections of tonsil derived B lymphocytes as explained in methodology. We observed significantly increased numbers of GFP positive B lymphocytes within the  $\Delta$ ORF11 infected samples (**Fig 4.5**). We hypothesized that this increase in infected cells could be due to (1) increased spread of KSHV- $\Delta$ ORF11 virus within the cultures or (2) increased proliferation of KSHV- $\Delta$ ORF11 infected cells. To test the first hypothesis, we analyzed KSHV genomes in the culture supernatant of infected B lymphocytes at 6 days post infection. Interestingly, this data did not show any changes in the viral production level between WT and  $\Delta$ ORF11 culture supernatants (**Fig.4.5**).

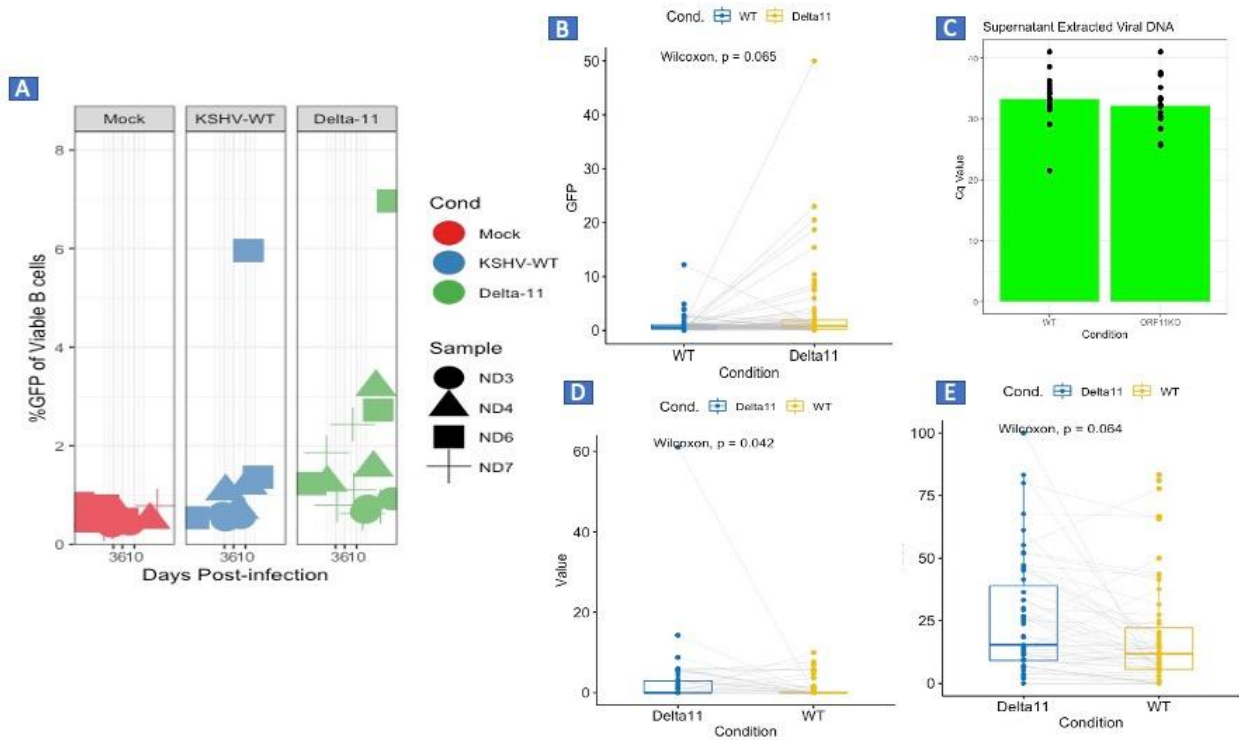


**Figure 4.3** Increased Infection with ORF11KO Is Observed However There Is No Significant Viral Particle Production Change. (A) Shows a comparison between different conditions over the course of time and how GFP is constantly higher in Delta11 samples. (B) shows statistical analysis of the GFP levels between WT and Delta11 where with P value of 0.065 Delta11 is showing higher levels of GFP. (C) Comparison of Viral DNA production between different samples from the viral DNA extracted from supernatant of infected B cells at 6 days post infection. (D) statistical analysis of GFP positive double negative B cells, with P value of 0.042.(E) statistical analysis of GFP positive Plasmablast B cells, with P value of 0.064.

#### 4.3.4 Increased Proliferation In $\Delta$ ORF11 Mutant Virus Infected Cells, Is Linked to Increased Proliferation of Plasmablasts and Plasma Cells.

Since the previous experiments had demonstrated that the increased infection we observe with KSHV- $\Delta$ ORF11 is not due to higher viral production, we speculated that the increase might be due to increased proliferation of B lymphocytes infected with KSHV- $\Delta$ ORF11. In order to examine whether B cell populations differed between KSHV-WT and KSHV- $\Delta$ ORF11, we employed a multicolor flow cytometry panel that we reported previously (Aalam F, 2020) and analyzed total B cell lineages and the distribution of infection within B cell lineages at 3, 6 and 10 days post-infection. As observed in (**Fig.4.6**), the total plasmablast population and the infected plasmablast population are both increased in KSHV- $\Delta$ ORF11 infected cultures compared to the KSHV-WT infected samples.

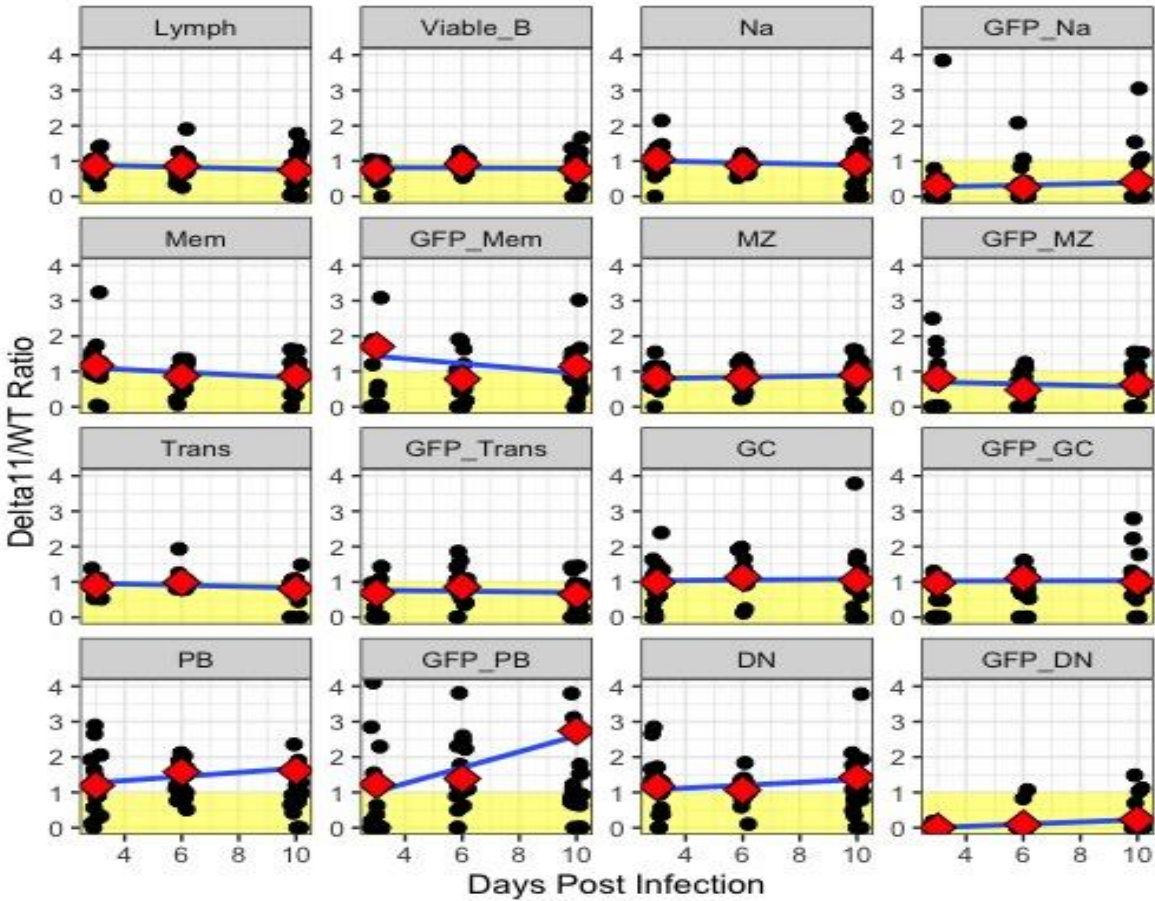


**Figure 4. 6** Observed changes in total population of B cells, as well as changes in GFP(Infected) only population of B cells. All B cells are shown as frequency of viable, CD19+ B cells. the GFP subsets are shown as the frequency of infected subsets of the particular parent subset. Na stands for Naïve B cell, Mem stands for Memory B cells, MZ stands for Marginal Zone B cells, Trans stands for transitional B cells, GC stands for Germinal Center B cells, PB stands for Plasmablasts, and finally DN stands for Double negative cells based on negative expression of CD27 and IgD observed in our gating scheme (Appendix A.1) similar to Fig4.5, the elevated levels of GFP in the infected Plasmablast and infected Double negative cells are statistically significant (P values are respectively 0.064 and 0.041 based on Wilcoxon test). A more detailed look into the surface markers each of the subsets express is available in Table 4.1.

In order to determine whether the increased plasmablast numbers observed with KSHV- $\Delta$ ORF11 were due to proliferation, we added BrdU at 100mM concentration to cultures at infection. At 3 and 6 dpi cells were stained with surface markers for B cell immunophenotypes and then fixed, permeabilized, treated with DNase to liberate BrdU epitopes and incubated overnight with Anti-BrdU antibody. These results show a statistically significant increase in total B cell proliferation with KSHV- $\Delta$ ORF11 (**Fig 4.9**). More importantly it can be observed that the higher proliferation in the samples is associated with significantly increased proliferation of plasmablasts and plasma cells (**Fig4.9**), these two B cell subsets are biologically/pathologically important cell types as plasmablasts are precursors of short- and long-lived plasma cells and they both are a proliferating fraction of antibody-secreting cells, which play complex roles in humoral immunity and host protection.

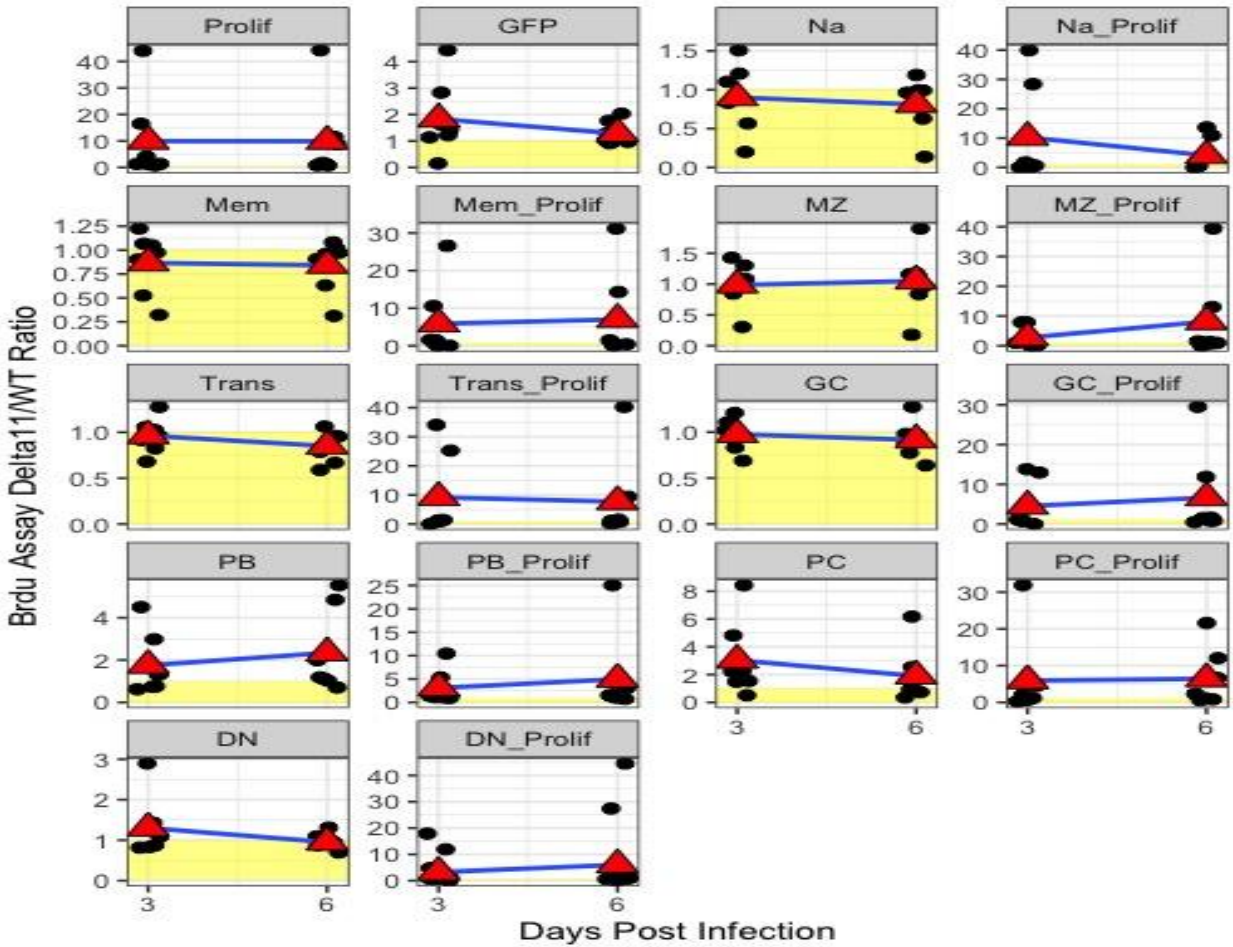


**Figure 4.7** BrdU analysis shows increased proliferation in total B cell population and individual subset proliferation. All B cells are shown as frequency of viable, CD19+ B cells. the Proliferating (Prolif) subsets are shown as the frequency of infected subsets of the particular parent subset. Na stands for Naïve B cell, Mem stands for Memory B cells, MZ stands for Marginal Zone B cells, Trans stands for transitional B cells, GC stands for Germinal Center B cells, PB stands for Plasmablasts, and finally DN stands for Double negative cells based on negative expression of CD27 and IgD observed in our gating scheme (Appendix A.1) similar to Fig4.9, the elevated levels of proliferation in the Plasmablasts and plasma cells, as well as overall proliferation are statistically significant (P values are respectively 0.0067 and 0.00024, and 0.0052). A more detailed look into the surface markers each of the subsets express is available in Table 4.1.

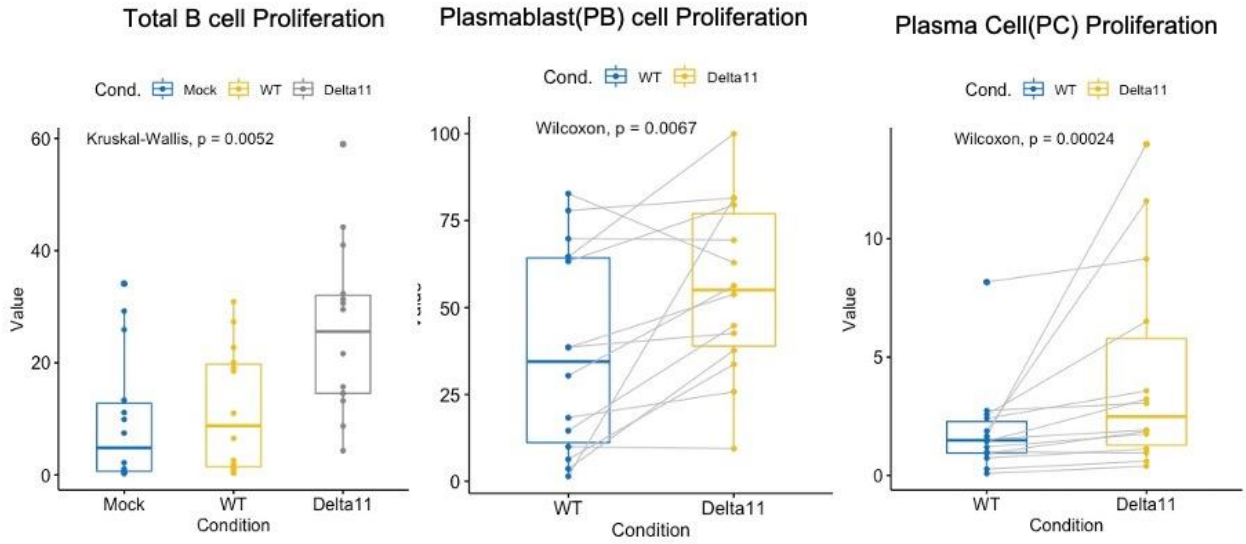


**Figure 4.8** Total B Cell Proliferation, Plasmablasts and, Plasma Cell Proliferation Increases Significantly Post Infection with ORF11KO, statistical analysis has been done using ggplot ggpaired statistical tests.

4.3.5 Increased proliferation phenotype is not linked to ORF11 protein packaged within the viral particles.

A possible explanation for the increased levels of proliferation could be the ORF11 protein packaged within the virion and its interaction with the host in early stages of infection. In order to test whether virion-associated ORF11 was responsible for suppressing B cell proliferation, we UV-inactivated the virion for 10 minutes prior to infection (**Appendix C.2**, shows our optimization experiments of UV-Inactivation exposure time effects on viral infectivity) to prevent any de novo gene expression, thus providing a chance to study the effects of proteins carried by the virion in absence of new proteins being produced from virion DNA after infection. The UV virus was then used in side-by-side infections of B cell lymphocytes using BrdU to assess proliferation. We observed that the UV inactivated KSHV- $\Delta$ ORF11 did not display the increased proliferation seen in non-UV treated infections, and more importantly it behaves similar to WT UV inactivated virion (**Fig.4.10**), these results suggest that it is ORF11 produced in the cells after infection and not ORF11 packaged into the virus particles that is affecting proliferation of plasmablasts and plasma cells in our experiments.

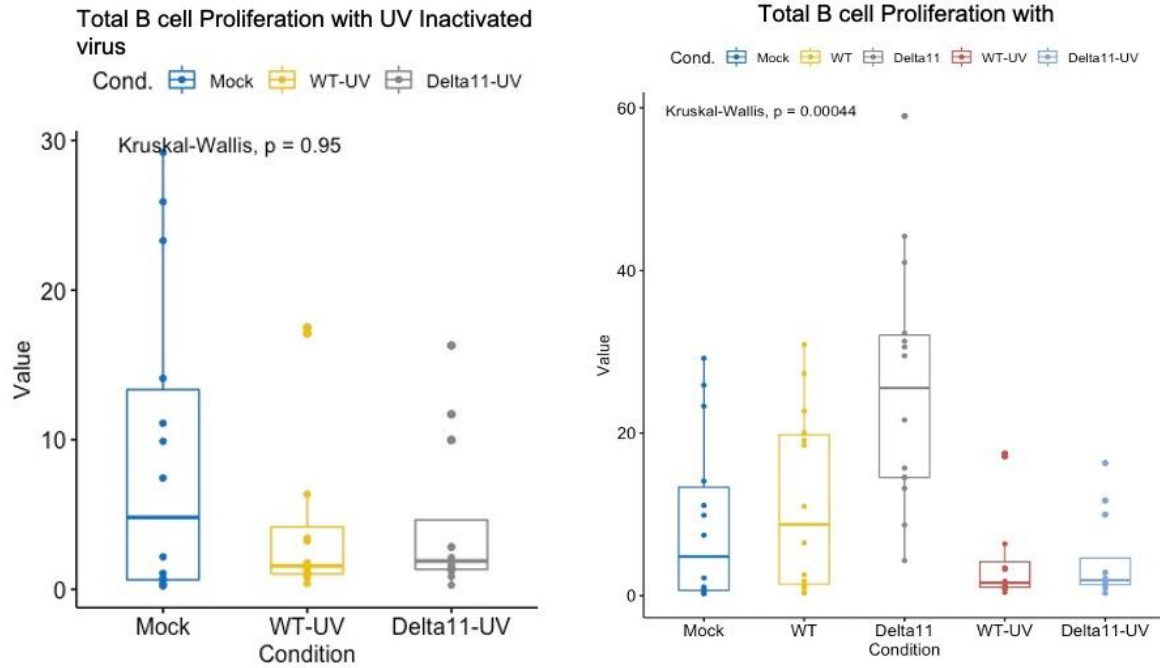


**Figure 4. 9** UV inactivated  $\Delta$ ORF11 infection of B cells does not yield any proliferation, indicating that it is not the ORF11 packaged within the virus that has an effect in the suppression of B cell proliferation but the role of newly expressed ORF11 within the infected cells, analysis is done by ggplot.

#### 4.4 Discussion and Future Directions

The ORF11 tegument protein, although highly conserved within gamma herpesviruses, is still a poorly characterized protein. This protein has been detected within the virion of KSHV (Zhu, 2005), (Bechtel, Winant, & Ganem, 2005), (Nabiee R., 2020). Furthermore, investigations on have revealed that ORF11 interacts with other tegument proteins such as ORF45, ORF64 and ORF63 suggesting a potential role in primary KSHV infection, such as virion morphology, latency establishment, or host interaction. (R. Rozen, 2008), (Zhu, 2005). Later with the discovery of a dUTPase like domain in ORF11 coding sequence, it was suggested that ORF11 protein may function as a dUTPase (A.J. Davison, 2005), yet as of now it is still not confirmed whether ORF11 is capable of such functions, due to lack of evidence (Ramirez CN, 2009.) later Chen et al. (Chen L. M. S., 2009) suggested that ORF11 promotor is not directly controlled by RTA and there might be an indirect regulation involved, however later on they also reported of identification of a silencer within ORF11 concluding that KSHV might be using a particularly novel gene regulation mechanism to precisely control ORF11 (Chen L. M. S., 2011) .

In our studies we have found that ORF11 is plasma membrane-localized and has a transmembrane domain with C-out topology.

More importantly it has been established that in MCD patients', the flare-ups episodes are closely linked to higher vIL6-expression (Sakakibara S. &, 2011), it had also been reported previously that deletion of vIL6 lead to increased expression of ORF11 (Chen L. M. L., 2006). In the current study, we report that an ORF11 knockout virus, causes selective proliferation of plasmablasts and plasma cells. Higher proliferation these two biologically/pathologically important cell types, combined with the prior knowledge of vIL6's role and contribution to lytic phase may indicate that ORF11 participates in persistence of latency through anti-proliferative effect on CD138+ B cells; a cell type which we have shown is highly targeted early in KSHV infection of tonsil lymphocyte samples (Aalam F, 2020).

One possible mechanism for this observation is that ORF11 can inhibit proliferation by inhibiting toll like receptor (TLR) signaling. TLRs are differentially expressed in various immune cells, moreover TLR ligands, such as bacterial and viral components, found at sites of infection or inflammation, affect the expression of their cognate TLRs. (Hornung V, 2002 ). It has also been reported that tonsillar B cells exhibit a constitutively high level of several TLRs. In particular, TLR1 and TLR10 (Månsson, 2006), further emphasizing the unique ability of B cells to respond directly, via TLRs, to a certain range of microbial patterns. During latency, KSHV inhibits TLR3-mediated IFN induction via vIRFs (Jacobs SR, 2013 ). In 2008 West et al. (West J, 2008 ) first reported that KSHV

upregulates the TLR3 pathway during infection to induce TLR3-specific cytokines and chemokines. More importantly it has been reported that TLR9 is the major pattern recognition receptor for KSHV infection (West JA, 2011 ). Lagos et al. found that KSHV suppresses TLR4 for immune escape during KSHV infection in endothelial cells (Lagos D, 2008 ), (Zheng, 2020). Thus, KSHV uses two mechanisms to avoid attack by the host immune system, leading to repeated infection in the host (Lagos D, 2008 ).

Such evidence strongly indicates the need for further investigation in the potential regulatory role of ORF11 in B lymphocytes KSHV infection.

### 5.1 Conclusions

Despite the vast body of research in the KSHV field, there are still major gaps in our basic understanding of KSHV host-pathogen interactions, such as the route of transmission, cellular tropism, and, more importantly, early infection events leading to establishment and persistence of KSHV in B lymphocytes. In the studies presented in this dissertation, we have aimed to address some of these gaps, by utilizing our laboratory's model system (Totonchy J, 2018 ) that benefits from the use of primary tonsil derived B cells, as well as the versatile BAC16 KSHV virion backbone and iSLK virion production cell line (Brulois, et al., 2012), (Myoung & Ganem, 2011 ). What follows is a summary of our important findings for each of our 3 aims, and their contribution towards a better understanding of KSHV virology.

#### 5.1.1 In Chapter 2:

We examined KSHV infection of tonsillar B lymphocytes from 40 human donors in order to determine whether KSHV has a particular B cell subtype tropism, as well as addressing how the presence or absence of certain immune cells influences the initial stages of KSHV infection. We observed that susceptibility to KSHV

infection does not rely on demographic factors, such as age, sex, or race.

Additionally, we observed that, although a variety of B cell subtypes derived from tonsils are susceptible to infection, KSHV has a significant tropism towards plasma cells (mature antibody-secreting B cells) in early infection events. This finding is particularly intriguing in the context of KSHV-mediated lymphoproliferative diseases, which often have a plasma cell or plasmablast-like phenotype, suggesting that the pathological cells observed in KSHV related diseases such as PEL may not be derived from KSHV-driven differentiation from less mature lineages, but instead could be the result of modifications of differentiated plasma cells by direct infection. We also studied the microenvironments present in these experiments and observed that T cell composition manipulation has a more profound effect on KSHV infection in tonsil specimens that were CD4<sup>+</sup> T cell rich at baseline. These results lay the foundation for further studies into the specific biology of KSHV in different types of B cells, an effort that may help us ultimately discover how to prevent the establishment of infection in these cells or reveal new ways to halt the progression of B cell cancers associated with KSHV infection.

### 5.1.2 In Chapter 3:

We revisited the KSHV virion proteome, which has not been re-examined since the early 2000's, even with substantial advances in both proteomics technology and the introduction of new KSHV cellular and molecular tools and cell models. Given the vital role virion packaged proteins play in early KSHV infection events, it was an unfilled gap in our basic understanding of KSHV. We re-examined the protein composition of purified KSHV virions via ultra-high resolution Qq time-of-flight mass spectrometry (UHR-QqTOF). Our results confirm the detection of all 24 previously reported virion proteins, in addition to 17 other viral proteins, some of which have been characterized as virion-associated using other methods, and 10 novel proteins identified as virion-associated for the first time in this study. These results add KSHV ORF9, ORF23, ORF35, ORF48, ORF58, ORF72/vCyclin, K3, K9/vIRF1, K10/vIRF4, and K10.5/vIRF3 to the list of KSHV proteins that can be incorporated into virions. The addition of these proteins to the KSHV virion proteome provides novel and important insight into early events in KSHV infection mediated by virion-associated proteins.

### 5.1.3 In Chapter 4:

We looked at a poorly characterized yet highly conserved tegument protein of KSHV called ORF11. As we had shown in the previous chapters of this thesis,

KSHV is the only known rhadinovirus capable of infecting B cells, and the highly conserved genes are likely to play roles specifically in B cell infection (Chapter I). In Chapter II, we were able to show that KSHV has a particular tropism for plasma cells, finally in Chapter III we demonstrated that ORF11 is abundantly present in the KSHV virion. Thus, we decided to utilize gain and loss of function approaches to further study the contribution of ORF11 to KSHV early infection events. Our studies reveal that KSHV- $\Delta$ ORF11 targets similar lineages at higher frequency compared to WT (increased number of GFP<sup>+</sup> cells with similar viral dose), indicating that ORF11 has regulatory roles in infection. In addition, KSHV- $\Delta$ ORF11 increases the frequency of specific B cell subsets (plasmablasts, and plasma cells) by increasing cellular proliferation of these cell types. These results indicate that ORF11 has a suppressive role in plasmablast proliferation and contributing to the establishment of latency. We also demonstrated that ORF11, localizes to the plasma membrane and has a transmembrane domain.

## **5.2 In Summary**

We aimed to study early KSHV infection events, in order to provide a better understanding of the less studied and poorly understood aspects of KSHV host-pathogen interactions. Our results demonstrated that KSHV has broad lymphotropism and favors infection of plasma cells. This information can further

be used to facilitate the study of KSHV transmission and conceptualize new therapeutics. Our results open doors to many other questions that could be asked within the same context, which will ultimately increase our understanding of the human immune system as well as KSHV's basic virology.

Moreover, our proteomics studies have introduced 10 new virion associated proteins, especially detection of vIRFs provides unique opportunities to study and understanding of the earliest stages of KSHV infection in new ways and how these proteins may participate in immune evasion early in KSHV infection, and how KSHV can utilize these packaged proteins to affect the environment of host cells before *de novo* transcription is started.

In chapter 4, we combined our newly found knowledge of KSHV's B cell subtype tropism and our findings of KSHV's virion proteome to further look into dynamics of KSHV-B cell interactions, and not only we were able to provide much needed information about the poorly characterized ORF11 protein but more importantly to provide information that suggests how KSHV uses its vast protein repertoire for the maintenance of latency and essentially using B cells as a viral reservoir before reactivation and infection of other human cells.

### 5.3 Future Directions

It is important to note that upon viral entry and during reactivation, the host mounts immune responses against KSHV infection mostly via innate immune receptors, especially toll-like receptor (TLR) responses, which have been shown to act as the first responders in many viral infections (Lester SN, 2014). It has also been reported that KSHV activates TLR3 (West, 2008), TLR4 (Lagos D, 2008 ), and TLR9 (West JA, 2011 ). In addition, we know that certain B cell subsets rely heavily on TLRs for regulation of proliferation and cytokine secretion (Hou, 2013). Specifically, in tonsils, they primarily rely on TLR9 (Månsson, 2006). Finally, it is worth noting that in most clinical studies, especially studies focused on MCD disease, high levels of plasmablast proliferation is consistently detected (Hassman LM, 2011 ). Moreover, elevated levels of particular viral proteins are reported, most notably vIL6 protein (Sakakibara & Tosato, 2011). Chen et al. (Chen, 2007) observed high levels of ORF11 post knockout of vIL6.

Taken together with our observations in the previous chapters, these results suggest that plasmablast differentiation during KSHV infection is regulated both positively and negatively by KSHV gene products, and these gene products may alternately influence disease progression in KSHV-associated lymphoproliferative disorders.

One way they could interact and influence these cellular responses could be via interactions with TLRs, particularly TLRs3, 4 and 9.

However, further studies are needed to more effectively shine light on host cellular signaling profile changes, especially in early infection events. Given the significant breakthroughs in deep gene sequencing, as well as cell-based small-molecule screening campaigns (Calderon, 2020), it might be beneficial to invest in utilization of these technologies combined with tools developed in our studies to be able to further analyze and study host-pathogen interactions in early KSHV events.

## References

- A. Krogh, B. L. (2001). Predicting transmembrane protein topology with a hidden Markov model: Application to complete genomes. . *Journal of Molecular Biology*, , 567-580.
- A.J. Davison, N. S. (2005). New genes from old: redeployment of dUTPase by herpesviruses . *J. Virol.*, , 12880-12892.
- Aalam F, Nabiee. R. (2020). Analysis of KSHV B lymphocyte lineage tropism in human tonsil reveals efficient infection of CD138+ plasma cells. . *PLOS Pathogens* , 16(10): e1008968.
- Akula SM, W. F. (2001 ). Human herpesvirus 8 interaction with target cells involves heparan sulfate. . *Virology*. , 245–255.
- Alkharsah KR, S. V. ( 2011 ). Deletion of Kaposi's sarcoma-associated herpesvirus FLICE inhibitory protein, vFLIP, from the viral genome comprises the activation of STAT1-responsive cellular genes and spindle cell formation in endothelial cells. *J Virol.*, 10375–10388.
- B. Lubyova, P. P. (2000 ). Characterization of a novel human herpesvirus 8-encoded protein, vIRF-3, that shows homology to viral and cellular interferon regulatory factors . *J. Virol.*, 8194-8201.
- Bacon CM, M. R.-Q. (2004 ). Pathology of bone marrow in human herpes virus-8 (HHV8)-associated multicentric Castlemans disease. . *Br J Haematol. John Wiley & Sons, Ltd;* , 585–591.
- Bai Z, H. Y. (2014). Genomewide mapping and screening of Kaposi's sarcoma-associated herpesvirus (KSHV) 3' untranslated regions identify bicistronic and polycistronic viral transcripts as frequent targets of KSHV microRNAs. . *J Virol.* , 377-392.
- Barasa A, Y. P. (2017). BALB/c mice immunized with a combination of virus-like particles incorporating Kaposi sarcoma associated herpesvirus (KSHV) envelope glycoproteins gpK8.1, gB, and gH/gL Induced comparable serum neutralizing antibody activity to UV-inactivated KSHV. . *Oncotarget* , 34481–34497.
- Bechtel, J. ., Winant, R., & Ganem, D. (2005). Host and Viral Proteins in the Virion of Kaposi's Sarcoma-Associated Herpesvirus. *journal of virology*, 4952-4964.
- Bekerman E, J. D. (2013 ). A role for host activation-induced cytidine deaminase in innate immune defense against KSHV. Gao S-J, editor. *PLoS Pathog. Public Library of Science*, e1003748.
- Bergson, S., Itzhak, I., Wasserman, T., Gelgor, A., Kalt, I., & Sarid, R. (2016). The Kaposi's-sarcoma-associated herpesvirus orf35 gene product is required for efficient lytic virus reactivation. . *Virology* , 499, 91–98.

- Bergson, S., Kalt, I., Itzhak, I., Brulois, K., Jung, J., & Sarid, R. (2014 ). Fluorescent Tagging and Cellular Distribution of the Kaposi's Sarcoma-Associated Herpesvirus ORF45 Tegument Protein. . *J. Virol.* , 12839–12852.
- Bhutani M, P. M. (2015 ). Kaposi Sarcoma–Associated Herpesvirus-Associated Malignancies \_ Epidemiology, Pathogenesis, and Advances in Treatment. *Seminars in Oncology.* . *Elsevier*, 223–246.
- Borza, C., & Hutt-Fletcher, L. (2002 ). Alternate replication in B cells and epithelial cells switches tropism of Epstein-Barr virus. . *Nat. Med.* , 594–599.
- Brulois, K., Chang, H., Lee, A.-Y., Ensser, A., Wong, L.-Y., Toth, Z., . . . al., e. (2012). Construction and manipulation of a new Kaposi's sarcoma-associated herpesvirus bacterial artificial chromosome clone. *J. Virol.*, 9708–9720.
- Brulois, K., Toth, Z., Wong, L.-Y., Feng, P., Gao, S.-J., Ensser, A., & Jung, J. (2014 ). Kaposi's sarcoma-associated herpesvirus K3 and K5 ubiquitin E3 ligases have stage-specific immune evasion roles during lytic replication. . *J. Virol.* , 9335–9349.
- Butnaru, M., & Gaglia, M. (2019). The Kaposi's Sarcoma-Associated Herpesvirus Protein ORF42 Is Required for Efficient Virion Production and Expression of Viral Proteins. . *Viruses* , 711.
- Carbone A, C. E. ( 2010 ). Understanding pathogenetic aspects and clinical presentation of primary effusion lymphoma through its derived cell lines. . *AIDS.*, 479–490.
- Carbone A, V. E. (2014 ). Diagnosis and management of lymphomas and other cancers in HIV-infected patients. *Nat Rev Clin Oncol.* . *Nature Publishing Group*, 223–238.
- Casper C, K. E.-L. (2007 ). Frequent and asymptomatic oropharyngeal shedding of human herpesvirus 8 among immunocompetent men. *J Infect Dis.* , 30–36.
- Casper C, R. M.-L. (2004). HIV infection and human herpesvirus-8 oral shedding among men who have sex with men. . *J Acquir Immune Defic Syndr.* , 233–238.
- Cesarman E, C. Y. ( 1995). Kaposi's sarcoma-associated herpesvirus-like DNA sequences in AIDS-related body-cavity-based lymphomas. . *N Engl J Med.*, 1186–1191.
- Chadburn A, H. E. (2008). Immunophenotypic analysis of the Kaposi sarcoma herpesvirus (KSHV; HHV-8)-infected B cells in HIV+ multicentric Castlemann disease (MCD). *Histopathology.* *Blackwell Publishing Ltd;* , 513-524.
- Chandran, B., Bloomer, C., Chan, S., Zhu, L., Goldstein, E., & Horvat, R. (1998). Human herpesvirus-8 ORF K8.1 gene encodes immunogenic glycoproteins generated by spliced transcripts. . *Virology* , 140–149.

- Chang, P., & Li, M. (2008). Kaposi's sarcoma-associated herpesvirus K-cyclin interacts with Cdk9 and stimulates Cdk9-mediated phosphorylation of p53 tumor suppressor. . *J. Virol.*, 278–290.
- Chang, Y., Cesarman, E., Pessin, M., Lee, F., Culpepper, J., Knowles, D., & Moore, P. (1994). Identification of herpesvirus-like DNA sequences in AIDS-associated Kaposi's sarcoma. *Science* ( 266), 1865–1869.
- Chang, Y., Moore, P., Talbot, S., Boshoff, C., Zarkowska, T., Godden-Kent, D., . . . Mitnacht, S. (1996). Cyclin encoded by KS herpesvirus. . *Nature*, 382, 410.
- Chaturvedi AK, M. S. (2008). Underestimation of relative risks by standardized incidence ratios for AIDS-related cancers. . *Ann. Epidemiol.*, 230–234.
- Chen L., M. L. (2006). The KSHV viral interleukin-6 is not essential for latency or lytic replication in BJAB cells. *J virology*, 425-435.
- Chen L., M. S. (2009). Identification and characterization of the promoter region of Kaposi's sarcoma-associated herpesvirus ORF11. *Virus Res.*, 160-168.
- Chen L., M. S. (2011). A silence element involved in Kaposi's sarcoma-associated herpesvirus ORF11 gene expression. *Acta virologica*.
- Chen, L. &. (2007). Establishment and maintenance of Kaposi's sarcoma-associated herpesvirus latency in B cells. *Journal of virology*, 14383–14391.
- Chow, D.-C., He, X., Snow, A., Rose-John, S., & Garcia, K. (2001). Structure of an Extracellular gp130 Cytokine Receptor Signaling Complex. . *Science*, 2150–2155.
- Coscoy, L., & Ganem, D. ( 2000 ). Kaposi's sarcoma-associated herpesvirus encodes two proteins that block cell surface display of MHC class I chains by enhancing their endocytosis. *Proc. Natl. Acad. Sci. USA*, 8051–8056.
- Dünn-Kittenplon, D., Kalt, I., Lellouche, J., & Sarid, R. (2019). The KSHV portal protein ORF43 is essential for the production of infectious viral particles. . *Virology*, 205–215.
- Dai, X., Gong, D., Wu, T.-T., Sun, R., & Zhou, Z. ( 2014 ). Organization of Capsid-Associated Tegument Components in Kaposi's Sarcoma-Associated Herpesvirus. . *J. Virol.*, 12694–12702.
- Davis, D., Rinderknecht, A., Zoetewij, J., Aoki, Y., Read-Connole, E., Tosato, G., . . . Yarrow, R. (2001). Hypoxia induces lytic replication of Kaposi sarcoma-associated herpesvirus. . *Blood*, 3244–3250.
- De Oliveira, D., Ballon, G., & Cesarman, E. (2010). NF- $\kappa$ B signaling modulation by EBV and KSHV. . *Trends Microbiol.*, 248–257.

- De Oliveira, D., Ballon, G., & Cesarman, E. (2010). NF- $\kappa$ B signaling modulation by EBV and KSHV. . *Trends Microbiol.* , 248–257.
- den Ridder, M., Daran-Lapujade, P., & Pabst, M. (2020 ). Shot-gun proteomics: Why thousands of unidentified signals matter. . *FEMS Yeast Res.* , foz088.
- Deutsch, E., Bandeira, N., Sharma, V., Perez-Riverol, Y., Carver, J., Kundu, D., . . . al., e. (2020). The ProteomeXchange consortium in 2020: Enabling ‘big data’ approaches in proteomics. *Nucleic Acids Res.* , 1145–1152.
- Dollery SJ, S.-C. R. (2018). Glycoprotein K8.1A of Kaposi's sarcoma-associated herpesvirus is a critical B cell tropism determinant, independent of its heparan sulfate binding activity. . *J Virol.* , 1–38.
- Drexler, H. e. (1998 ). “Lymphoma cell lines: in vitro models for the study of HHV-8+ primary effusion lymphomas (body cavity-based lymphomas).”. *Leukemia* , 1507-1517.
- Dyson, O., Walker, L., Whitehouse, A., Cook, P., & Akula, S. (2012). Resveratrol Inhibits KSHV Reactivation by Lowering the Levels of Cellular EGR-1. . *PLoS ONE* , e33364.
- Ford, T., Graham, J., & Rickwood, D. (1994 ). Iodixanol: A Nonionic Iso-osmotic Centrifugation Medium for the Formation of Self-Generated Gradients. . *Anal. Biochem.* , 360–366.
- Friborg J Jr, K. W. (1998 ). Distinct biology of Kaposi's sarcoma-associated herpesvirus from primary lesions and body cavity lymphomas. . *J Virol.* , 10073–10082.
- G. Miller, L. H. (1997). Chang Selective switch between latency and lytic replication of Kaposi's sarcoma herpesvirus and Epstein–Barr virus in dually infected body cavity. *J. Virol*, 314-324.
- G. Miller, L. H. (1997 ). Selective switch between latency and lytic replication of Kaposi's sarcoma herpesvirus and Epstein–Barr virus in dually infected body cavity lymphoma cells. *J. Virol.*, 314-324.
- Gao, S., Boshoff, C., Jayachandra, S., Weiss, R., Chang, Y., & Moore, P. (1997). KSHV ORF K9 (vIRF) is an oncogene which inhibits the interferon signaling pathway. . *Oncogene* , 1979–1985.
- Garrigues, H., Rubinchikova, Y., DiPersio, C., & Rose, T. (2008 ). Integrin  $\alpha$ V $\beta$ 3 Binds to the RGD Motif of Glycoprotein B of Kaposi's Sarcoma-Associated Herpesvirus and Functions as an RGD-Dependent Entry Receptor. . *J. Virol.* , 1570–1580.
- Giffin, L., West, J., & Damania, B. (2015 ). Kaposi's Sarcoma-Associated Herpesvirus Interleukin-6 Modulates Endothelial Cell Movement by Upregulating Cellular Genes Involved in Migration. . *mBio* , e01499-15.

- Godden-Kent, D., Talbot, S., Boshoff, C., Chang, Y., Moore, P., Weiss, R., & Mittnacht, S. (1997). The cyclin encoded by Kaposi's sarcoma-associated herpesvirus stimulates cdk6 to phosphorylate the retinoblastoma protein and histone H1. . *J. Virol.* , 4193.
- Gonçalves PH, U. T. (2017 ). HIV-associated Kaposi sarcoma and related diseases. . *AIDS.* , 1903–1916.
- Gong, D., Wu, N., Xie, Y., Feng, J., Tong, L., Brulois, K., . . . al., e. (2014). Kaposi's Sarcoma-Associated Herpesvirus ORF18 and ORF30 Are Essential for Late Gene Expression during Lytic Replication. . *J. Virol.* , 11369–11382.
- Großkopf AK, S. S. (2019). EphA7 Functions as Receptor on BJAB Cells for Cell-to-Cell Transmission of the Kaposi's Sarcoma-Associated Herpesvirus and for Cell-Free Infection by the Related Rhesus Monkey Rhadi Rhadinovirus. . *Jung JU, editor. J Virol*, 1029.
- Grundhoff, A., & Ganem, D. (2004 ). Inefficient establishment of KSHV latency suggests an additional role for continued lytic replication in Kaposi sarcoma pathogenesis. . *J. Clin. Investig.* , 124–136.
- H. Deng, M. S. (2002 ). Transcriptional regulation of the interleukin-6 gene of human herpesvirus 8 (Kaposi's sarcoma-associated herpesvirus) . *J. Virol.*, 8252-8264.
- H. Nakamura, M. L. (2003). Global changes in Kaposi's sarcoma-associated virus gene expression patterns following expression of a tetracycline-inducible Rta transactivator . *J. Virol.* , 4205-4220.
- Hahn A, B. A. (2009 ). Kaposi's sarcoma-associated herpesvirus gH/gL: glycoprotein export and interaction with cellular receptors. *J Virol. American Society for Microbiology Journals*, 396–407.
- Hassman LM, E. T. (2011 ). KSHV infects a subset of human tonsillar B cells, driving proliferation and plasmablast differentiation. *J Clin Invest.* , 752–768.
- Hikita, S., Yanagi, Y., & Ohno, S. (2015). Murine gammaherpesvirus 68 ORF35 is required for efficient lytic replication and latency. *J. Gen. Virol.* , 96, 3624–3634.
- Holzerlandt, R., Orengo, C., Kellam, P., & Albà, M. ( 2002). Identification of new herpesvirus gene homologs in the human genome. . *Genome Res.*, 12, 1739–1748.
- Hornung V, R. S. (2002 ). Quantitative expression of toll-like receptor 1-10 mRNA in cellular subsets of human peripheral blood mononuclear cells and sensitivity to CpG oligodeoxynucleotides. *J Immunol.*, 68(9):4531-7.
- Hu D, W. V. (2016 ). Induction of Kaposi's Sarcoma-Associated Herpesvirus-Encoded Viral Interleukin-6 by X-Box Binding Protein 1. . *Frueh K, editor. J Virol. American Society for Microbiology Journals;* , 368–378.

- Hwang, S., Kim, D., Jung, J., & Lee, H. (2017). KSHV-encoded viral interferon regulatory factor 4 (vIRF4) interacts with IRF7 and inhibits interferon alpha production. *Biochem. Biophys. Res. Commun.*, 700–705.
- Ibrahim HAH, B. K. (2016). Bone marrow manifestations in multicentric Castleman disease. . *Br J Haematol. John Wiley & Sons, Ltd;*, 923–929.
- Iwakoshi NN, L. A.-H. (2003). Plasma cell differentiation and the unfolded protein response intersect at the transcription factor XBP-1. . *Nat Immunol. Nature Publishing Group;*, 321–329.
- Jacobs SR, G. S. (2013). The viral interferon regulatory factors of kaposi's sarcoma-associated herpesvirus differ in their inhibition of interferon activation mediated by toll-like receptor 3. . *J Virol.*, 87(2):798-806.
- Jarousse N, T. D.-A. (2011). Virally-induced upregulation of heparan sulfate on B cells via the action of type I IFN. . *J Immunol. American Association of Immunologists*, 5540–5547.
- Jenner, R., Albà, M., Boshoff, C., & Kellam, P. (2001). Kaposi's sarcoma-associated herpesvirus latent and lytic gene expression as revealed by DNA arrays. . *J. Virol.*, 891–902.
- JN., M. (2007. ). The epidemiology of KSHV and its association with malignant disease. In: Arvin A, Campadelli-Fiume G, Mocarski E, et al., editors. Human Herpesviruses: Biology, Therapy, and Immunoprophylaxis. . *Cambridge: Cambridge University Press;*, Chapter 54.
- Johnson KE, T. V. (2020). Gammaherpesviruses and B Cells: A Relationship That Lasts a Lifetime. . *Viral Immunol.*, 316–326.
- Jones, T., Ramos da Silva, S., Bedolla, R., Ye, F., Zhou, F., & Gao, S. ( 2014 ). Viral cyclin promotes KSHV-induced cellular transformation and tumorigenesis by overriding contact inhibition. *Cell Cycle*, 845–858.
- K. Borchers, M. G. (1994). Genome organization of the herpesviruses: minireview . *Acta Vet. Hung*, 217-225.
- K.A. Staskus, W. Z. (1997). Haase Kaposi's sarcoma-associated herpesvirus gene expression in endothelial (spindle) tumor cells. *J. Virol.*, 715-71.
- Kang S, M. J. (2017). Primary lymphocyte infection models for KSHV and its putative tumorigenesis mechanisms in B cell lymphomas. . *J Microbiol. The Microbiological Society of Korea*, 319–329.
- Karass, M. e. (2017). “Kaposi Sarcoma Inflammatory Cytokine Syndrome (KICS): A Rare but Potentially Treatable Condition..”*The oncologist vol. 22,5*, 623-625.

- Karass, M., Grossniklaus, E., Seoud, T., Jain, S., & Goldstein, D. (2017). Kaposi Sarcoma Inflammatory Cytokine Syndrome (KICS): A Rare but Potentially Treatable Condition. *Oncologist*, 623–625.
- Katano, H., Sato, Y., Kurata, T., Mori, S., & Sata, T. (2000). Expression and localization of human herpesvirus 8-encoded proteins in primary effusion lymphoma, Kaposi's sarcoma, and multicentric Castleman's disease. *Virology*, 335–344.
- Knowlton ER, R. G. (2014). Human herpesvirus 8 induces polyfunctional B lymphocytes that drive Kaposi's sarcoma. *MBio.*, e01277–14.
- Lagos D, V. R. (2008). Toll-like receptor 4 mediates innate immunity to Kaposi sarcoma herpesvirus. *Cell Host Microbe.*, 470-83.
- Lagunoff, L. C. (2007). The KSHV viral interleukin-6 is not essential for latency or lytic replication in BJAB cells. *J. Virology*, 425-435.
- Lang, S., Bynoe, M., Karki, R., Tartell, M., & Means, R. (2013). Kaposi's sarcoma-associated herpesvirus K3 and K5 proteins down regulate both DC-SIGN and DC-SIGNR. *PLoS ONE*, e58056.
- Lee, H.-R., Doğanay, S., Chung, B., Toth, Z., Brulois, K., Lee, S., . . . Jung, J. (2014). Kaposi's sarcoma-associated herpesvirus viral interferon regulatory factor 4 (vIRF4) targets expression of cellular IRF4 and the Myc gene to facilitate lytic replication. *J. Virol.*, 2183–2194.
- Li, M., Lee, H., Yoon, D., Albrecht, J., Fleckenstein, B., Neipel, F., & Jung, J. (1997). Kaposi's sarcoma-associated herpesvirus encodes a functional cyclin. *J. Virol.*, 1984–1991.
- Longnecker R, N. F. (2007). Introduction to the human  $\gamma$ -herpesviruses. In: Arvin A, Campadelli-Fiume G, Mocarski E, et al., editors. Human Herpesviruses: Biology, Therapy, and Immunoprophylaxis. *Cambridge: Cambridge University Press*; , Chapter 22.
- Lorenzo, M., Jung, J., & Ploegh, H. (2002). Kaposi's sarcoma-associated herpesvirus K3 utilizes the ubiquitin-proteasome system in routing class major histocompatibility complexes to late endocytic compartments. *J. Virol.*, 5522–5531.
- Lukac DM, Y. Y.-F. (2007). Human Herpesviruses: Biology, Therapy, and Immunoprophylaxis. *Cambridge: Cambridge University Press*; , Chapter 26.
- M.M. Alba, D. L. (2001). VIDA: a virus database system for the organization of animal virus genome open reading frames. *Nucleic Acids Res.*, 133-136.
- Mahnke YD, B. T. (2013). The who's who of T-cell differentiation: human memory T-cell subsets. *EurJ Immunol. John Wiley & Sons, Ltd*; , 2797–2809.

- Majerciak, V., Pripuzova, N., McCoy, J., Gao, S., & Zheng, Z. (2007). Targeted disruption of Kaposi's sarcoma-associated herpesvirus ORF57 in the viral genome is detrimental for the expression of ORF59, K8alpha, and K8.1 and the production of infectious virus. *J. Virol.* , 1062–1071.
- Majerciak, V., Yamanegi, K., & Zheng, Z. G.-a.-1. (2006). Gene structure and expression of Kaposi's sarcoma-associated herpesvirus ORF56, ORF57, ORF58, and ORF59. *J. Virol.* , 11968–11981.
- Månsson, A. A. (2006). A distinct Toll-like receptor repertoire in human tonsillar B cells, directly activated by PamCSK, R-837 and CpG-2006 stimulation. *Immunology* , 118(4), 539–548. .
- Meads, M., & Medveczky, P. (2004). Kaposi's sarcoma-associated herpesvirus-encoded viral interleukin-6 is secreted and modified differently than human interleukin-6: Evidence for a unique autocrine signaling mechanism. *J. Biol. Chem.* , 51793–51803.
- Medina F, S. C.-C.-G. (2002). The heterogeneity shown by human plasma cells from tonsil, blood, and bone marrow reveals graded stages of increasing maturity, but local profiles of adhesion molecule expression. *Blood.* , 2154-2161.
- Meggetto F, C. E. (2001). Detection and characterization of human herpesvirus-8—Infected cells in bone marrow biopsies of human immunodeficiency virus—Positive patients. *Human Pathology.* , 288–291.
- Mesri EA, C. E. (2010). Kaposi's sarcoma and its associated herpesvirus. *Nat Rev Cancer.* , 707–719.
- Minhas, V. &. (2014). Epidemiology and transmission of Kaposi's sarcoma-associated herpesvirus. *Viruses*, 4178–4194.
- Moore, P., Boshoff, C., Weiss, R., & Chang, Y. (1996). Molecular mimicry of human cytokine and cytokine response pathway genes by KSHV. *Science* , 1739–1744.
- Moore, P., Gao, S., Dominguez, G., Cesarman, E., Lungu, O., Knowles, D., . . . Chang, Y. (1996). Primary characterization of a herpesvirus agent associated with Kaposi's sarcomae. *J. Virol.* , 549–558.
- Muniraju M, M. L. (2019). Kaposi Sarcoma-Associated Herpesvirus Glycoprotein H Is Indispensable for Infection of Epithelial, Endothelial, and Fibroblast Cell Types. *Longnecker RM, editor. J Virol.* , 140.
- Myoung J, G. D. (2011). Active lytic infection of human primary tonsillar B cells by KSHV and its noncytolytic control by activated CD4+ T cells. *J Clin Invest.* , 1130–1140.
- Myoung J, G. D. (2011). Infection of primary human tonsillar lymphoid cells by KSHV reveals frequent but abortive infection of T cells. *Virology.* , 1–11.

- Myoung, J., & Ganem, D. (2011). Generation of a doxycycline-inducible KSHV producer cell line of endothelial origin: Maintenance of tight latency with efficient reactivation upon induction. *J. Virol. Methods*, 12–21.
- Nabiee R., B. S. (2020). An Update of the Virion Proteome of Kaposi Sarcoma-Associated Herpesvirus. *Viruses*, 1382.
- Naranatt, P., Krishnan, H., Svojanovsky, S., Bloomer, C., Mathur, S., & Chandran, B. (2004). Host Gene Induction and Transcriptional Reprogramming in Kaposi's Sarcoma-Associated Herpesvirus (KSHV/HHV-8)-Infected Endothelial, Fibroblast, and B Cells. *Cancer Res*, 72-84.
- Neipel, F., Albrecht, J., Ensser, A., Huang, Y., Li, J., Friedman-Kien, A., & Fleckenstein, B. (1997). Human herpesvirus 8 encodes a homolog of interleukin-6. *J. Virol.*, 839–842.
- Neuwirth E. RColorBrewer: ColorBrewer Palettes [Internet]. Available: <https://CRAN.R-project.org/package=RColorBrewer>.
- Newton, R., Labo, N., Wakeham, K., Marshall, V., Roshan, R., Nalwoga, A., . . . al., e. (2018). Determinants of Gammaherpesvirus Shedding in Saliva Among Ugandan Children and Their Mothers. *J. Infect. Dis.*, 892–9.
- Nicol SM, S. S. (2016). Primary B Lymphocytes Infected with Kaposi's Sarcoma-Associated Herpesvirus Can Be Expanded In Vitro and Are Recognized by LANA-Specific CD4+ T Cells. *Frueh K, editor. J Virol. American Society for Microbiology*, 3849–3859.
- Nishimura, M., Watanabe, T., Yagi, S., Yamanaka, T., & Fujimuro, M. (2017). Kaposi's sarcoma-associated herpesvirus ORF34 is essential for late gene expression and virus production. *Sci. Rep.*, 329.
- Ohno, S., Steer, B., Sattler, C., & Adler, H. (2012). ORF23 of murine gammaherpesvirus 68 is non-essential for in vitro and in vivo infection. *J. Gen. Virol.*, 93 Pt 5, 1076–1080.
- Pauk J, H. M. (2000). Mucosal shedding of human herpesvirus 8 in men. *N Engl J Med. Massachusetts Medical Society*, 1369–1377.
- Paulose-Murphy, M., Ha, N.-K., Xiang, C., Chen, Y., Gillim, L., Yarchoan, R., . . . Zeichner, S. (2001). Transcription Program of Human Herpesvirus 8 (Kaposi's Sarcoma-Associated Herpesvirus). *J. Virol.*, 4843–4853.
- Perez-Riverol, Y., Csordas, A., Bai, J., Bernal-Llinares, M., Hewapathirana, S., Kundu, D., . . . al., e. (2019). The PRIDE database and related tools and resources in 2019: Improving support for quantification data. *Nucleic Acids Res.*, 442–450.
- Perez-Riverol, Y., Xu, Q., Wang, R., Uszkoreit, J., Griss, J., Sanchez, A., . . . al, e. (2016). PRIDE Inspector Toolsuite: Moving towards a universal visualization tool for proteomics data standard formats and quality assessment of ProteomeXchange datasets. *Mol. Cell. Proteom.*, 305–317.

- Petra D, P. K. (2015). Polyclonal, newly derived T cells with low expression of inhibitory molecule PD-1 in tonsils define the phenotype of lymphocytes in children with Periodic Fever, Aphthous Stomatitis, Pharyngitis and Adenitis (PFAPA) syndrome. . *Molecular Immunology. Elsevier*, 139-147.
- Powles T, R. D. (2009 ). Highly Active Antiretroviral Therapy and the Incidence of Non-AIDS-Defining Cancers in People With HIV Infection. . *Journal of Clinical Oncology*. , 884–890.
- Pozharskaya, V., Weakland, L., Zimring, J., Krug, L., Unger, E., Neisch, A., . . . Offermann, M. (2004 ). Short duration of elevated vIRF-1 expression during lytic replication of human herpesvirus 8 limits its ability to block antiviral responses induced by alpha interferon in BCBL-1 cells. *J. Virol.* , 6621–6635.
- Qi, J., Han, C., Gong, D., Liu, P., Zhou, S., & Deng, H. (2015 ). Murine Gammaherpesvirus 68 ORF48 Is an RTA-Responsive Gene Product and Functions in both Viral Lytic Replication and Latency during In Vivo Infection. *J. Virol.* , 5788–5800.
- Quiceno, J. (2010). *Characterization of Kaposi's Sarcoma-Associated Herpesvirus Open Reading Frames 58 and 27. Thesis.* South Orange, NJ, USA, : Seton Hall University, .
- R. Renne, W. Z. (1996 ). Lytic growth of Kaposi's sarcoma-associated herpesvirus (human herpesvirus 8) in culture . *Nat. Med.*, 342-346.
- R. Rozen, N. S. (2008). Virion-wide protein interactions of Kaposi's sarcoma-associated herpesvirus. *J. Virol.* , 4742-4750.
- R. Sarid, O. F. (1998 ). Transcription mapping of the Kaposi's sarcoma-associated herpesvirus (human herpesvirus 8) genome in a body cavity-based lymphoma cell line (BC-1) . *J. Virol.* , 1005-1012.
- R. Sun, S. L. (1998 ). A viral gene that activates lytic cycle expression of Kaposi's sarcoma-associated herpesvirus . *Proc. Natl. Acad. Sci. U.S.A.*, , 10866-10871.
- R.G. Jenner, M. A. (2001). Kaposi's sarcoma-associated herpesvirus latent and lytic gene expression as revealed by DNA arrays . *J. Virol.* , 891-902.
- R: A language and environment for statistical computing [Internet]. Vienna, Austria: R Foundation for Statistical Computing. Available: <https://www.R-project.org>.
- Rabkin CS, B. R. (1991 ). Increasing incidence of cancers associated with the human immunodeficiency virus epidemic. . *Int J Cancer*. , 692–696.
- Ramirez CN, C. S. (2009.). *KSHV 12th International Workshop.* KSHV 12th International Workshop.

- Rappocciolo G, H. H. (2008 ). Human herpesvirus 8 infects and replicates in primary cultures of activated B lymphocytes through DC-SIGN. . *J Virol. American Society for Microbiology Journals*, 4793–4806.
- Roizman, B., Carmichael, L., Deinhardt, F., De-The, G., Nahmias, A., Plowright, W., . . . Wolf, K. (1981 ). Herpesviridae. Definition, provisional nomenclature, and taxonomy. The Herpesvirus Study Group, the International Committee on Taxonomy of Viruses. *Intervirology* , 201–217.
- Russo, J., Bohenzky, R., Chien, M.-C., Chen, J., Yan, M., Maddalena, D., . . . al., e. (1996 ). Nucleotide sequence of the Kaposi sarcoma-associated herpesvirus (HHV8). . *Proc. Natl. Acad. Sci. USA* , 14862–148.
- Sakakibara, S. &. (2011). Viral interleukin-6: role in Kaposi's sarcoma-associated herpesvirus: associated malignancies. *Journal of interferon & cytokine research : the official journal of the International Society for Interferon and Cytokine R. journal of interferon & cytokine research : the official journal of the International Society for Interferon and Cytokine Research*, 791-801.
- Sakakibara, S., & Tosato, G. (2011). Viral interleukin-6: Role in Kaposi's sarcoma-associated herpesvirus: Associated malignancies. . *J. Interferon Cytokine Res.* , 791–801.
- Sander, G., Konrad, A., Thureau, M., Wies, E., Leubert, R., Kremmer, E., . . . Stürzl, M. (2007 ). Intracellular Localization Map of Human Herpesvirus 8 Proteins. . *J. Virol.* , 1908–1922.
- Sathish N, W. X. (2012 ). Tegument Proteins of Kaposi's Sarcoma-Associated Herpesvirus and Related Gamma-Herpesviruses. . *Front Microbiol.* , 98.
- Schmidt, K., Wies, E., & Neipel, F. (2011 ). Kaposi's sarcoma-associated herpesvirus viral interferon regulatory factor 3 inhibits gamma interferon and major histocompatibility complex class II expression. . *J. Virol.* , 4530–4537.
- Shevchenko, A., Tomas, H., Havlis, J., Olsen, J., & Mann, M. (2006 ). In-gel digestion for mass spectrometric characterization of proteins and proteomes. . *Nat. Protoc.* , 2856–2860.
- Shin, H., Decotiis, J., Giron, M., Palmeri, D., & Lukac, D. (2013). Histone Deacetylase Classes I and II Regulate Kaposi's Sarcoma-Associated Herpesvirus Reactivation. . *J. Virol.* , 1281–1292.
- Soulier J, G. L.-H. (1995). Kaposi's sarcoma-associated herpesvirus-like DNA sequences in multicentric Castleman's disease. . *Blood*, 1276–1280.
- Speck, S., & Ganem, D. (2010). Viral Latency and Its Regulation: Lessons from the  $\gamma$ -Herpesviruses. . *Cell Host Microbe*, 100–115.
- Stanisce L, S. E. ( 2018 ). Differential cellular composition of human palatine and pharyngeal tonsils. . *Archives of Oral Biology.*, 80–86.

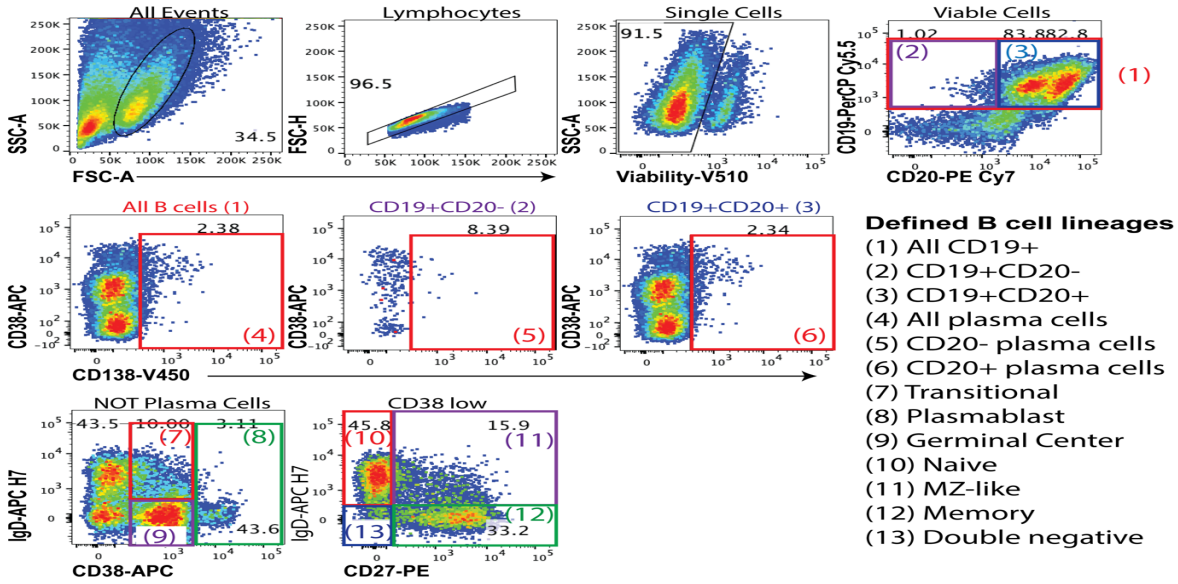
- Swanton, C., Mann, D., Fleckenstein, B., Neipel, F., Peters, G., & Jones, N. (1997). Herpes viral cyclin/Cdk6 complexes evade inhibition by CDK inhibitor proteins. . *Nature* , 184–187.
- Thakur, S., Geiger, T., Chatterjee, B., Bandilla, P., Fröhlich, F., Cox, J., & Mann, M. (2011). Deep and hoverly sensitive proteome coverage by LC-MS/MS without prefractionation. . *Mol Cell Proteom.* , 10.
- Totonchy J, O. J. (2018). KSHV induces immunoglobulin rearrangements in mature B lymphocytes. . *Coscoy L, editor. PLoS Pathog.* , e1006967.
- Trus BL, H. J. (2001). Capsid structure of Kaposi's sarcoma-associated herpesvirus, a gammaherpesvirus, compared to those of an alphaherpesvirus, herpes simplex virus type 1, and a betaherpesvirus, cytomegalovirus. . *J Virol.* , 2879-2890.
- Tsirigos KD, P. C. (2015). The TOPCONS web server for consensus prediction of membrane protein topology and signal peptides. *Nucleic Acids Res.* , 43.
- Uldrick TS, W. V. (2010). An interleukin-6-related systemic inflammatory syndrome in patients co-infected with Kaposi sarcoma-associated herpesvirus and HIV but without Multicentric Castleman disease. . *CLIN INFECT DIS.* , 350–358.
- van Zelm MC, S. T. (2007). Replication history of B lymphocytes reveals homeostatic proliferation and extensive antigen-induced B cell expansion. . *J Exp Med. Rockefeller Univ Press;* , 645–655.
- Varon LS, D. R. (2017). Characterization of tonsillar IL10 secreting B cells and their role in the pathophysiology of tonsillar hypertrophy. *Sci Rep. Springer US;* , 1–9.
- Vieira J, H. M. (1997). Transmissible Kaposi's sarcoma-associated herpesvirus (human herpesvirus 8) in saliva of men with a history of Kaposi's sarcoma. . *J Virol. American Society for Microbiology (ASM)*, 7083–7087.
- Vieira, J., O'Hearn, P., Kimball, L., Chandran, B., & Corey, L. (2001). Activation of Kaposi's Sarcoma-Associated Herpesvirus (Human Herpesvirus 8) Lytic Replication by Human Cytomegalovirus. . *J. Virol.* , 1378–1386.
- Wabinga HR, P. D.-M. (1993). Cancer in Kampala, Uganda, in 1989–1991: changes in incidence in the era of AIDS. *Int J Cancer.* , 26–36.
- West J, D. B. (2008). Upregulation of the TLR3 pathway by Kaposi's sarcoma-associated herpesvirus during primary infection. *J Virol.* , 5440-9.
- West JA, G. S. (2011). Activation of plasmacytoid dendritic cells by Kaposi's sarcoma-associated herpesvirus. *J Virol.*, 895-904.
- Wickham H. ggplot2: Elegant Graphics for Data Analysis [Internet]. New York: Springer-Verlag. Available: <http://ggplot2.org/year>.

- Wies, E., Mori, Y., Hahn, A., Kremmer, E., Stürzl, M., Fleckenstein, B., & Neipel, F. (2008 ). The viral interferon-regulatory factor-3 is required for the survival of KSHV-infected primary effusion lymphoma cells. . *Blood J. Am. Soc. Hematol.* , 320–327.
- Wu, F., Ahn, J.-H., Alcendor, D., Jang, W.-J., Xiao, J., Hayward, S., & Hayward, G. (2001). Origin-independent assembly of Kaposi's sarcoma-associated herpesvirus DNA replication compartments in transient cotransfection assays and association with the ORF-K8 protein and cellular PML. *J. Virol.* , 75, 1487–1506.
- Wu, J., Avey, D., Li, W., Gillen, J., Fu, B., Miley, W., . . . Zhu, F. (2015). ORF33 and ORF38 of Kaposi's Sarcoma-Associated Herpesvirus Interact and Are Required for Optimal Production of Infectious Progeny Viruses. . *J. Virol.* , 1741–1756.
- Yates, J. 3. (1998 ). Mass spectrometry and the age of the proteome. . *J. Mass Spectrom.* , 1–19.
- Ye, F., Zhou, F., Bedolla, R., Jones, T., Lei, X., Kang, T., . . . Gao, S.-J. (2011). Reactive Oxygen Species Hydrogen Peroxide Mediates Kaposi's Sarcoma-Associated Herpesvirus Reactivation from Latency. . *PLoS Pathog.* , e1002054.
- Yu, F., Harada, J., Brown, H., Deng, H., Song, M., Wu, T.-T., . . . al., e. (2007). Systematic Identification of Cellular Signals Reactivating Kaposi Sarcoma–Associated Herpesvirus. . *PLoS Pathog.* .
- Zhang, J., Xin, L., Shan, B., Chen, W., Xie, M., Yuen, D., . . . Ma, B. (2012). PEAKS DB:De Novo Sequencing Assisted Database Search for Sensitive and Accurate Peptide Identification. . *Mol. Cell. Proteom.* , 11.
- Zhang, Y., Fonslow, B., Shan, B., Baek, M.-C., & Yates, J. (2013 ). Protein Analysis by Shotgun/Bottom-up Proteomics. . *Chem. Rev.* , 2343–2394.
- Zheng, W. X. (2020). Toll-like receptor-mediated innate immunity against herpesviridae infection: a current perspective on viral infection signaling pathways. . *J Virology* , 192.
- Zhou, F.-C. e. (2002). “Efficient infection by a recombinant Kaposi's sarcoma-associated herpesvirus cloned in a bacterial artificial chromosome: application for genetic analysis..”*Journal of virology vol. 76,12*, 6185-96.
- Zhu, F. (2005). Virion Proteins of Kaposi's Sarcoma-Associated Herpesvirus. . *J. Virol.* , 800-811.
- Zhu, F., King, S., Smith, E., Levy, D., & Yuan, Y. A. (2002). Kaposi's sarcoma-associated herpesviral protein inhibits virus-mediated induction of type I interferon by blocking IRF-7 phosphorylation and nuclear accumulation. *Proc. Natl. Acad. Sci. USA* , 5573–5578.
- Zhu, F., Sathish, N., & Yuan, Y. (2010). Antagonism of Host Antiviral Responses by Kaposi's Sarcoma-Associated Herpesvirus Tegument Protein ORF45. . *PLoS ONE* , e10573.

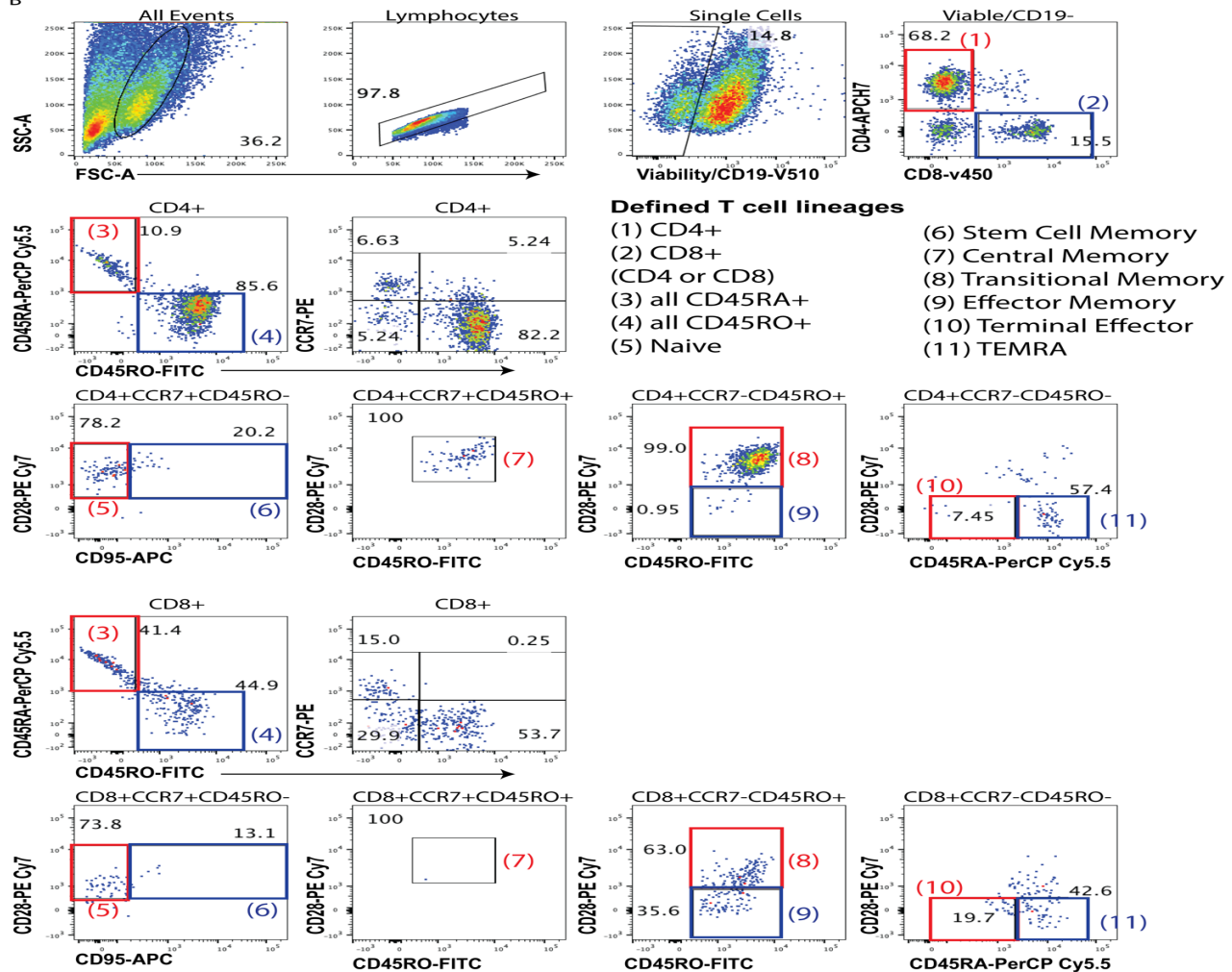
# **Appendix A. Supplementary data from Chapter 2**

## **A.1 Gating schemes for tonsil lymphocyte lineages.**

A



B



**Supplemental Figure 1: Gating schemes tonsil lymphocyte lineages.** Flow cytometry data for a baseline uninfected sample from a 2-year-old male donor showing representative gating and lineage definitions used in the study for (A) B cell lineages based on 31 and (B) T cell lineages based on 32.

Flow cytometry data for a baseline uninfected sample from a 2-year-old male donor showing representative gating and lineage definitions used in the study for (A) B cell lineages based on vanZelm et. al. 2007 (van Zelm MC, 2007 ) and (B) T cell lineages based on Mahnke et. al. 2013 (Mahnke YD, 2013 ).

## **A.2 Analyzed flow cytometry data.**

Values derived from flow cytometry analysis for baseline B cell and T cell lineage frequencies, overall infection frequency at 3dpi and lineage-specific infection frequencies for B cells. Comments associated with column headers contain detailed definitions for each subset. <https://doi.org/10.1371/journal.ppat.1008968.s002> (XLSX)



### **A.3 Analyzed flow cytometry data for B cell lineages at 3 days post infection.**

Values derived from flow cytometry analysis for overall B cell lineage frequencies in Mock and KSHV-infected cultures at 3 days post-infection. Abbreviations and lineage definitions are as in S1 Table comments. <https://doi.org/10.1371/journal.ppat.1008968.s003> (XLSX)

CD19B	CD19_PC	AIIB	All_PC	DN	Mem	Na	NE	GC	PB	Trans	DP	DPPC	Sample	Cond
1.74	4.64	49.6	0.95	5.88	7.95	2.4	2.7	42.6	13.7	23.8	47.6	0.82	ND11	Mock
1.2	2.02	53.7	0.45	4.61	5.96	2.39	2.43	33.3	22.4	28.5	52.4	0.42	ND11	Mock
1.45	5.51	49.6	1.95	4.96	8.45	1.52	2.73	45	15.1	20.4	48.1	1.82	ND11	KSHV
0.98	6.98	57	1.81	4.15	6.18	2.23	3.51	34.8	20.9	26.5	55.9	1.73	ND11	KSHV
1.11	0.35	84.1	0.37	10.5	40.9	2.01	28.5	19.9	7.11	64	83	0.37	ND12	Mock
1.23	0.37	85.8	0.39	10.2	41.2	2.12	27.3	19.6	5.76	65	84.6	0.39	ND12	Mock
1.14	3.23	86.5	0.36	9.86	43.1	20.7	26.4	20.5	5.99	63.5	85.3	0.32	ND12	KSHV
1.39	2.35	85.4	0.43	9.88	44	22.6	23.5	21.8	5.92	62.8	84	0.39	ND12	KSHV
1.38	0	55	0.25	4.27	5.65	2.89	2.26	47.8	8.41	28.6	53.4	0.26	ND14	Mock
0.76	0	57.2	0.56	3.67	7.13	1.67	3.23	48.4	8.8	26.5	56.3	0.57	ND14	KSHV
2.53	0	87.7	0.16	1.61	57.4	8.73	32.3	19.2	0.7	62.8	85.2	0.16	ND15	Mock
2.38	1.02	85.7	0.28	1.94	58	9.89	30.2	18.8	0.86	60.4	83.3	0.25	ND15	KSHV
1.63	0	80.7	0.21	8.77	32.1	25.8	33.4	31.5	1.78	56.8	79.1	0.21	ND18	Mock
1.05	1.23	82.9	0.29	10.3	35	21.6	33.1	33.6	2.82	55.7	81.8	0.27	ND18	KSHV
0.47	1.67	88.2	0.12	5.2	23	39	32.8	16.1	0.8	74.9	87.7	0.12	ND19	Mock
0.61	16.7	86	0.3	4.18	29.4	31.3	35.1	16.8	0.99	71.7	85.3	0.18	ND19	KSHV
0.27	3.12	84	0.21	6.94	30.8	24	38.2	16.4	0.76	74	83.7	0.2	ND20	Mock
0.43	3.64	83.5	0.39	6.14	33.9	21.6	38.4	16.9	0.8	72.2	83.1	0.38	ND20	KSHV
8.19	0.82	85.4	1.13	1.84	9.28	1.08	5.3	38.4	6.01	37.1	76.5	1.18	ND21	Mock
5.55	0	82.9	1.89	1.76	9.73	1.29	4.74	37.5	6.48	36.5	77	2.03	ND21	KSHV
0.91	0	54.4	0.36	1.56	3.36	3.4	2.2	34.1	13.5	41.5	53.3	0.37	ND23	Mock
1.02	1.41	57.3	0.4	1.4	2.96	2.93	0.62	32.7	18.2	39.2	56.1	0.38	ND23	KSHV
0.58	3.12	41.8	0.79	1.7	4.28	2.31	2.27	38.6	16.5	33.4	41.1	0.75	ND23	KSHV
0.77	2.44	48.3	0.39	1.36	3.85	2.6	2.53	36.5	17.2	35.5	47.5	0.36	ND23	KSHV
0.69	2.74	53.2	1.19	4.11	4.52	3.94	2.27	43.9	16.2	23.8	52.5	1.17	ND25	Mock
0.74	0	56	0.23	4.53	2.94	7.31	1.73	40.5	11.3	31.4	55.2	0.23	ND25	KSHV
0.23	0	54.1	1.03	1.2	1.33	1.11	0.6	24.7	27.5	42.6	53.9	1.03	ND26	Mock
0.14	0	56.3	0.65	0.76	0.97	1.59	0.76	20.8	30.1	44.3	56.1	0.65	ND26	Mock
0.2	0	57.8	0.7	1.13	1.48	1.3	1	34	20.7	39.8	57.6	0.7	ND26	KSHV
0.38	0	49.5	1.25	1.68	1.64	1.73	1.06	31.4	24.1	37.2	49.1	1.26	ND26	KSHV
1.76	0.37	80.5	0.29	1.5	1.69	2.73	1.04	36.6	9.3	46.9	78.6	0.29	ND27	Mock
2.14	0	70.4	0.49	2.47	2.61	2.13	1.5	53.7	6.61	30.4	68	0.51	ND27	KSHV
2.73	0	85.8	0.56	4.03	26	8.8	7.68	10.6	0	41.3	84	0.57	ND31	Mock
3.92	0	85.6	0.84	3.74	24.2	8.97	5.33	12.9	0	43.3	82.3	0.87	ND31	KSHV
2.57	1.36	83.3	0.46	3.45	7.43	4.33	0.62	36.6	0.54	65	80.4	0.43	ND32	Mock
2.25	1.6	83.5	0.47	2.78	7.14	4.35	1.03	15.8	0.73	67	80.9	0.44	ND32	Mock
1.9	1.5	88.2	0.22	2.99	6.98	4.12	1.02	16.5	0.79	66.6	86	0.19	ND32	KSHV
1.63	1.25	87.9	0.31	2.72	7.28	4.01	1.21	16.9	0.82	66.1	86	0.28	ND32	KSHV
3.56	0.24	91.2	0.39	2.56	6.73	4	1.96	19.7	1.27	62.8	87.5	0.39	ND33	Mock
3.65	0.16	94.1	0.36	2.21	5.25	4.61	1.92	16.5	1.03	67.5	90.5	0.37	ND33	KSHV
1.15	0.72	93.1	0.24	1.93	6.65	16.6	7.18	11.9	0.89	54.8	91.9	0.24	ND39	Mock
1.06	0.6	94.2	0.32	1.89	6.41	13.7	6.89	12.7	1.07	57.2	93.2	0.32	ND39	Mock
1.23	1.05	93.1	0.53	1.79	6.83	13	6.9	14.1	1.16	55.9	91.9	0.52	ND39	KSHV
1.15	1.98	92.9	0.35	2.38	6.36	12.3	7.13	14	1.47	56.2	91.7	0.33	ND39	KSHV
0.37	3.51	69.9	0.62	5.6	54	10.8	29.5	25.3	3.02	51.5	69.5	0.61	ND4	Mock
0.44	5.38	67.4	0.83	4.42	54.9	10.1	30.6	26.2	3.19	49.2	66.9	0.8	ND4	Mock
0.54	7.45	70.4	1.15	4.02	52.3	11.9	31.8	23.1	1.91	49.9	69.8	1.1	ND4	KSHV
0.72	8.26	69.3	0.94	3.96	55.2	9.32	31.5	25.5	2.33	48.1	68.5	0.87	ND4	KSHV
7.34	0	82.1	0.14	1.61	9.52	12.8	6.76	9.84	0.45	59	74.7	0.16	ND40	Mock
9.29	0	78.5	0.17	1.49	11.7	14	5.85	11.8	0.36	54.8	69.2	0.19	ND40	Mock
6.11	0.84	80.4	0.34	3.07	10.1	11	4.87	14.3	0.54	55.6	74.2	0.29	ND40	KSHV
6.76	2.42	84.1	0.39	1.93	9.42	15.7	7.57	8.14	0.097	56.9	77.3	0.16	ND40	KSHV
3.68	0.42	83.4	0.2	1.68	22.8	12.4	8.5	17.3	0.39	36.2	79.5	0.19	ND41	Mock
5.12	0.19	81.6	0.39	2.9	24.1	8.92	8.29	24.7	0.62	29.6	76.2	0.4	ND41	Mock
5.98	0.092	85.1	0.35	2.8	21.2	12	7.92	23.3	0.57	31.3	78.8	0.36	ND41	KSHV
6.63	0.5	88	0.82	2.3	22.1	11.9	7.31	25.8	1.02	28.1	81	0.85	ND41	KSHV
1.18	3.66	69.3	0.89	1.43	11.2	5.49	3.95	23.6	3	50.4	68.1	0.84	ND42	Mock
0.84	1.39	70.1	0.65	1.86	10.6	5.89	5.44	21.2	1.48	52.7	69.3	0.64	ND42	Mock
1.13	8.86	71.2	1.43	1.57	10.9	5.68	5.32	22.2	3.04	49.8	70.1	1.31	ND42	KSHV
1.06	9.43	66.3	1	1.18	10.3	4.48	4.66	22.4	3.72	52	65.2	0.83	ND42	KSHV
0.72	0	89.2	0.45	1.74	9.42	26.3	17.3	8.43	0.19	38.1	88.5	0.46	ND43	Mock
1.13	3.57	93.4	0.4	1.65	8.19	25	16	10.5	0.22	37.5	92.1	0.36	ND43	KSHV
6.24	0.96	52.2	0.78	3.97	23.2	7.31	7.54	31.1	1.83	23.8	45.7	0.76	ND44	Mock
6.96	1.87	54.3	0.84	2.83	23	6.61	5.52	36.8	2.11	21.6	46.9	0.69	ND44	KSHV
2.07	0.81	50.3	1.47	6.23	20.7	5.63	5.83	35.6	1.54	22	48.1	1.51	ND45	Mock
1.22	4.35	44.4	2.06	5.6	19	4.09	4.8	42.3	1.94	19.5	43.2	2	ND45	KSHV
1.73	1.96	90.7	0.84	2.1	10.5	27.7	10.9	5.92	0.09	42.3	89	0.82	ND46	Mock
2.38	1.28	90.4	0.95	1.93	10.8	27	11.4	5.51	0.13	42.6	88	0.94	ND46	Mock
2.89	2.14	91.4	0.88	1.94	10.5	28.5	11.7	5.27	0.15	41.2	88.5	0.84	ND46	KSHV
2.84	2.79	89.6	1.56	2.37	11.4	23.4	11	7.24	0.16	43.1	86.7	1.51	ND46	KSHV
5.69	0.63	83.4	1.51	2.11	30	3.38	8.82	31	1.51	21.5	77.7	1.57	ND47	Mock
5.1	1.62	89.1	2.32	3.25	26.1	4.68	7.4	28.3	1.48	26.5	84	2.36	ND47	KSHV
2.9	0.62	84.3	1.48	2.63	15	3.62	6	37.3	2.09	31.8	81.4	1.52	ND48	Mock
3.13	1.11	89.2	1.47	2.72	14.8	3.28	5.8	36.8	1.9	38.1	81.2	1.49	ND48	Mock
2.04	4.82	84.6	1.64	2.31	14.1	2.63	5.68	37.2	3.54	32.8	82.5	1.56	ND48	KSHV
1.66	1.7	79.7	1.36	2.43	13	2.33	4.8	40.4	3.99	31.6	78.1	1.35	ND48	KSHV
4.98	1.56	41.6	1.69	5.62	44.9	25.3	12.9	3.56	0.19	5.62	36.4	1.71	ND49	Mock
4.89	14.1	68.8	2.66	4.22	33.2	27.6	14.8	3.77	0	13.7	63.7	1.8	ND49	KSHV
3.28	0.57	92	0.8	2.72	21.5	17.2	18.1	13.7	0.21	25.4	88.6	0.81	ND50	Mock
3.19	1.39	92.2	1.11	2.89	22.6	20	19.4	11.4	0.14	22.3	88.8	1.1	ND50	Mock
3.3	1.43	92	1.72	3.19	22.7	17.7	17	13.5	0.25	23.7	88.4	1.73	ND50	KSHV
2.13	1.05	91.7	1.47	2.88	20.9	14.8	14.9	18	0.33	26.4	89.5	1.47	ND50	KSHV
8.16	0.24	94.6	0.35	1.27	8.93	8.4	5.04	21.9	1.15	52	86	0.36	ND51	Mock
10.1	0.049	94.2	0.31	1.22	9.73	9.32	5.29	23.2	1.03	49	83.6	0.35	ND51	Mock
6.54	0.37	96.2	0.8	0.99	8.84	7.2	5.2	22	2.02	52.1	89.1	0.83	ND51	KSHV
8.36	0.045	96.6	0.54	1.16	9.5	8.5	5.82	21.8	1.38	50.6	87.8	0.59	ND51	KSHV
1.15	3.77	60.6	2.14	2	21	3.75	12.5	21.3	4.21	33	59.5	2.11	ND52	Mock
1.64	1.68	80.5	1.5	2.39	15.2	2.92	6.66	33.2	7.58	30.5	78.9	1.49	ND52	KSHV
1.38	0.88	94.8	0.31	1.38	6.05	15.5	18	8.21	1.18	49.4	93.4	0.3	ND53	Mock
1.15	4.52	93.9	0.62	1.38	6.34	12.4	17.1	9.6	1.51	51.1	92.8	0.57	ND53	KSHV
3.48	0.39	92.7	0.14	0.82	7.01	9.83	4.85	7	0.38	70.1	89.2	0.13	ND54	Mock
3.77	0.74	91.8	0.75	1	8.56	15.4	5.38							

# Appendix B. Supplementary data from Chapter 3

## B.1 Supplementary Table1: Hits reported previously by other labs through Mass-Spectrometry and detected in our analysis as well using Trypsin as digesting enzyme.

Gene	Protein	Amino-Acid	Number of Unique Peptide Hits	Sequences of Correspondence detected
ORF6	Major DNA-binding protein (MBP)	1133	7	244-251: R.QFVHDQYK.I 569-587: K.GIDSTVEAELLKFINC(+57.02)M(+15.99)IK.N 691-712: F.C(+57.02)DLFDTDAIIGGMFAPARMQVR.I 43-49: G.NGYPEAK.V 574-580: T.VEAELLK.F 740-752: E.SIQAGFMKPASQR.D 1012-1031: R.DNPNLPKTVVLELVKHLGSS.C
ORF7	Tripartite terminase subunit 1 (TRM1)	695	6	327-355: R.GTPKHFFDC(+57.02)FRPDSLETLC(+57.02)GGLFSSVED.T 546-568: L.FPSPPNVTLAQ(+57.02)FEAAGMLPHQK.M 23-33: L.SYADPATLDTK.S 414-426: R.QLVGGDKPEEVL.R.D 355-362: L.TPESC(+57.02)VKA.C 454-470: A.SAGLFTFQPLLSNSTHR.K
ORF8	Envelope glycoprotein B (gB)	845	10	650-662: R.LASSVFDLETMFR.E 834-845: L.TQSLDISPETGE 197-215: R.YFSQPVIYAEPGWFPFIYR.V 692-705: R.DLSEIVADLGGIGK.T 163-173: K.VNVNGVENTFT.D 778-788: P.SGGAPTREEIK.N 581-588: T.NNQVETC(+57.02)K.D 70-78: S.ASITGELFR.F 674-686: G.LRELDNTIDMKN.E 165-175: N.VNGVENTFTDR.D
ORF11	ORF11	407	9	24-42: R.GEPVWDSVIHPSHIVISNR.V 67-78: R.AYPNFTFDNTHR.K 118-147: R.ASVSANIAGGLKIIIALTLVHAQGVYLR.C 151-164: K.DLSTPHC(+57.02)APAIVQR.E 165-195: R.EVLSSGFEPQFTVTGIPVTSSNLNQC(+57.02)YFLVR.K 230-261: R.ISVTAPAQETPVWGLVTTSFSLTPTAPLAFDR.N 275-285: R.HYIPVIYSGPK.I 294-309: R.QVVWHNNSYSSLP(+57.02)K.V 310-339: K.VTAIVSNHC(+57.02)C(+57.02)NC(+57.02)DIFLEDSEWRPNKPAPLK.L
ORF17	Capsid Scaffolding Protein (CSP)	534	3	386-397: W.HAGPPSSSSAAA.A 421-433: K.EHGGTYVHPPIYV.Q 264-285: F.LSMLQSSIDGMKTTAAKMSHTL.S
ORF21	Thymidine kinase	580	8	382-395: R.LSFDHFFQLLSIFR.A 486-504: K.NLHEQSLPMTGVLDPVR.H 364-373: R.HLLSPAVVFP.L 252-264: R.NVYLLYLEGVM(+15.99)GV.G 274-294: V.C(+57.02)GILPQERVTSFPEPMVYWR.A 328-354: K.FSLPFRNTATAILRMMQPWNVGGGSGR.G 382-392: R.LSFDHFFQLLS.I 244-251: R.TPVTVDYR.N
ORF22	Envelope glycoprotein H (gH)	730	7	565-597: K.IIATVPLPHVTYIISSEALSNAVVEVSEIFLK.S 154-163: I.FASKWSLFAR.D 164-184: R.DTPEYRVFYPMNV(+15.99)AVKFSIS.I 661-668: R.VQTNLF.LD.K 629-636: S.TPRRGC(+57.02)PL.C 158-169: K.WSLFARDTPEYR.V 165-210: D.TPEYRVFYPMNV(+15.99)AVKFSISIGNNESGVALYGVVSEDFVVVTLHNR.S
ORF24	ORF24	752	4	395-412: T.DARTLGSSTVSDMLEPTK.H 86-96: Q.EGTLGKVGRR.Y 422-444: I.TIFNTNM(+15.99)VINTKISC(+57.02)HVPNTLQK.T 372-391: Y.APKDRRAAMKGNLQAC(+57.02)FQRY.A
ORF25	Major capsid protein (MCP)	1376	5	123-143: HHIGAEIELAAADIPELLFAEK 158-172: TITSALQFGMDALER 1057-1070: ASTSMFVGLPSVVR 1243-1255: R.GSLGDVLYNITFR.Q 1293-1335: R.LAGAPATSTDLQYVVVNGTDVFLDQPC(+57.02)HMLQEAYPTLAASHR.V

ORF26	Triplex capsid protein 2 (TRX-2)	305	5	203-220: R.VLDDLSMYLC(+57.02)ILSALVPR.G 268-285: R.VMFSYLQSLSSIFNLGPR.L 90-96: P.SDN(+.98)LQIK.N 232-251: R.HDRHPLTEVFEGVVPEVTR.I 175-189: L.DLYTTNVSEFM(+15.99)GRTYR.L
ORF27	ORF27	290	6	1-26: M(+15.99)ASSDILSVARTDDGSVC(+57.02)EVSLRGGR.K 169-189: Y.SM(+15.99)ALRRFAVAVMNTSC(+57.02)AGVTL.C 104-110: V.TPSSIEFA 44-60: T.DAIKDAFLSDGIVDMAR.K 35-60: P.DTEPWVETDAIKDAFLSDGIVDM(+15.99)AR.K 179-191: V.MVNTSC(+57.02)AGVTL.C(+57.02)R.G
ORF28	ORF28	102	2	63-73: ATVAYQVLR 74-96: TLGPQAGSHAPPTVGIATQEPYR
ORF33	Cytoplasmic envelopment protein 2 (CEP-2)	334	7	117-126: R.FPYIAPPPSR.E 117-145: R.FPYIAPPPSREHVDPDLTRQELVHTSQVVR.R 135-145: R.QELVHTSQVVR.R 160-196: R.NVNPVWLGGSVWLLFLGVDYMAFC(+57.02)PGVDGMPSLAR.V 257-270: R.NFLGLLFDPIVQSR.V 276-303: K.ITSHPTPTHVENVLTGVLDDGTLVPSSK.A 318-324: R.LLIYEC(+57.02)K.K
ORF39	Envelope glycoprotein M (gM)	400	6	6-16: SDRFLMSSWVK 105-149: AKHVHATTMMMSM(+15.99)QSWIALLGSHSVLYVAILRM(+15.99)WSM(+15.99)QLFIHVLVSYK 136-149: M(+15.99)WSMQLFIHVLVSYK 270-290: QVGFYVGVFVGYLILLLPVIR 370-379: VKDISTPAPR 380-400: TQYQSDHESDEIDETQMIFI
ORF45	ORF45	407	5	266-288: HFSHQPPSSEEDGEDQGEVLSQR 356-381: GHLPQSPSTSAHSISSGTTTAGSR 17-25: R.MLPIEGAPR.R 201-218: Y.GLSPASRNSVPGTQSSPY.S 50-68: R.GYAGPTVIDMSAPDDVFAE.D
ORF47	Envelope glycoprotein L (gL)	528	5	17-25: MLPIEGAPR 121-137: AMAMFVRTSSSTHDEER 121-146: AM(+15.99)AM(+15.99)FVRTSSSTHDEERM(+15.99)LPPIEGAPR 387-409: HFSHQPPSSEEDGEDQGEVLSQR 477-503: GHLPQSPSTSAHSISSGTTTAGSR
ORF52	ORF52	131	9	98-117: R.IDVC(+57.02)MSDGGTAKPPPGANNR.R 47-78: L.TATEKEAQLTATVGALSAAAARKIEARVRTIF.S 52-68: K.EAQLTATVGALSAAAARK 43-51: R.DRPLTATEK.E 21-29: K.ISQLTVENR.E 99-117: L.D(+57.02)(+57.02)VC(+57.02)MSDGGTAKPPPGANNR.R 98-117: R.IDVC(+57.02)MSDGGTAKPPPGAN(+98)NR.R 98-118: R.IDVC(+57.02)MSDGGTAK(+42.01)PPPGANNRR.R 52-68: K.EAQ(+98)LTATVGALSAAAARK
ORF53	Envelope glycoprotein N (gN)	110	1	103-110: FVDEVVHA
ORF62	Triplex capsid protein 1 (TRX-1)	331	4	45-53: K.YAASTRPTV.G 211-217: S.C(+57.02)PMVQRR.E 4-10: V.QAENAAR.L 68-73: R.QPTYGDFLVYSQTFSPQ.E
ORF63	Inner tegument protein	927	7	445-452: R.ALAFVPP.A 480-491: K.TTWGGAVPANL.A.R 501-512: T.QHISSTPPPTL.K.D 604-624: R.HSQDALYNLLDC(+57.02)IQELFTHIR.Q 725-741: R.EATVAMTTIAKPIYPAY.I 461-495: R.VYAALPSQLM(+15.99)RAIFEISVKTWGGAVPANLARDID.T 748-781: R.LEYLNRLNHHILRIPFPQDALSELQETYLAAFAR.L
ORF64	Large tegument protein deneddylase	2635	6	129-135: R.NYAGTVQ.Y 1979-1985: M.EFGPPPK(+42.01).T 384-406: R.EPPPTPATPGATALLSDLTATR.G 2358-2365: R.T(+75.98)ALQPPRT.E 2428-2445: R.DTS(+238.23)PPAEKRAAPVIRVMA.P 1265-1273: Y.Q(+57.02)D(+57.02)QVSFFLR.T
ORF65	Small capsomere-interacting protein (SCP)	170	4	8-14: DPVIQER 28-45: M(+15.99)NTLDQGNM(+15.99)SQAEYLVQK 28-46: M(+15.99)NTLDQGNMSQAEYLVQKR 47-64: HYLVFLIAHHYYETYLRR
ORF68	Packaging protein UL32 homolog	545	3	290-324: K.NGTASVC(+57.02)LLC(+57.02)EC(+57.02)LAHPPEAPKALQTLQC(+57.02)EVMGHIE.N 454-467: LDLAHPQSQTSHLYA 5-15: K.EPSAVHPDAPR.I
ORF75	ORF75	1296	8	63-84: DVEIQTVLAVLSPLLGYPHVIR 139-153: K.ITQTLLPHPPQFIR.A 442-495: R.AHLPADPAAGPDAVEAAVAEHFLNVYC(+57.02)SLVFVVAESGAVPGDLGETPLEVLQR.A 552-575: R.VSGHPEDVDWGLFATGSTIHKLLR.H 630-647: R.VSGHPEDVDWGLFATGSTIHKLLR.H 792-799: R.YRVTPDVK.V 1206-1224: R.GEITLYHGNAADETL.PAR.H 1229-1245: R.NPTGNSTVAGLTSSDGR.H

K8.1	gp35/37	228	4	33-53: SHLGFWQEGWWSGQVYQDWLGR 65-87: L.EAVSLNGTRLAAGSPSSEYPNV.S.V 137-155: L.ISAFSGSYSSGEPSTRTRLR 173-183: VPFSATTTTTR
------	---------	-----	---	---

## B.2 Supplemental Table2: Hits unique to our mass spectrometry but reported previously through other methods using Trypsin as digesting enzyme.

Name	Amino Acid Size	Protein detected	Reported previously by other methods	Number of unique peptide hits	Sequences of Correspondence detected	-10lgP
ORF18	257	Protein UL79 homolog	Gong et al 2014	4	22-32: S.LEMRLVTMC(+57.02)VK.E 47-57: M(+15.99)YNFGLNVYLLR 119-140: K.L.SVGREAVYLHVGLSERGRFLT.L 148-159: L.FNLGSLVLP(+57.02)R	28.41 41.6 27.45 33.37
ORF32	454	Capsid vertex component 1 (CVC-1)	Dai et al 2014	7	224-232: R.LSFNPVNAD.V 149-167: S.VLDARDTPGFRARPLPTRS.D 274-293: E.EPVPPPGLVFM(+15.99)DDLFINTK.Q 301-313: T.LEAAC(+57.02)RTQGYTLR.Q 133-146: R.SPTVDGVSPPGAV.A 102-155: R.ISC(+57.02)PGSNLSLTVRFLYLSLVVAMGAGRNNARSPTVDGVSPPGAVAHLEELQR.L 10-17: R.YVGPRC(+57.02)HR.L	37.48 37.41 35.18 28.43 28.27 27.63 25.1
ORF38	61	Cytoplasmic envelopment protein 3 (CEP-3)	Wu et al 2016	4	10-32: RPSQPVDVDGEPLDVVVDYDPIR 33-51: VSEKGM(+15.99)LLEQSQSPYPALK 37-51: GMLLEQSQSPYPALK 20-36: G.EPLDVVVDYDPIRVSEK.G	44.09 25 25 27.74
ORF42	278	Cytoplasmic envelopment protein 1 (CEP-1)	Butnaru et al 2019	3	35-42:K.GNGELMMR.A 170-189: I.ETLTATAAFVYELSVDDHFR.A 9-21: A.RLTGVPM(+15.99)STHAPK.T	32.87 27.17 25.6
ORF43	605	Portal Protein	DD Dünn-Kittenplon et al, 2019	6	480-506: E.SHLGSSSYC(+57.02)YMC(+57.02)SDSAINTANIYC(+57.02)LIR.Y 464-479:K.DLTNLWESEMFTYKLA 555-565:L.VTPPFENVPGK.G 44-54:L.RNPGVFFRQLF.I 156-163:L.VNSIQEQL.M 377-385:L.RKDTC(+57.02)SMSLA	27.15 33.22 30.47 28.11 27.03 40.1
ORF48	402	ORF48	Sander,G. et al .2007	6	336-343:D.VTLVHTAR.M 192-222:V.EFRRELSLISSC(+57.02)LNVC(+57.02)WLYHIFIEHITS DVR.R 214-222:F.IEHITSDV.R.R 313-321:R.LDLSHFDRR.R 362-384:K.VSLLHIC(+57.02)SYSMEADVVPVPGQLN.T 190-201:R.M(+15.99)ESTRIIGAC(+57.02)PF.A	25.76 37.34 35.49 36.05 32.42 31.38
ORF56	843	DNA primase	Davis et al 2015	6	525-538: R.EAILDIIQLLGPVD.P 497-507: R.WVLDLDFLPVC(+57.02)R.D 535-548:L.GPVDPRTHPVYFFK.S 426-439:K.QFFTMLQEDGLERY.W 595-605:V.ALTGILNRTIK.L 701-708:R.NENFLENK.T	27.05 25 25.67 25.14 27.35 25.31
ORF K2	204	Viral Interleukin 6 Homolog	Katano,H. et al.2000	12	33-56: K.DLLIQRNLNWMWLWVIDEC(+57.02)FRDLC(+57.02)YR.T 39-51:R.LNWMWLWVIDEC(+57.02)FR.D 62-73:K.GILEPAAIFHLK.L 62-96:K.GILEPAAIFHLKLPAINDTDHC(+57.02)GLIGFNETSC(+57.02)LKK.L 96-117:K.KLADGFFEFVLFKFLTTEFGK.S 96-109:K.KLADGFFEFVLFK.F 97-117:K.LADGFFEFVLFKFLTTEFGK.S 97-109:K.LADGFFEFVLFK.F 118-130:K.SVINVDVMELLTK.T 131-142:K.TLGWDIQEELNK.L 166-182:K.YWVRHFASFYVLSAMEK.F 170-182:R.HFASFYVLSAMEK.F	48.85 66.32 40.95 25.72 64.76 47.06 25.94 25.66 50.54 47.99 27.17 51.43

## B.3 Supplementary Table3: Hits unique to our Study using Trypsin as digesting enzyme.

Name	Amino Acid Size	Protein detected	Number of unique peptide hits	Sequences of Correspondence detected	-10lgP
ORF9	1012	DPOL	6	69-82: K.RGEVFAGETGSIWK.T 70-82: R.GEVFAGETGSIWK.T 396-404: Y.DFKLQDFTK.I 470-482: K.DDISYKDIPPLFK.S 671-677: K.TLDDKQQ.L 938-950: R.IPYVFVDAPGSLR.S	26.31 26.87 44.45 26.41 45.15 30.99
ORF23	404	ORF23	6	30-67: T.SPAAVMVGSNPEVPMPLLFKFGTTPDSSTLPLYAAR.H 356-389: Q.SAAWLGAGVVELIC(+57.02)DGNPLSEVLGFLAKYMPIQK.E 225-251: R.LGESPVVC(+57.02)DFNTVTIM(+15.99)ERANNSITFLPK.L 354-360: D.RQSAAWL.G 193-215: H.NIAQVC(+57.02)ERDIVSLNTDNEAASM.F.Y 269-291: R.SMGLENIVSC(+57.02)FSSLYGAELAPAK.T	31.71 59.54 40.2 36.59 72.52 33.22
ORF35	150	ORF35	4	94-105: D.IDALVDAVADLKE 87-102: L.KSASNAEELIASEPLA 45-52: R.NLASPDHV.R 120-130: L.TFSAVGVLHTD.G	29.35 43.54 28.98 27.76
ORF58	357	ORF58	5	54-66: W.DVEFFRLVAAPVF.K 32-38: P.AYFGSVL.V 30-42: L.FPAYFGSVLVALR.T 101-120: R.VPFIPGLC(+57.02)VLNC(+57.02)LLLLPYPLA 172-178: V.GGLLAFR.H	28.43 28.21 32.22 28.78 25.43
ORF72	257	viral cyclin homolog	4	153-160: A.IESGLYDR.L 146-154: R.TEAVLATDV.T 21-44: R.IFYNILEIEPRFLTSDSVFGTFQQ.S 54-82: LLGTWFMFVC(+57.02)HEYNLEPNVVALALNLLDR	35.76 32.47 26.09 25.94
ORF K3	333	E3 ubiquitin-protein ligase MIR1	5	2-35: EDEDVPVC(+57.02)WIC(+57.02)NEELGNERFRAC(+57.02)GC(+57.02)TGELENVHR 26-51: AGPSSLVDM(+15.99)LPQGLPGGGYGSMGVIR 250-271: DDNVEPTAVGC(+57.02)DC(+57.02)NNLGAERYR 308-321: Q.GLPGGGGYSGMGVIR.K 279-292: Y.VGAQSGDGAYSVSC(+57.02).H	25.06 26 25 42.27 29.5
vIRF-1	449	Viral IRF like protein 1	5	246-281: T.AEGQEAVIDWGRFLFIRM(+15.99)YYNGEQVHELLTTSQSGC(+57.02)R.I 94-110: K.DWIVC(+57.02)QVNSGKFPGVVEW.E 92-117: S.IKDWIVC(+57.02)QVNSGKFPGVVEWEDEERTR.F 26-67: F.KAWSVGATRNVPMGAGRGGGPC(+57.02)JLC(+57.02)ARNINTKTPFPPTPTAVEV.C 52-58: R.NINTKTP.F	30 25.33 25.21 33.62 30.86
vIRF-3	566	Viral IRF like protein 3	7	72-80: L.GSPITAFGK.I 128-136: L.HSGSSLWEIL 30-52: K.ASEVC(+57.02)AADVSGVPRPADMTEPTK.L 559-566: R.ENVLSSSP 478-490: R.MEVPLSFRPEEWR.V 15-24: L.RSASGIASGLD 35-52: C.AADVSGVPRPADMTEPTK.L	31.89 25.72 32.53 31.04 27.9 26.18 25.26
vIRF-4	911	Viral IRF like protein 4	11	505-547: T.QGGASATPSAGAPPTPEVAERQEPSSSGIPYVC(+57.02)QGDNM(+15.99)ATGYR.R 752-785: EGDAGEAMLC(+57.02)SWPVGDTLGHLC(+57.02)QSFPELLLRIPR 152-158: R.RSDTREQ.S 435-467: F.EPQPSPAPAGYAKPSC(+57.02)YNWSPLAEPPTATPIR.A 161-175: S.APAHRPPSPLTWLWR.T 549-568: R.VTSSGALEVEIIDLTDGSD.T 858-868: R.YLATAAIPQT.P 677-696: G.NILSELQEPSSSTRQATDR.R 825-836: Q.VEGWWFGNPNRSR.Y 492-501: W.SSGGAPNQL.S 407-421: R.ETGAEGAC(+57.02)GASTEGR.A	30.84 26.13 37.95 25 53.33 44.03 37.87 36.42 34.83 29.55 28.06

#### B.4 Supplemental Table 4: Hits reported previously by other labs through Mass-Spectrometry and detected in our analysis as well using Chymotrypsin as digesting enzyme.

Gene	Protein	Amino-Acid	Previous Report by Mass-Spectroscopy	Number of Unique Peptide Hits	Sequences of Correspondence detected
ORF6	Major DNA-binding protein (MBP)	1133	Zhu et al 2005	6	77-88: LDATTASVKLTSY.H 111-120: L.EKLC(+57.02)RESREL.F 627-650: L.LTVIQDIC(+57.02)LTSC(+57.02)M(+15.99)MYEQDNPAVGL.V 755-761: S.YIVGGPY.M 984-990: L.VKRIVGLN 961-968: F.KKNVSSML.L

ORF7	Tripartite terminase subunit 1 (TRM1)	695	Zhu et al 2005	3	31-37: L.DTKSLAL.T 99-113: L.LHLDITC(+57.02)NKHRSVRF.N 666-672: L.VDKKYGW.I
ORF8	Envelope glycoprotein B (gB)	845	Zhu et al 2005, Bechtel et al 2005	20	57-63: G.PKSVDYF.Y.Q 63-77: F.Y(+79.97)QFRVC(+57.02)SASIT(+79.97)GELF.R 67-76: R.VC(+57.02)SASITGEL.F 82-92: L.EQTC(+57.02)PDTK(+42.02)DKY.H 82-92: L.EQTC(+57.02)PDTKDKY.H 93-105: Y.HQEGILLVYKKN.I.V 117-125: R.KIATSVTVY(+6.01).R 138-155: Y.ELPRPVPLYEISHMDSTY.Q 147-158: Y.E(+57.02)(+57.02)ISH(+57.02)MDSTYQC(+57.02)F.S 202-209: P.V(+42.01)IYAEPGW.F 275-281: L.NHTVVVY.S 287-295: T.SPTQON(+203.08)RIF.V 364-371: L.TSDINTTL.N 377-390: A.KLASTHVPNGTVQY.F 392-398: F.HT(+27.05)TGGLY.L 402-408: W.QPMSAIN(+14.02).L 466-473: Y.DKLRDGIN.Q 469-476: L.R(+27.99)DGINQVLE 511-518: Y.GRPVSC(-18.01)AKF.V 519-548: F.VGDAISVTEC(+57.02)INVDQSSVNIHKSRLTNSKD.V 532-555: V.DQSSVNIHKSRLTNSKDVC(+57.02)YARPL.V 534-542: Q.S(+28.03)SVNIHKS.L.R 572-579: L.GARNEIIL.T 588-594: C.KDTC(+57.02)E(+57.02)HY.F 651-657: L.ASSVFDL.E 675-689: L.RELDNTID(+1572.99)MNKERF.V 726-739: F.INFIKHPLGGMLM.I.I 734-740: L.GGMLM.I.I 738-747: L.M(+15.99)IIIVIAI.L.I 751-759: F.M(+31.99)LSRRTNTL.A 767-791: M.IYPDVDRRAPPSGGAPTREIKNIL.L 809-820: L.KKS(+162.05)TPSVFQRTA.N 817-823: F.Q(+42.01)(+98)RTANGL.R
ORF11	ORF11	407	Zhu et al 2005	5	13-32: F.AVC(+57.02)SSKRQLGRGPEVWDSV.I.H 65-73: L.HRAYPNFTF.D 166-175: E.VLSSGFEPQF.T 194-201: L.VRKPXSRL.A 229-242: L.RISVTAPAQETPVW.G
ORF17	Capsid Scaffolding Protein (CSP)	534	Zhu et al 2005	3	64-91: H.GIFC(+57.02)TGAITSPAFLELASRLADTSHVAR.A 181-197: R.LEDLSTPNFVSPLETLM(+15.99).A 183-199: E.DLSTPNFVSPLETLM(+15.99)AK.A
ORF21	Thymidine kinase	580	Zhu et al 2005, Bechtel et al 2005	3	96-106: L.IRHPSEKGSIF.A 129-167: F.QSPRV(+57.02)GRPPLPPPNNHPPATRPADASM(+15.99)GDVGVADLQGL.K 392-401: L.SIFRATEGDV.V
ORF22	Envelope glycoprotein H (gH)	730	Zhu et al 2005, Bechtel et al 2005	5	233-241: L.KGHATYDEL.T 315-321: F.QMLVAHF.L 584-601: L.SNAVVEVSEIFLKSAMF.I 597-614: L.KSAMFISAIKPCDC(+57.02)SGFN.F.S 629-636: S.TPRRGC(+57.02)PL.C
ORF24	ORF24	752	Bechtel et al 2005	7	127-139: S.WELTDDC(+57.02)DKPC(+57.02)EF.R 172-179: W.EFEQC(+57.02)FHA.F 319-326: L.VYPGTPAI.Y 372-391: Y.APKDRRAAMKGNLQAC(+57.02)FQRY.A 485-493: I.NINISGDM.L.H 543-557: F.WTTNFPSVVSSKDGL.N 709-715: F.AALKPQI.V
ORF25	Major capsid protein (MCP)	1376	Zhu et al 2005, Bechtel et al 2005	6	547-554: P.C(+57.02)PGARGSY.R 836-845: Y.NGPVFADV.N.A 860-868: L.KDILQAGDI.R 1063-1086: F.VGLPSVVRREVRSDAVTFEITHEI.A 1316-1337: F.LDQPC(+57.02)HMLQEAYPTLAASHRVM(+15.99).L 1342-1349: Y.MSNKQTHA.P
ORF26	Triplex capsid protein 2 (TRX-2)	305	Zhu et al 2005, Bechtel et al 2005	3	72-87: AVLEEVRPDSLRLTRM 156-171: HIYSKISAGAPDDVNM 238-266: TEVFEVGVPEVTRIDLQ.L.SVPDDITRM
ORF27	ORF27	290	Zhu et al 2005,	4	24-32: R.GGRKKTIVY.L 45-51: D.AIKDAFL.S 52-72: L.SDGIVDM(+15.99)ARKLHRGALPSNSH.N 104-110: V.TPSSIEF.A
ORF28	ORF28	102	Zhu et al 2005	3	1-13: MSMTSPSPVTGGM 39-52: VIGACYCCIRVFL 76-102: GPQAGSHAPPTVGIATQEPY RTIYMPD
ORF33	Cytoplasmic envelopment protein 2 (CEP-2)	334	Zhu et al 2005, Bechtel et al 2005	7	35-51: C.TSISPVY(+79.97)DPELVTSYAL.S 47-56: V.TSYALSVPAY.N 50-64: Y.A(+57.02)LSVPAYN(+98)VSVAILL.H 138-144: L.VHTSQVV.R 185-194: F.C(+57.02)P(+31.99)GVDGMPSL.A

					234-240: L.SNIC(+57.02)PC(+57.02)I.K 291-298: T.GVLDDGTL.V
ORF39	Envelope glycoprotein M (gM)	400	Zhu et al 2005	3	1-8: M(+15.99)RASKSDR.F 58-66: L.TVRNSAKHL.T 367-400: A.RAKVKDISTPAPRTQYQSDHESDSEIDETQMIFI
ORF45	ORF45	407	Zhu et al 2005	4	18-45: LPIEGAPRRRPPVKFIFPPP PLSSLPGF 94-121: DEDEDEDEEENDDVQEEDE PEGYPADF 293-395: DVGQKRKRQSTASSGSEVDV RCQRQPNSLRKAVASVIIS SGSDTDEEPSSAVSVIVSPS STKGHLPTQSPSTSAHSISS GSTTTAGSRCSDPTRLAST PPL 321-395: SRKAVASVIISGSDTDEE PSSAVSVIVSPSSTKGHLPT QSPSTSAHSISSGSTTTAGS RCSDPTRLASTPPL
ORF47	Envelope glycoprotein L (gL)	528	Zhu et al 2005	3	22-39: VALPCCAIQASAASTLPL 114-140: TVGFNATTADSSIHNVNIII ISVGKAM 141-167: NRTGVSQTRAKSSSRRRA HAGQKGG
ORF52	ORF52	131	Zhu et al 2005	5	18-24: L.T(+79.97)AKISQ(+98)L.T 25-31: L.TVENREL.R 32-41: L.RKALGSTADP.R 36-42: L.GSTAD(+57.02)PR.D 97-131: L.RIDVC(+57.02)MSDGGTAK(+14.02)PPPGANNRRRRGASTTR(+14.02)AGVDD
ORF53	Envelope glycoprotein N (gN)	110	Zhu et al 2005	2	18-42: HCWVTANSTGVASSTERSSP STAG.L 52-58: T.SVITTPGF.Y
ORF62	Triplex capsid protein 1 (TRX-1)	331	Zhu et al 2005, Bechtel et al 2005	3	46-65: AASTRPTVGSLEALRQAPF 244-263: L.TFFQSGKGFVAVM(+15.99)IKDHF.T 297-315: DSHPVHQSLNVKGTSLPVL
ORF63	Inner tegument protein	927	Zhu et al 2005, Bechtel et al 2005	5	540-610: Y.FHIM(+15.99)DILEERHSQDALY.N 601-613: L.EERHSQDALYNLL.D 134-140: Y.ADQIAGF.K 104-129: S.QPPQNTAPAQPPTSDDTLNNC(+57.02)TLLKLL 529-547: Y.DEDIVRSPLFADAFKSHLL
ORF64	Large tegument protein deneddylase	2635	Zhu et al 2005	12	893-900: I.TDPNGAHF.H 46-58: E.TPLVDRASLDDVL.E 779-787: L.QSAATAEHH.L 571-585: Y.STAAPSKCTHVLQFF.I 892-900: N.ITDPNGAHF.H 146-155: A.GAIVVK(+57.02)DK(+42.01)TY.Y 1178-1192: H.GEQAWKKIQAFKDF.N 1541-1551: L.S(+75.98)PLRVKGGKAA.V 681-706: T.ARLKPNFNIVC(+57.02)ARQDAQTIQDGVGLL.R 2397-2410: L.ETKTTTPSTPPHAI.D 1566-1574: L.VQEAEQAGL.L 90-104: L.RTDDWATKIFQSPEF.Y
ORF65	Small capsomere-interacting protein (SCP)	170	Zhu et al 2005	3	5-24: KVRDPVIQERLDHDIYAHHPL 78-100: RDQKPRERADRVAASAYDA GTF 148-170: SSTTETAAPAVADARKPPSG KKK
ORF68	Packaging protein UL32 homolog	545	Zhu et al 2005	4	40-57: TQIHQSLQPSSPCRVQQL 174-224: KTSWPRTDKEEATGPTPCQ ITDITTTAPASGIPELARATF CGASRPTKPSL 183-195: K.EEATGPTPC(+57.02)C(+57.02)QIT.D 355-367: IRGCTPQEIHKHL
ORF75	ORF75	1296	Zhu et al 2005, Bechtel et al 2005	6	124-135: L.QEWARVEVGRHL.V 168-192: L.EVPEGPQPVARPHIEDDVIM(+15.99)QAVMIS 180-201: P.HIEDDVIM(+15.99)QAVMISLGADLLPL.A 666-690: A.WRQAMAMGEQAYKMATNVSTGATY.A 1011-1024: F.SC(+57.02)PTSPRRVAALVL.P 1122-1133: L.GVVGRSESSPYT.Y
K8.1	gp35/37	228	Zhu et al 2005	4	70-121: NGTRLAAGSPSEYPNVSVS VEDTSASGSGEDAIDESGSG EEERPVTSHVTF 123-132: TQSVQATTEL 145-151: Y.S(-18.01)SGEPSR.T 145-197: SSGEPSRTRIRVSPVAENG RNSGASNRVPFSATTTTTTRG RDAHYNAEIRTHL

**B.5 Supplemental Table 5: Hits reported previously by other labs through Mass-Spectrometry and detected in our analysis as well using Chymotrypsin as digesting enzyme.**

Name	Amino Acid Size	Protein detected	Reported previously by other methods	Number of unique peptide hits	Sequences of Correspondence detected	-10lgP
ORF18	257	Protein UL79 homolog	Gong et al 2014	4	51-81: REATANAGTYDEVVLGRKVP AEVW 100-108: L.C(+57.02)EAYRDSLW.M 205-226: VWASETYGYPGVEAVCRDIR SM 233-248: AVSGYLPAPSEAQLAY	25 28.53 26.66 26.95
ORF32	454	Capsid vertex component 1 (CVC-1)	Dai et al 2014	4	48-79: SRSPGSSRRLVVCGRVLP EENQLASSPSGL 159-165: R.ATPDPAL.T 204-237: DPPVSQKGPARTRHRPPV R LSFNPNADVPATW 313-334: RQRVPVAIPRDAELADAVKS HF	25 29.43 25.01 25
ORF38	61	Cytoplasmic envelopment protein 3 (CEP-3)	Wu et al 2016	3	5-28: LSICKRPSQPVDVDGPELDV VVDY 11-28: R.PSQPVDVDGPELDVVVDY.D 41-61: EQSQSPYPALKKKKKKEAI Y	26 45.19 25
ORF42	278	Cytoplasmic envelopment protein 1 (CEP-1)	Butnaru et al 2019	3	16-51: STHAPKTRESEEA CPVYPHP VVPRLVLEVHRKNNAL 133-147: L.ENC(+57.02)RDMSPFLRSII.C 222-243: KLESSGENEDDKQTCADPVN IF	26 25.18 25
ORF43	605	Portal Protein	DD Dünn-Kittenplon et al, 2019	5	156-163: L.VNSIQEQL.M 383-406: L.EKERELC(+57.02)M(+15.99)KRLKC(+57.02)IETQLSHQPG.D 4-19: R.M(+15.99)NPGLGSSISVHPSEL.S 383-416: L.EKERELC(+57.02)M(+15.99)KRLKC(+57.02)IETQLSHQPGDAKPGSVNL.L 429-442: L.QDPSLQLTSSSHIPS.G	35.01 25.49 25.53 27.14 25.97
ORF48	402	ORF48	Sander,G. et al 2007	3	214-221: F.IEHITSDV.R 214-223: F.IEHITSDVRR.L 260-276: R.KPWKELSVSRINVEAR.L.L	26.82 25.08 28.26
ORF56	843	DNA primase	Davis et al 2015	4	247-254: L.ETEADIRT.I 726-735: E.TLSGRSIEDW.L 353-360: L.VGERC(+57.02)VYW.C 40-46: F.FSVLHDL.F	40.18 29.4 25.88 25.95
ORF K2	204	Viral Interleukin 6 Homolog	Katano,H. et al.2000	7	176-183: Y.VLSAMEKF.A 45-55: W.VIDEC(+57.02)FRDLC(+57.02)Y.R 178-185: L.S(+154.00)AMEKFAG.Q 184-203: F.AGQ(+.98)AVRVLN(+.98)SIPDVTDPVHD.K 192-199: L.NSIPDVT.P.D 8-15:W.SILLVGSLL 17-29: L.V(+42.01)SGTRGK(+42.01)LPDAPE.F	86.52 36.29 34.9 29.75 27.62 26.81 26

### B.6 Supplemental Table 6: Hits reported previously by other labs through Mass-Spectrometry and detected in our analysis as well using Chymotrypsin as digesting enzyme.

Name	Amino Acid Size	Protein detected	Number of unique peptide hits	Sequences of Correspondence detected	-10lgP
ORF9	1012	DPOL	4	154-164: Y.FYTLAPQGVNL.T 323-336: L.HTVGNDKPYTRMLL.G 933-940: P.QIHDRIPY.V 989-999: F.QNNTSATVAIL.Y	34.08 30.27 27.7 31.12
ORF23	404	ORF23	4	103-124: HSKPVVRGHEFEDTQILPEC.RL 169-190: DPESLPRHPITPRAGQTRS IL 193-215: H.NIAQVC(+57.02)ERDIVSLNTDNEAASMF.Y 325-338: REPIRQPPDCSKVL	25.01 26.97 27.23 25.31
ORF35	150	ORF35	3	2-15: DSTNSKREFIKSAL 83-97: RQPRDLPRVADIDAL 116-137: EENGEETPTHSSSEIKDTIV RW	25.62 28.53 25.93
ORF58	357	ORF58	4	65-74: L.C(+57.02)PAAQKQLDR.R 116-130: L.LPYPLATATAVYQAP.P 215-222: Y.C(+57.02)RREVVVF.V 350-357: L.SVINKVVG	27.92 29.48 25.43 25
ORF72	257	viral cyclin homolog	4	1-11: MATANNPPSGL 85-93: IKQVSKEHF 185-204: VDPKTGSLPASIIASAAGCAL 206-224: VPANVIPQDTHSGGVVPQL	30 26.23 25.9 25
ORF K3	333	E3 ubiquitin-protein ligase MIR1	3	76-91: L.TYQEGLELIVFIFIMT.L 139-152: L.GAFFHM(+15.99)MRHVGRAY.A 279-292: Y.VGAQSGDGAYSVSC(+57.02).H	25.04 27.54 25.13

vIRF-1	449	Viral IRF like protein 1	4	23-73: SQGSPGTSGSGAPCDEPSRS ESPGEGPSGTGGSAAGDIT RQAVVAITEW 175-189: L.QEIGKGISQDGHFL.V 334-340: L.TSSC(+57.02)NGLF 385-399: ANSLPAPSHVTCPL	25.03 26.47 25.44 25
vIRF-3	566	Viral IRF like protein 3	3	79-96: GKICTTSRRLRRLPGEEY 128-136: L.HSGSSLWELL 278-293: L.GIPEDVLIATSQPGGDT.D	25 26.08 25.01
vIRF-4	911	Viral IRF like protein 4	5	141-177: L.LSPPMQTTATRRSDTREQSYEEAGAAAPAPPKAPSGL.R 492-501: W.SSGGAPNQL.S 672-679: W.EEGLGNIL.S 555-572: L.EVEIIDLTGDSPTST.T 871-879: L.SVNPVTC(+57.02)GT.V	26.12 30.02 29.65 25.01 25

### B.7 Supplemental Table 7: Hits detected in our study using Chymotrypsin as digesting enzyme, not found by Trypsin.

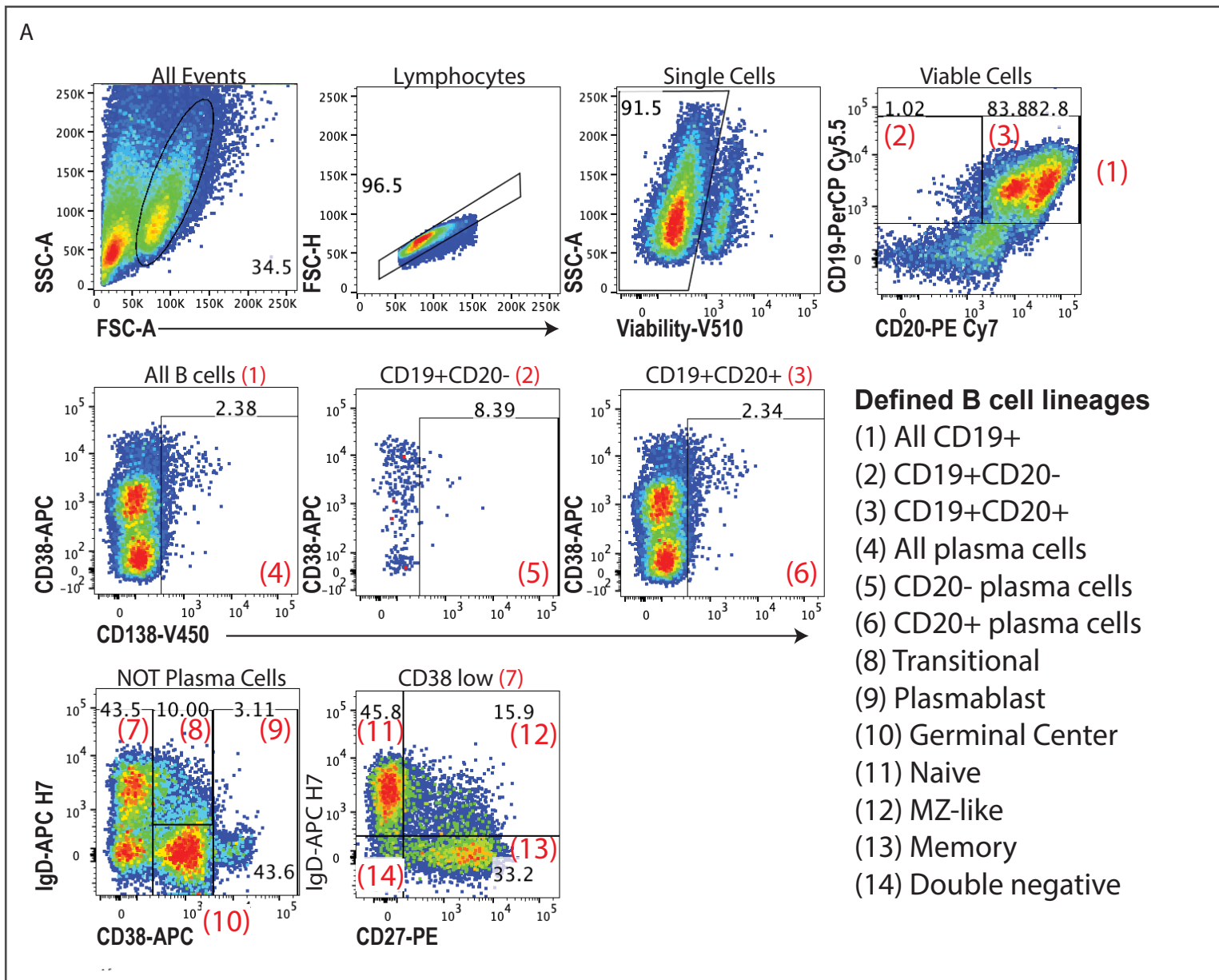
Name	Amino Acid Size	Protein detected	Number of unique peptide hits	Sequences of Correspondence detected	-10lgP
ORF44	788	DNA Replication Helicase	5	12-19: D.EPSPGFIL.N 55-64: F.DPLEDEGPFL.P 225-241: W.LDTPLYRNGAVPC(+57.02)IVC(+57.02)V.G 511-520: H.GVKQGHEEFL.R 616-622: F.VSTSPGL.H	30.76 30.37 26.11 35.07 27.95

### B.8 Supplemental Table 8: Example of de novo hits via de novo sequencing feature of PEAKS DB with cut-off ALC% at 75%.

Sequence	aa Length	ALC%	aa Scoring	PTMs
EC(+57.02)C(+57.02)HGDLLC(+57.02)ADDRWRR	17	93	98 98 98 97 86 94 95 98 98 97 96 94 94 91 82 86	Carbamidomethylation
APSAEVEMTAYVLLAHVTAQPAPGMVGHKS	30	93	98 97 96 96 98 99 100 100 99 99 99 99 100 100 99 99 98 97 96 96 96 94 83 89 89 59 60 84 97	N/A
LKEC(+57.02)C(+57.02)DKPLLEK	12	92	97 96 97 99 98 97 96 94 95 78 74 81	Carbamidomethylation
GDSGGPLLLHK	11	88	87 97 97 94 93 97 99 99 85 71 57	N/A
VPLPVSVSVEF	11	87	98 96 99 91 85 73 92 86 73 78 90	N/A
HTM(+15.99)SGVASVESSGSAVGSPNR	22	85	95 94 89 89 49 71 92 95 97 99 98 99 99 90 96 95 90 71 87 46 54 82	N/A
C(+57.02)VALLTLTY	9	85	96 96 98 99 99 90 73 55 63	Carbamidomethylation
SPQELLC(+57.02)GASLLSDR	15	85	97 97 95 97 99 99 99 88 93 94 93 88 35 41 62	Carbamidomethylation
LLLYALLPDGEVVGDWK	17	84	87 88 79 93 93 97 99 98 97 89 97 97 94 63 78 39 48	N/A
ELNDLLSQLGLRKLK	15	83	95 96 95 99 100 100 98 93 94 30 60 90 89 60 54	N/A
ASFSVLGDLLGSAM(+15.99)R	15	80	68 73 85 94 96 99 96 97 98 96 68 73 66 40 59	N/A
LTESALSPL	9	77	95 67 62 88 54 71 98 90 73	N/A
FLLPQLVK	8	76	92 97 97 86 73 41 41 80	N/A
LFFTHADLGM(+15.99)LEAEQL	16	75	95 91 67 68 94 94 94 82 94 95 50 21 21 43 93	Oxidation (M)
RTSTPLPVSVSVEFAVAATDC(+57.02)ALK	24	75	51 55 45 89 93 96 59 55 56 90 91 88 92 96 92 91 92 91 80 75 60 22 48 86	Carbamidomethylation

# Appendix C. Supplementary data from Chapter 4

## C.1 The B cell analysis gating Scheme utilized in this study based on our previous studies (Aalam F, 2020).



## C.2 UV Inactivation to study the early effects of $\Delta 11$ mutant virus vs. WT virus.

